AD-A129 391 SPATIAL ORIENTATION AND MOTION CUE ENVIRONMENT STUDY IN THE TOTAL IN-FLIG..(U) GULF AND WESTERN APPLIED SCIENCE LABS WALTHAM MA J BORAH ET AL. JUN 83 AFHRL-TP-82-28 1/2

UNCLASSIFIED F33615-78-C-0062 F/G 5/9 NL

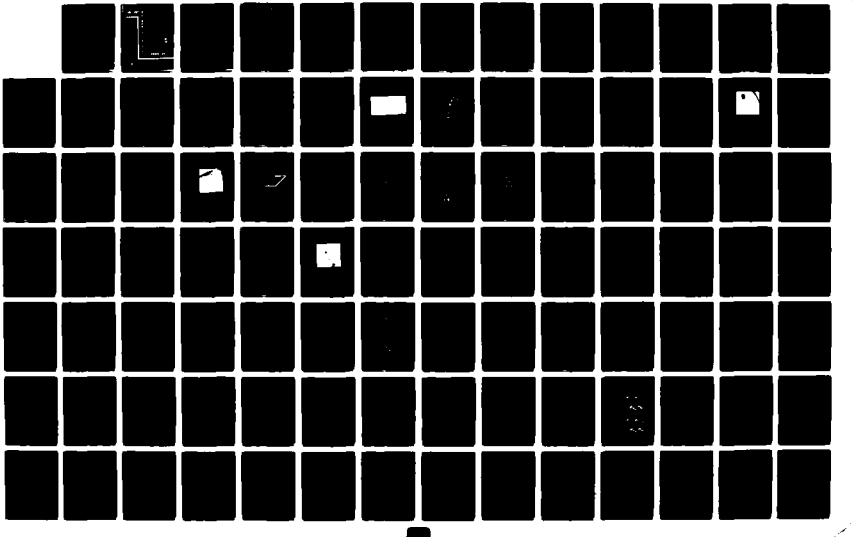

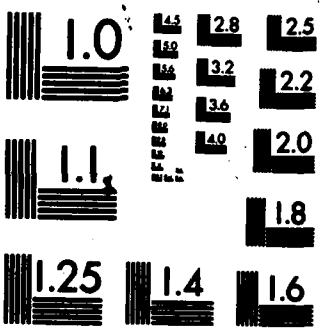

MICROCOPY RESOLUTION TEST CHART
NATIONAL BUREAU OF STANDARDS-1963-A

AFHRL-TP-82-38

AIR FORCE HUMAN RESOURCES LABORATORY

SPATIAL ORIENTATION AND MOTION CUE ENVIRONMENT STUDY IN THE TOTAL IN-FLIGHT SIMULATOR

By

Joshua Borah
Lawrence R. Young
Gulf and Western
Applied Science Laboratories
335 Bear Hill Road
Waltham, Massachusetts 02154

OPERATIONS TRAINING DIVISION
Williams Air Force Base, Arizona 85224

June 1983

Final Technical Paper

AIR FORCE SYSTEMS COMMAND
BROOKS AIR FORCE BASE, TEXAS 78235

NOTICE

When Government drawings, specifications, or other data are used for any purpose other than in connection with a definitely Government-related procurement, the United States Government incurs no responsibility or any obligation whatsoever. The fact that the Government may have formulated or in any way supplied the said drawings, specifications, or other data, is not to be regarded by implication, or otherwise in any manner construed, as licensing the holder, or any other person or corporation; or as conveying any rights or permission to manufacture, use, or sell any patented invention that may in any way be related thereto.

The Public Affairs Office has reviewed this paper, and it is releasable to the National Technical Information Service, where it will be available to the general public, including foreign nationals.

This paper has been reviewed and is approved for publication.

DAVID POHLMAN
Contract Monitor

MILTON E. WOOD, Technical Director
Operations Training Division

CARL D. ELIASON, Colonel, USAF
Chief, Operations Training Division

Unclassified

SECURITY CLASSIFICATION OF THIS PAGE *(When Data Entered)*

REPORT DOCUMENTATION PAGE

READ INSTRUCTIONS BEFORE COMPLETING FORM

1. REPORT NUMBER
AFHRL-TP-82-28

2. GOVT ACCESSION NO.
AD-A129 391

3. RECIPIENT'S CATALOG NUMBER

4. TITLE *(and Subtitle)*
SPATIAL ORIENTATION AND MOTION CUE ENVIRONMENT STUDY IN THE TOTAL IN-FLIGHT SIMULATOR

5. TYPE OF REPORT & PERIOD COVERED
Final

6. PERFORMING ORG. REPORT NUMBER

7. AUTHOR(s)
Joshua Borah
Laurence R. Young

8. CONTRACT OR GRANT NUMBER(s)
F33615-78-C-0062

9. PERFORMING ORGANIZATION NAME AND ADDRESS
Gulf and Western, Applied Science Laboratories
335 Bear Hill Road
Waltham, Massachusetts 02154

10. PROGRAM ELEMENT, PROJECT, TASK AREA & WORK UNIT NUMBERS
62205F
61141913

11. CONTROLLING OFFICE NAME AND ADDRESS
HQ Air Force Human Resources Laboratory (AFSC)
Brooks Air Force Base, Texas 78235

12. REPORT DATE
June 1983

13. NUMBER OF PAGES
148

14. MONITORING AGENCY NAME & ADDRESS *(if different from Controlling Office)*
Air Force Human Resources Laboratory
Operations Training Division
Williams Air Force Base, Arizona 85224

15. SECURITY CLASS *(of this report)*
Unclassified

15.a. DECLASSIFICATION/DOWNGRADING SCHEDULE

16. DISTRIBUTION STATEMENT *(of this Report)*

Approved for public release; distribution unlimited.

17. DISTRIBUTION STATEMENT *(of this abstract entered in Block 20, if different from Report)*

18. SUPPLEMENTARY NOTES

19. KEY WORDS *(Continue on reverse side if necessary and identify by block number)*

electromyographic (EMG)
head/neck biodynamics
modeling
motion cuing
pressure sensing seat pads
simulation
spatial orientation
tactile cue environment
total in-flight simulator (TIFS)

20. ABSTRACT *(Continue on reverse side if necessary and identify by block number)*

A study was performed using the Air Force Total In-Flight Simulator (TIFS) to gather data concerning spatial orientation, head/neck biodynamics, and the tactile cue environment during certain aircraft maneuvers. The maneuvers included coordinated turns, uncoordinated rolling and pitching motions, roller-coaster motions, lateral accelerations and sustained longitudinal accelerations. Measurements were made of perceived direction of vertical, perceived roll rate (magnitude estimates), and perceived translatory acceleration (magnitude estimates) using a special indicator and employing an otherwise passive subject. The dynamics of seat-pan and backrest pressure distributions for both the pilot and passive subject were measured with a set of pressure transducers laid over the seats. Videotape

DD Form 1473 1 Jan 73 EDITION OF 1 NOV 65 IS OBSOLETE

Unclassified

SECURITY CLASSIFICATION OF THIS PAGE *(When Data Entered)*

Item 20 (Continued)

recordings of the pilot's and passive subject's head position with respect to the cockpit were made, and neck muscle activity was measured using electromyographic (EMG) electrodes. Full documentation of the aircraft's specific forces, angular rates and Euler angles were obtained from an onboard inertial system.

The pattern of orientation illusions during coordinated turns can be explained in terms of biological sensory mechanisms and is compared to the predictions of an optimal estimator model for human dynamic spatial orientation. The EMG and video head motion data are used to partially describe head/neck/torso response to lateral inertial forces, and a proprioceptive component of the spatial orientation model is compared to some of the EMG data. The seat pressure results suggest that, for low frequency acceleration stimuli, the body/seat interaction can be adequately represented by a simple mass model, and implications for g-seat drive design are discussed.

AFHRL Technical Paper 82-28 June 1983

SPATIAL ORIENTATION AND MOTION CUE ENVIRONMENT STUDY IN THE TOTAL IN-FLIGHT SIMULATOR

By

Joshua Borah
Laurence R. Young

Gulf and Western
Applied Science Laboratories
335 Bear Hill Road
Waltham, Massachusetts 02154

OPERATIONS TRAINING DIVISION
Williams Air Force Base, Arizona 85224

Reviewed and submitted for publication by

Thomas H. Gray
Chief, Operational Unit Training Branch

PREFACE

The objective of the spatial orientation and motion cue environment study in the Total In-Flight Simulator was to collect in-flight data for human perception of spatial orientation, head-neck biodynamics, and the tactile cue environment. These data are needed to supplement existing information for the purpose of validating and improving a computer model of human motion sensing mechanisms. This study is in support of TPO 3, Air Combat Tactics and Training Engagement Simulation Technology whose objective is identification and demonstration of cost effective training strategies and training equipment capabilities for use in developing and maintaining the combat effectiveness of Air Force aircrew members. It is also responsive to the specific goal of TPO 3 to develop software techniques and hardware for use in aircrew training systems.

The project was sponsored by the Air Force Human Resources Laboratory and was under the direction of Mr. Don Gum. Mr. Joshua Borah was the principle investigator for G+W Applied Science Laboratories and Dr. Laurence R. Young was the principle consultant. Mr. Max Fiore of AFHRL participated in the experiment.

The study relied heavily on the Air Force Total In-Flight Simulator (TIFS) aircraft which is maintained and operated by Calspan Corporation, Buffalo, New York. Installation of equipment in the TIFS, implementation of flight protocol, and in-flight data recording were all handled by Calspan Corporation under the direction of Dr. Phillip Reynolds, TIFS program manager, and Mr. James Dittenhauser, project engineer.

TABLE OF CONTENTS

TABLE OF CONTENTS (CONT.)

LIST OF FIGURES

LIST OF FIGURES (Cont.)

LIST OF FIGURES (Cont.)

LIST OF FIGURES (Cont.)

LIST OF FIGURES (Cont.)

LIST OF FIGURES (Cont.)

LIST OF TABLES

1.0 INTRODUCTION

Experiments were performed, using the Air Force Total In-Flight Simulator (TIFS), to fill some specific gaps in the understanding of human spatial orientation, head-neck biodynamics, and the tactile cue environment during aircraft flight. Flight maneuvers included coordinated turns, roller coaster oscillations, lateral accelerations, and sustained longitudinal accelerations. They were designed to emphasize stimuli which cannot be represented adequately in existing motion-base simulators. The measurements comprise three related but separate experiments (spatial orientation, biodynamics, and tactile cue environment) that were conducted simultaneously in order to make the most efficient use of equipment and flight time.

1.1 Background

In order to design motion simulation devices effectively, it is important to understand how motions are perceived, both by the visual and non-visual senses. These mechanisms have been modeled, and the literature contains experimental data documenting perceptual responses to several standard patterns of motion. Included among these are responses to pure tilting motions with respect to gravity (Schone, 1964) and rotations of only the gravito-inertial force vector (Cohen, Crosbie, and Blackburn, 1973). Tilting motions, in which the subject feels no change in orientation with respect to the gravito-inertial force vector, such as during a coordinated aircraft turn have not been quantified previously. This type of maneuver is of potential importance, since most fixed wing aircraft maneuvers are so "coordinated". It is of more general interest because human motion sensing mechanisms evolved in a world where, over the long term, the specific force vector remains aligned with gravity. Perceptual responses to coordinated turns are especially interesting in the absence of visual cues, since the system must estimate orientation by resolving seemingly conflicting inertial cues, a roll rate which leaves one aligned with the apparent vertical. Quantitative data of this nature are needed to help validate and refine a recently developed computer model of the motion sensing mechanisms (Borah, Young, Curry, in press).

Inertial forces acting on the head can be detected by proprioceptive sensors (muscle force and position

detectors) in the neck and may provide an important motion cue. The spatial orientation model mentioned previously includes a preliminary model of head-neck system biodynamics. Although aircraft simulator researchers have considered building devices to produce artificial head forces, there is very little data in the literature describing head motions or neck muscle response to lateral accelerations and tilts. Data of this type, for pilots as well as passive subjects, is needed both for model development and design of cueing devices.

The somatosensory system provides still another important spatial orientation cue, and some advanced simulators now use g-seats to simulate the "seat-of-the-pants" feel of aircraft motion. Static body/seat pressure distributions have been measured, but there has been very little in the literature describing the dynamics of the tactile stimuli produced by changing inertial forces. Such data are essential for development and testing of g-seat drive algorithms.

1.2 Summary

Coordinated turns, uncoordinated rolling and pitching motions, rollercoaster motions, lateral accelerations, and sustained longitudinal accelerations were performed using the TIFS aircraft. Measurements were made of perceived direction of vertical, perceived roll rate (magnitude estimates) and percieved translatory acceleration (magnitude estimates) using a special indicator manipulated by an otherwise passive subject. The dynamics of seat-pan and backrest pressure distributions for both the pilot subject and the passive subject in this study were measured with a set of pressure transducers laid over the seats. Video tape recordings were made of the two subjects' head positions, with respect to the cockpit. These were complemented by measure of neck muscle activity using electromyogram (EMG) electrodes. Full documentation of the aircraft's specific forces, angular rates, and Euler angles was obtained from an onboard inertial system.

The subjective orientation data was used to describe the somewhat illusory sensations experienced by most subjects during coordinated turns. These responses are compared to predictions of a previously developed model of the motion sensing mechanisms. A small quantity of low noise neck muscle EMG data was obtained in the experiment and is compared to the forces in the head/neck biodynamics

component of the spatial orientation model mentioned previously. Although complete analysis of the video data (requiring an automated data reduction technique) was not part of the current program, a small amount of the data was reduced by hand and, along with the EMG data, is used for partial description of the head/neck/torso response to lateral inertial forces. More complete analysis will be possible with thorough reduction of the video data. The seat pressure results suggest that, for many stimuli, body/seat interaction can be adequately represented by a simple mass model, and the implications for g-seat drive designs are discussed.

1.3 Report Organization

Experimental methods (including aircraft configuration, maneuvers, specialized equipment, and subject tasks) are discussed in detail in Section 2.0. The format of the resulting data is described in Section 3.0. Sections 4.0 through 6.0 describe the results of the orientation, head-neck biodynamics, and tactile cue experiments, followed in section 7.0 by comparison of all pertinent data with a previously developed spatial orientation model. Conclusions are summarized in Section 8.0. Additional details concerning equipment construction, protocol, and data format are provided in the appendices.

The report has been designed so that the results presented in Sections 4.0 through 7.0 are reasonably self-contained. If desired, the methods and data format sections (2.0 and 3.0) can be skipped and used solely for reference without loss of continuity.

2.0 METHODS

2.1 Aircraft Configuration

Experimental data was gathered in the Air Force Flight Dynamics Laboratory's Total-In-Flight Simulator (TIFS). Figure 2.1 is a photograph of the aircraft, and Figure 2.2 shows the interior arrangement used in the orientation and motion cue environment study. TIFS is an NC-131H turboprop transport that has been modified to provide high fidelity reproduction of the motions and handling qualities of medium to large-size airplanes. It is equipped with a six-degree-of-freedom computer flight control system, moveable side force surfaces, and a separate simulation cockpit in the nose.

For the orientation and motion cue environment study, the simulation cockpit was divided in half by a black curtain. All instruments and controls were removed from the right half of the cockpit, and windows on this side were completely blacked out. In contrast, the left side of the simulation cockpit had full pilot controls and instrumentation as well as an unobstructed out-the-window view.

Both the left and right transport style seats in the simulation cockpit were equipped with especially designed pressure sensing seat pads. A video camera was installed on each side of the cockpit to view the back of each seat occupant's head. Both seats also contained leads for EMG electrodes used to measure neck muscle activity. The right side of the simulation cockpit was equipped with a special pointing device and meter for use by the occupant of the right seat. All of the above instrumentation is described in more detail in Section 2.2.

Just aft of the command cockpit was an instrumentation table containing a video tape recorder, video monitor, and amplification and control boxes for the various specialized instrumentation. Further aft, at the test engineer number two (TE2) station (see Figure 2.2) was a digital tape recording system on which all data were stored. The analog computer and VSS electronics used for flight control during most experimental runs were located at the rear of the cabin, and the strip chart to monitor equipment function during the flights was located at the test director station as shown in Figure 2.2.

Figure 2.1 Total-In-Flight-Simulator (TIFS)

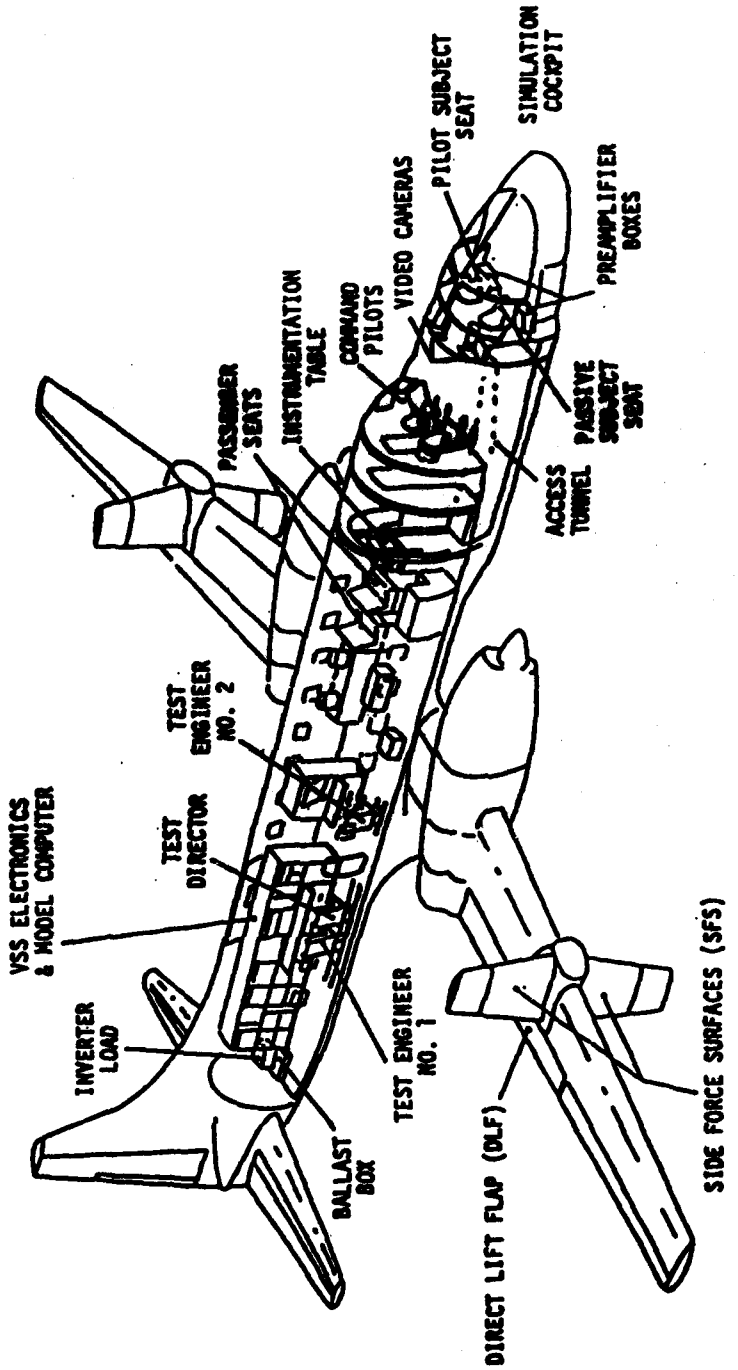

Figure 2.2 TIFS Arrangement

Eight persons were on board the aircraft during each flight: two command pilots, two subjects, two test engineers, the test director, and the instrumentation table operator. The TIFS can be controlled from either the command cockpit, the test engineer number one station (TE1), or the simulation cockpit. TIF control is at the discretion of the command pilots who can assume control of the aircraft at any time. Most experimental runs were controlled primarily by the analog computer from the TE1 station, but several selected runs were flown by the left-seat, pilot-subject in the simulation cockpit.

The intercom system was set up so that the right seat subject (in the simulation cockpit) could be excluded from listening to intercom conversation but could always be heard by the rest of the crew.

2.2 Instrumentation

Body/seat pressure sensing pads, electromyographic processing equipment, and a pointer/meter device were designed and constructed by Applied Science Laboratories for the TIFS experiment. In addition, video camera and recording equipment, furnished by the Government, were installed to monitor and record head movements.

2.2.1 Pointer/Meter Device

A two-degree-of-freedom pointing device was constructed to enable a subject to indicate perceived orientation by aligning a balanced thin rod with the apparent direction of earth vertical. The device is shown schematically in Figure 2.3. Potentiometers provided signals proportional to pitch and roll orientation of the pointing rod with respect to the cockpit. The pointer also controlled the needle on the meter face shown in Figure 2.4, and was used by subjects, at various times during the experiment, to make magnitude estimates of their roll angular velocity, or at other times, their forward acceleration. The pointer and meter were illuminated by a small light behind the seat.

Figure 2.5 shows the placement of the pointer and meter with respect to the subject, and Figure 2.6 is a photo of the right seat location showing both the pointer and meter. After the first test run in TIFS, a fore-aft

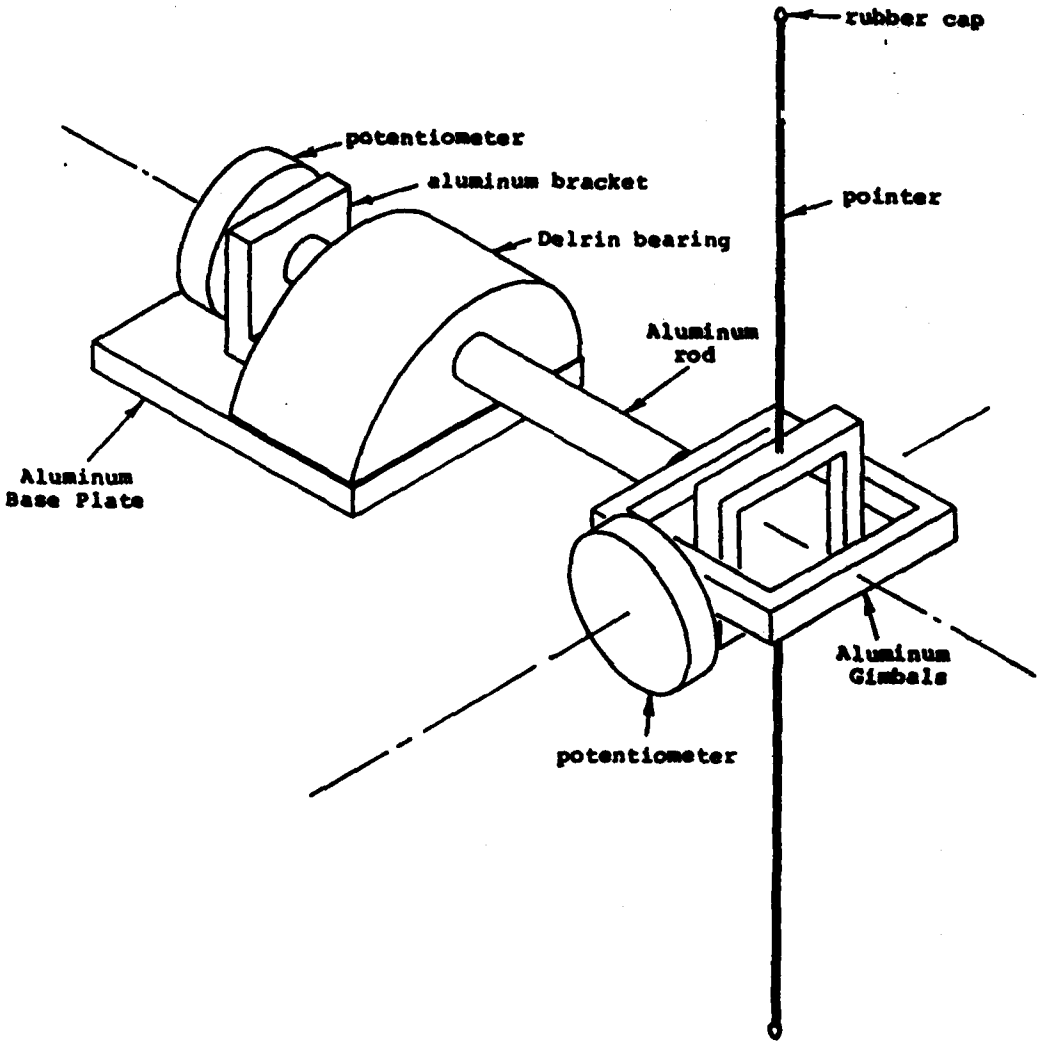

Figure 2.3 Instrumented Pointer Device

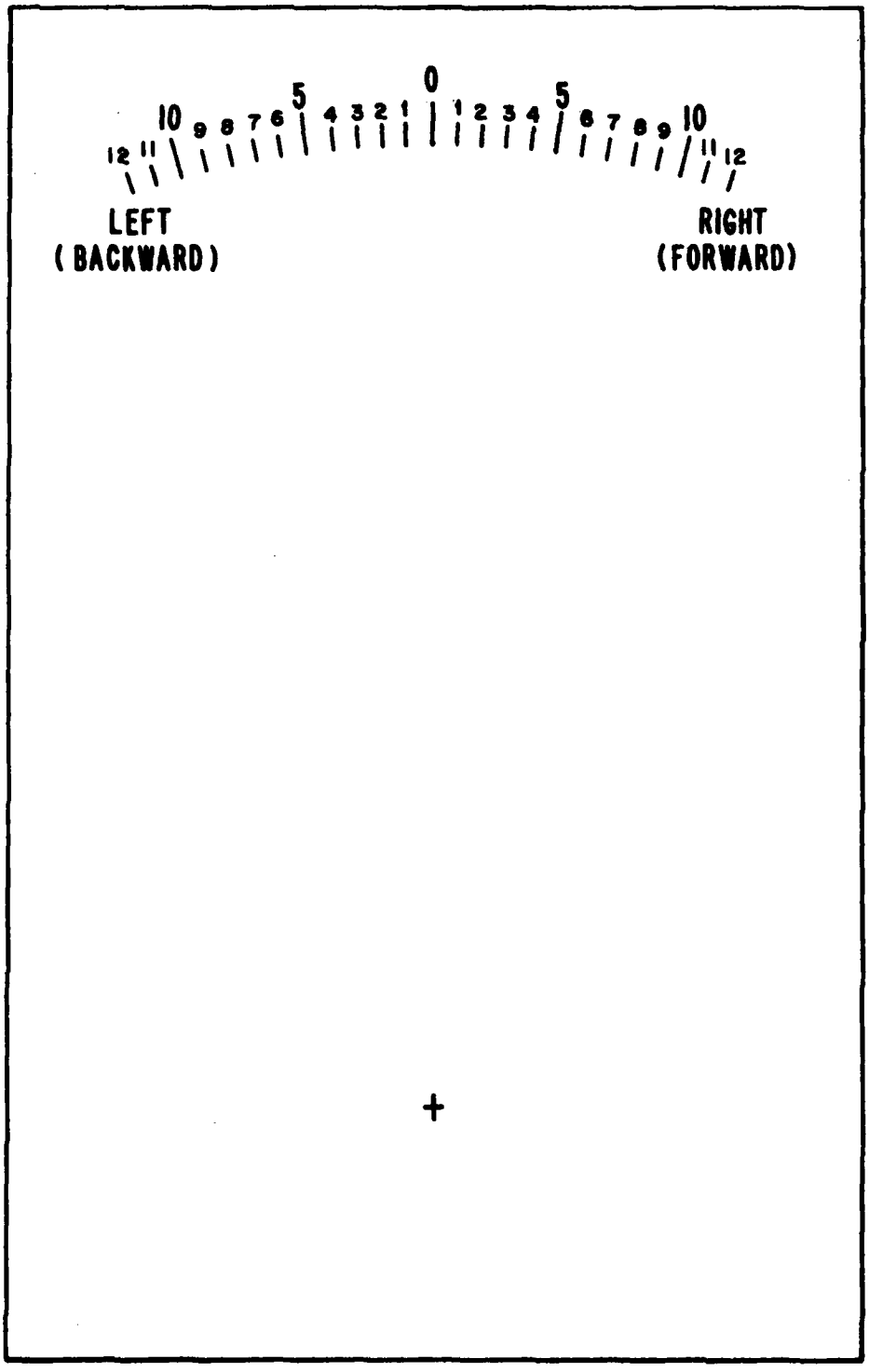

Figure 2.4 Meter Face

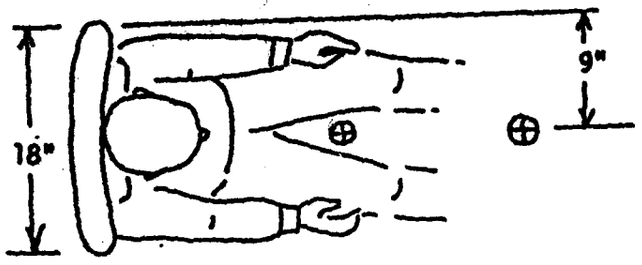

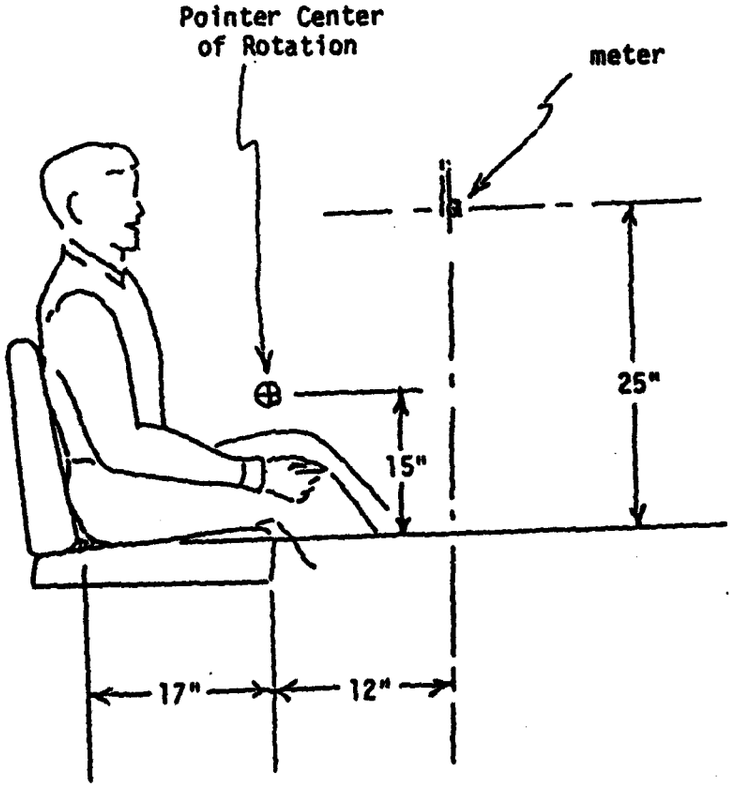

Figure 2.5 Location of meter and pointer with respect to right seat of TIFS evaluation cockpit.

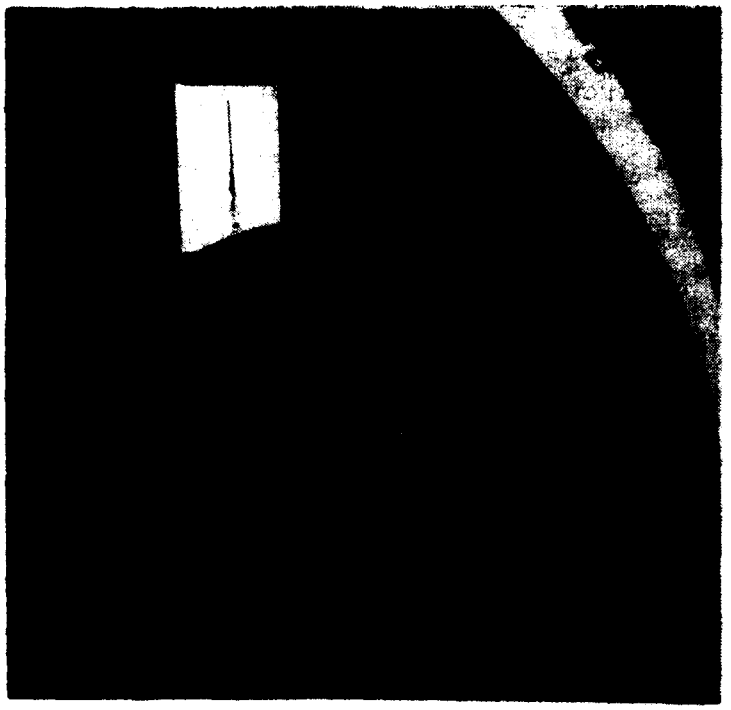

Figure 2.6 Photo showing pointer and meter at the right seat station in the TIFS simulation cockpit.

horizontal rod was added to the pointer to help the subject estimate pitch angles, as shown in Figure 2.6. A black cover was used to obscure the meter face during portions of the experiment for which it was not needed.

A control box on the TIFS instrumentation table allowed the meter needle to be controlled by either the roll or pitch axis of the pointer. The same box contained scaling and offset adjustments for the device. Details of the electronic circuitry are in Appendix A.

2.2.2 EMG Equipment

Both of the simulation cockpit subjects had EMG surface electrodes placed on their necks to monitor neck muscle activity. EMG signals required preprocessing since the TIFS data recording system (discussed in Section 2.3) can handle frequencies up to only about 20 Hz. Muscle tension has been shown to be approximately proportional to the RMS amplitude of an EMG signal; therefore, the RMS amplitude signal was extracted and recorded. Although the relation of EMG spike frequency to muscle tension is far more complex, frequency information was also extracted and recorded.

Each subject wore five electrodes -- a pair of active electrodes on each side of the neck, positioned approximately over the sternocleidomastoideus muscles, and a ground electrode on one shoulder just below the collarbone. The signal processing for each pair of active electrodes is shown schematically in Figure 2.7. Electrode positioning is shown by Figure 2.8. The circuitry used to implement the Figure 2.7 schematic can be found in Appendix A. Preamp boxes for the EMG signals were located in the simulation cockpit next to each seat, and the RMS amplitude and frequency extraction circuitry is in a box that was strapped to the instrumentation table.

Small, silver conductor, snap type disposable electrodes (Ludlow Medical Products Stock #9596) were applied shortly before each flight. Prior to application of each electrode, the skin was prepared by cleaning the area with an alcohol swab and making a small scratch with a sterile needle. The scratch which was needed to penetrate the high impedence top layer of dead skin and oil did not draw blood or pierce the skin deeply.

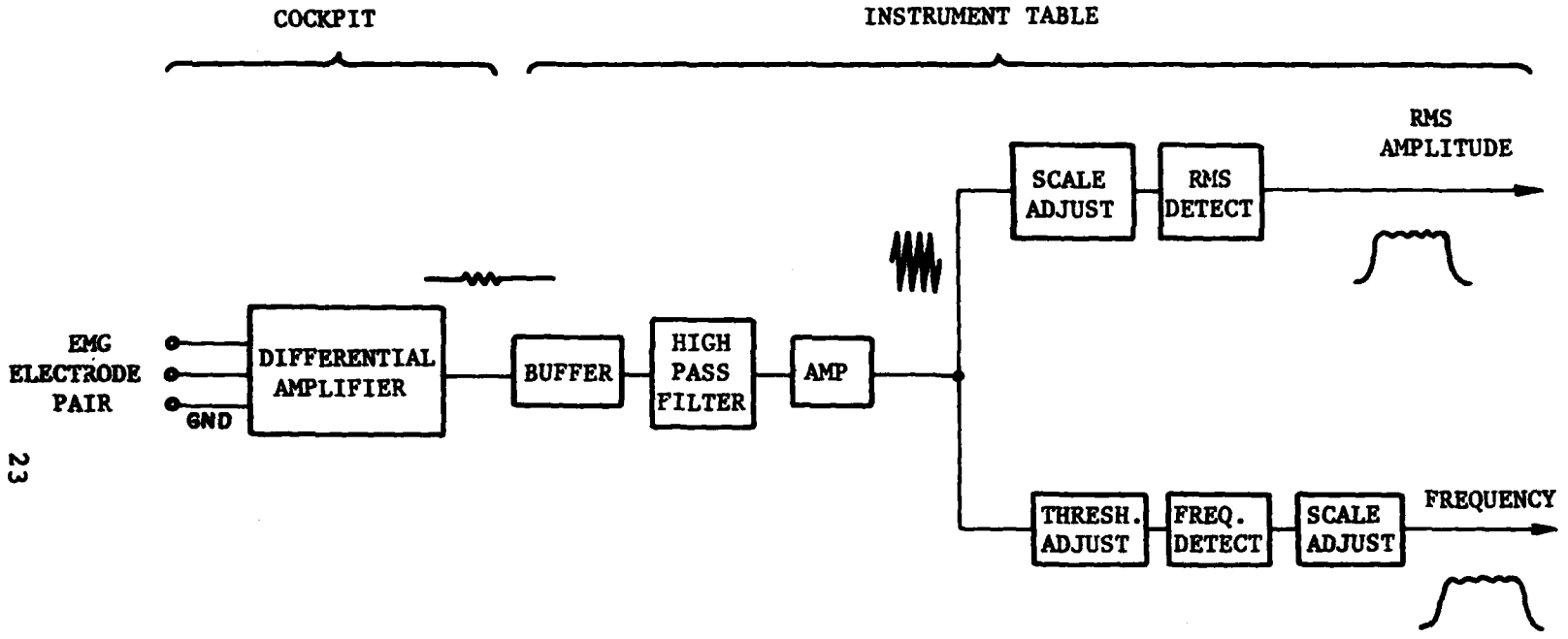

Figure 2.7 EMG Signal Processing Schematic

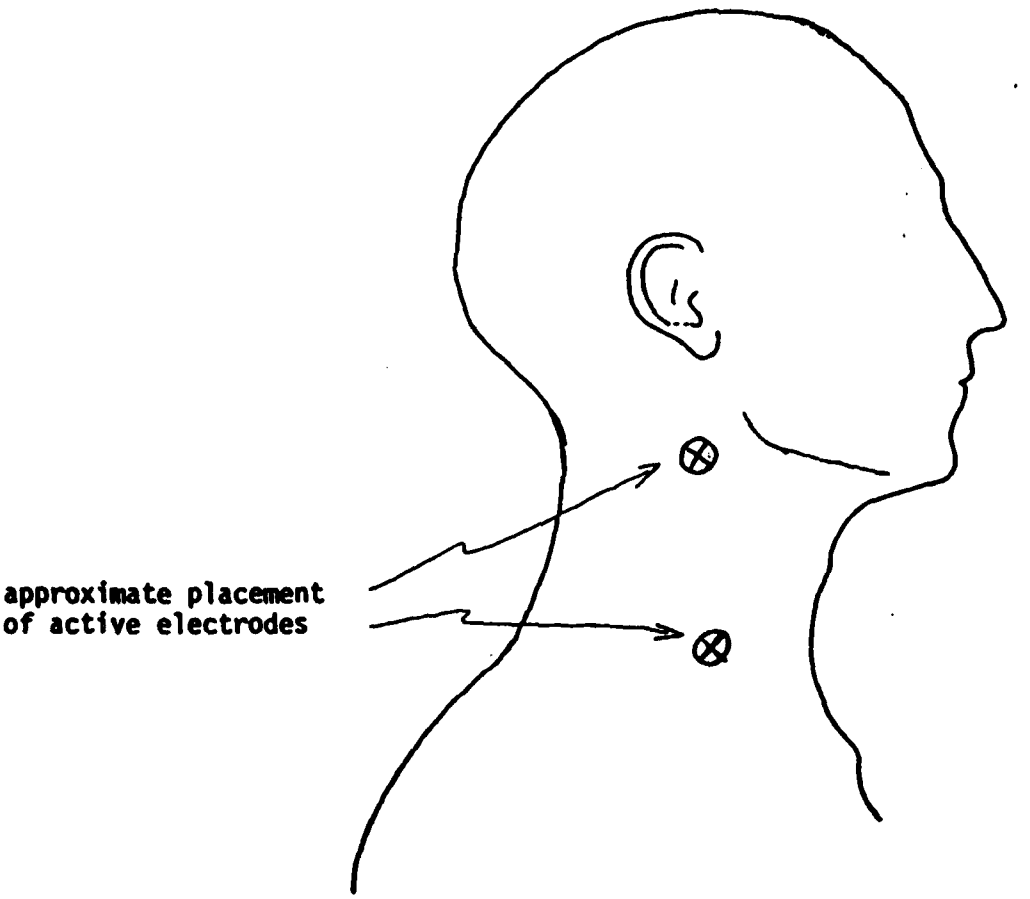

(ground electrode is placed on the right shoulder)

Figure 2.8 EMG Electrode placement (two electrodes are also placed on the left side of the neck).

2.2.3 Pressure Sensing Seat Pads

The thin seat pads, each containing an array of load cells, were designed and constructed to measure the dynamics and distribution of body/seat contact force during flight maneuvers. Pressure sensing pads were installed in both the left and right simulation cockpit seats as shown by the photograph in Figure 2.9. Note that the seat pan was of the partially split type to permit simulations with center stick controllers.

The seat pads, which fasten to both the seat-pan and backrest with velcro, have the sandwich-like construction diagrammed in 2.10. The inner layer is a .107 inch thick neoprene rubber cushion with square cutouts for 1 inch square, 0.1 inch thick load cells, and for lead wires. The load cells, which are sensitive in the direction perpendicular to the pads, are individually shimmed with fiberboard to match, as precisely as possible, the thickness of the rubber cushion. The rubber cushion is enclosed by a piece of nylon fabric glued to one side and folded to cover the other side. The upper and lower flaps of the nylon cover are fastened together with velcro.

Figure 2.11 is a rear view of a person seated on a cushion. Figures 2.12 to 2.14 show sensor placement relative to seat-pan and backrest pressure distribution data, and Figure 2.15 specifies the sensor numbering scheme used on seat-pan and backrest pads.

Preamplifiers for the load cell sensors were located in boxes just outboard of each seat in the simulation cockpit (the right seat preamp box can be seen in the Figure 2.9 photograph). A single box containing second stage amplification, as well as gain and offset adjustments, was strapped to the instrumentation table.

The load cells, made especially for this purpose by Besco Industries, Chatsworth, California, had four different force ranges: 0-10 lb., 0-6 lb., 0-5 lb., and 0-3 lb. Ten pound and 6 pound units were used in the positions closest to the ischial tuberosities (see Figure 2.11) on the seat pan. Six pound and 5 pound units were used elsewhere on the seat pan, and more sensitive 3 pound units were used for the backrest pads. Details of the amplification and scaling circuitry are in Appendix A.

Figure 2.9 Seat with Pressure Sensing Pads

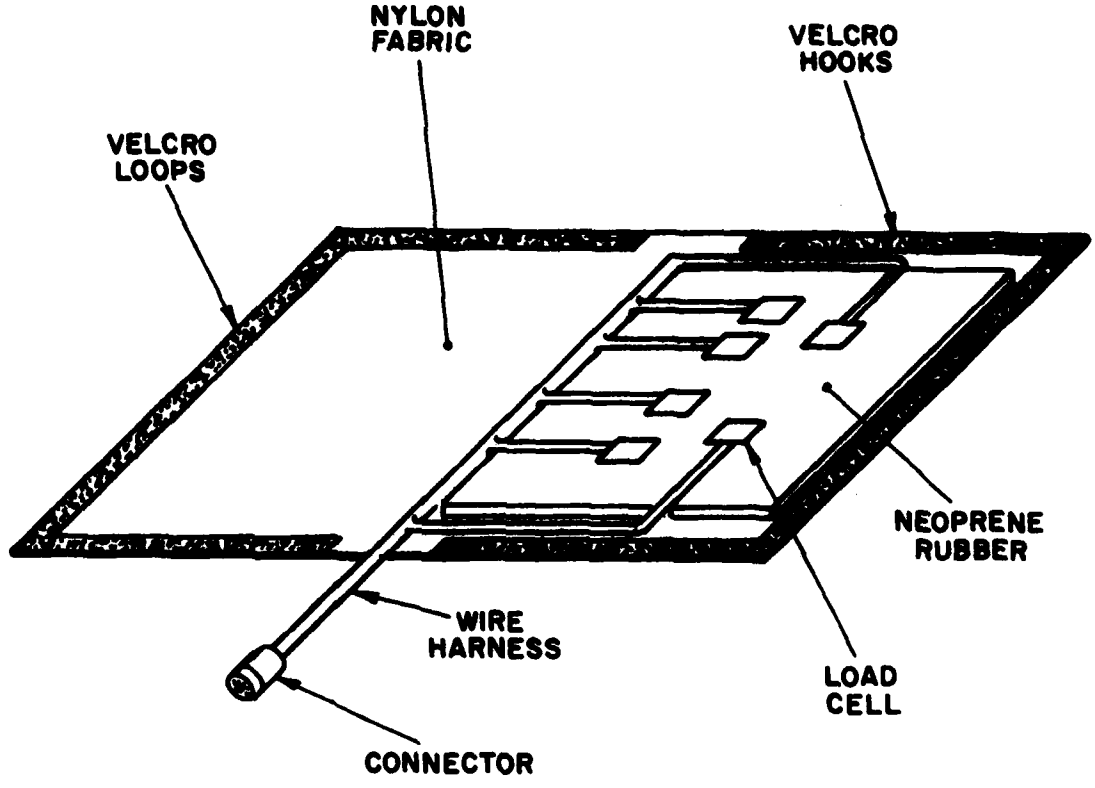

Figure 2.10 Pressure Sensing Seat Pad with Nylon "Cover" Opened

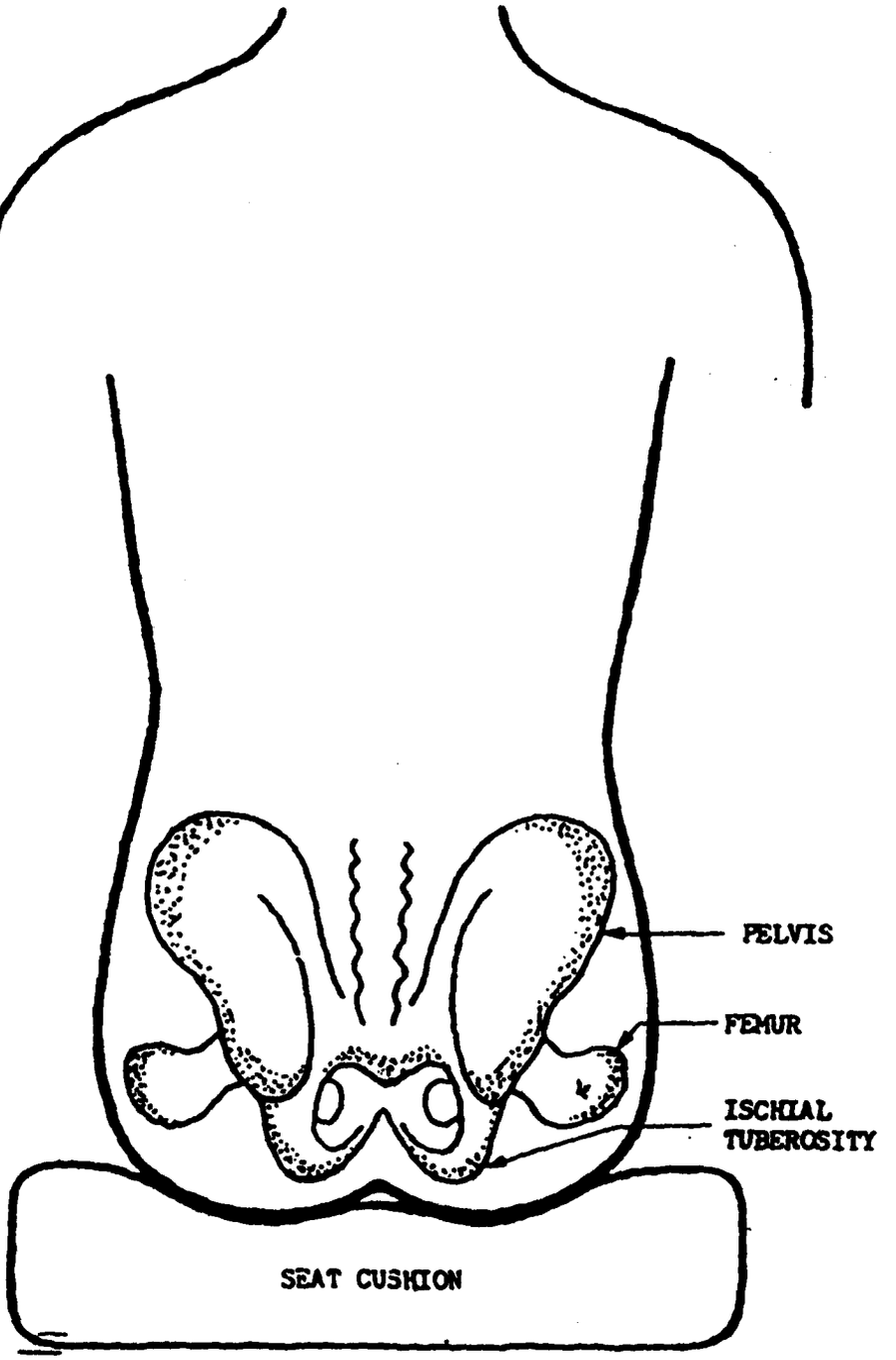

Figure 2.11 Body/Seat Diagram (from Gum, 1970)

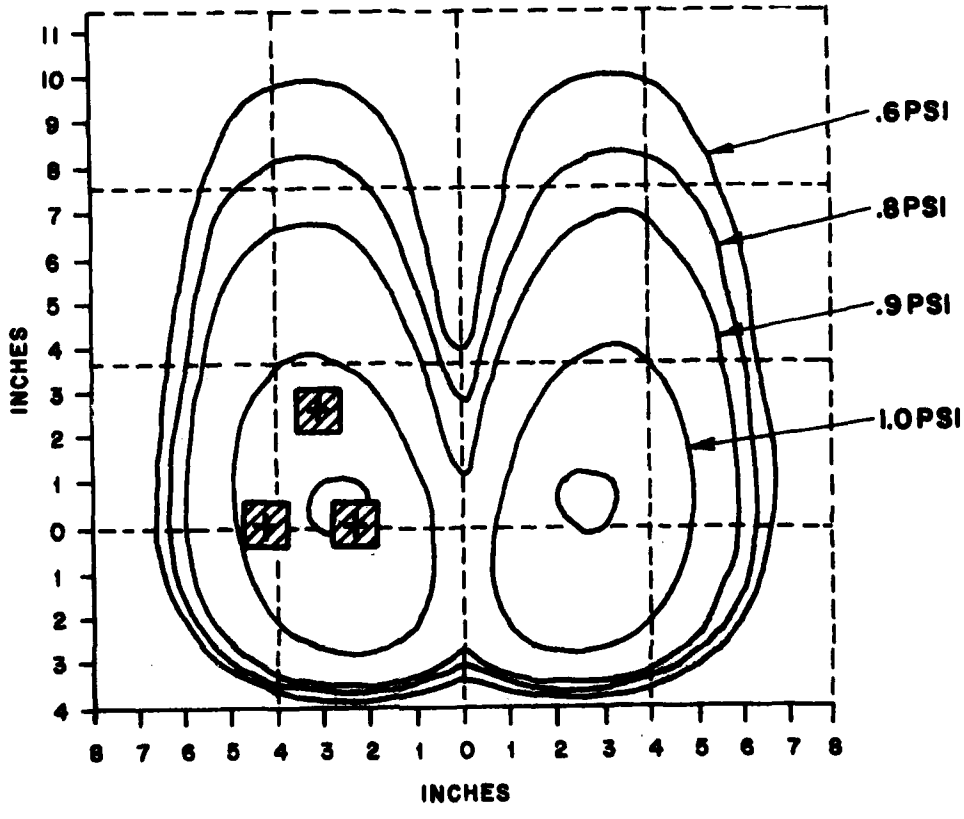

Figure 2.12 Seat Pan Sensor placement with respect to seat pan pressure contour from Kron (1975) after Lay & Fisher (1940)

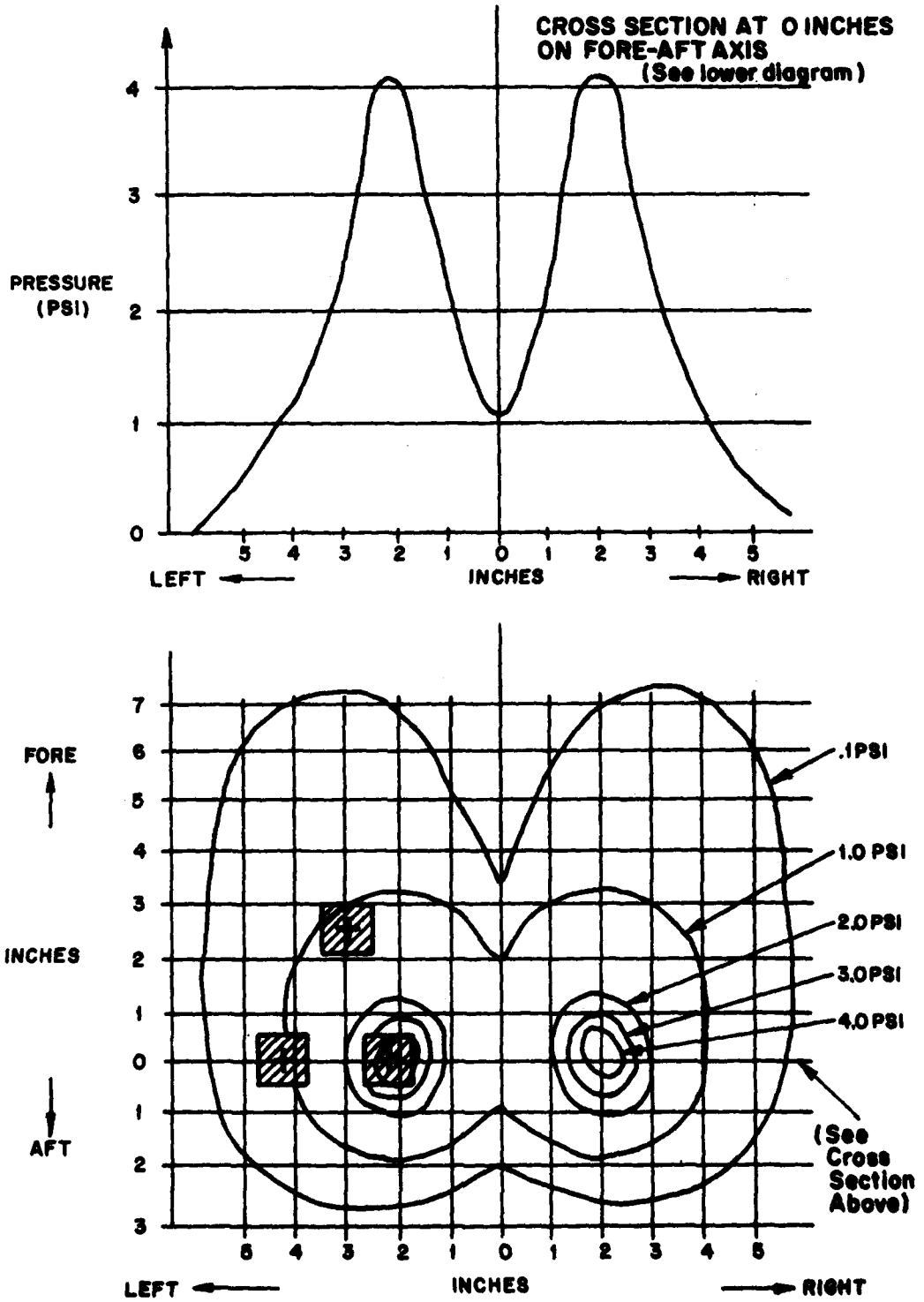

Figure 2.13 Seat Pan Sensor placement with respect to pressure distribution and pressure contours from Gum (1973) after Hertzberg (1955)

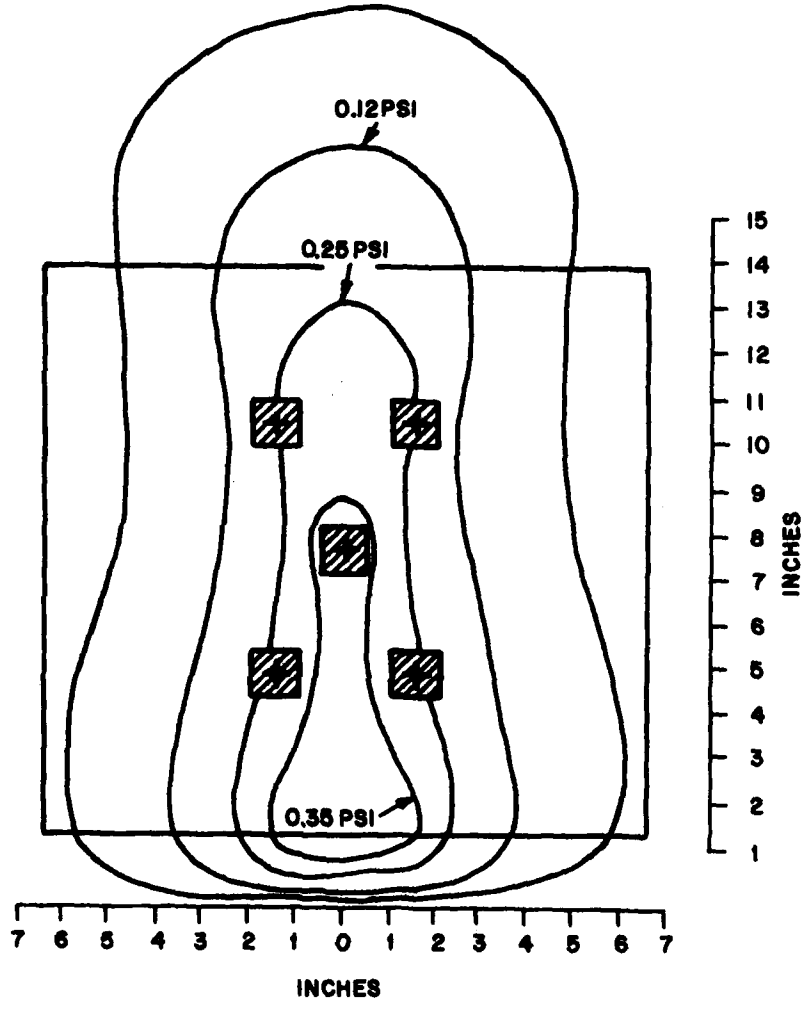

Figure 2.14 Backrest Seat Sensor placement with respect to data from Kron (1975), after Lay and Fisher (1940).

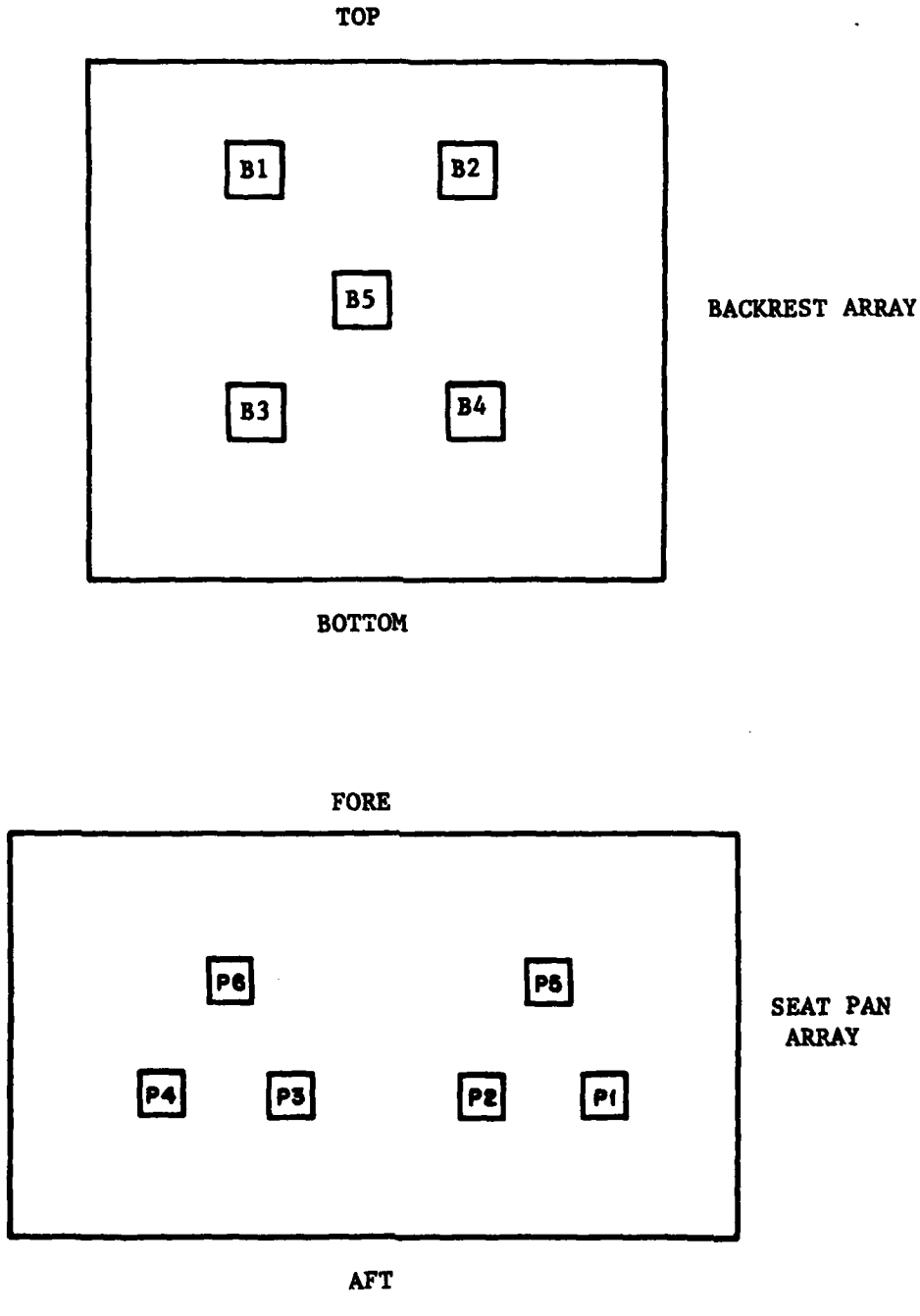

Figure 2.15 Seat Pad Transducer Layout

Each seat-pan array channel was calibrated with respect to pressure by placing known uniform loads over the seat pad area containing the load cell corresponding to that channel. The seat-pan array elements were adjusted for best linearity in the range of .5 to 3 psi, and, at the time of calibration, were precise to ±.15 psi in that range. The backrest elements were optimized in the range of 0 to .75 psi and, at the time of calibration, were precise to ±.075 psi in that range. Allowing for small changes during shipment and installation on TIFS, it is reasonable to assume ±.2 psi and ±.15 psi precision for the seat pan and backrest pads respectively. Note that this does not reflect the performance of the load cells themselves, but rather that of the load cell/cushion combination in response to distributed loads. For meaningful interpretation of data from the seat pads, it is necessary to assume that a soft, flexible surface rests on the pads, and that pressure distributions are approximately uniform over the 1 inch square area of each sensor. Furthermore, the shape and stiffness of this seat cushion must be considered in generalizing the result.

Performance of the seat pads was marked by a significant warm-up drift. The gain (volts/psi) was not affected, but the offset (voltage at 0 psi) of each sensor channel usually followed a roughly exponential curve after power was applied, with a time constant ranging from 10 to 20 minutes and an amplitude ranging from 1% to 50% full scale. The severity of this problem was not realized until experimental flights had begun and was exacerbated by the fact that internal electrical power, being dependent on the aircraft engines, could not be used until just before the start of each flight.

In order to extract maximum information from the data, drift curves were plotted for each sensor after the flights had concluded, and this information was used to correct for the drift. Figure 2.16 is an example showing drift curves for one of the seat pads. Even after making corrections in this way, the absolute static pressure values obtained at the start of each run are uncertain, especially for those runs near the beginning of the flight. However, the excursions from these static values during each brief run can be determined accurately (±.2 psi and ±.15 psi for the seat pan and backrest respectively). The drift problem has since been significantly reduced, although not completely eliminated, by improvements to the preamplification circuit.

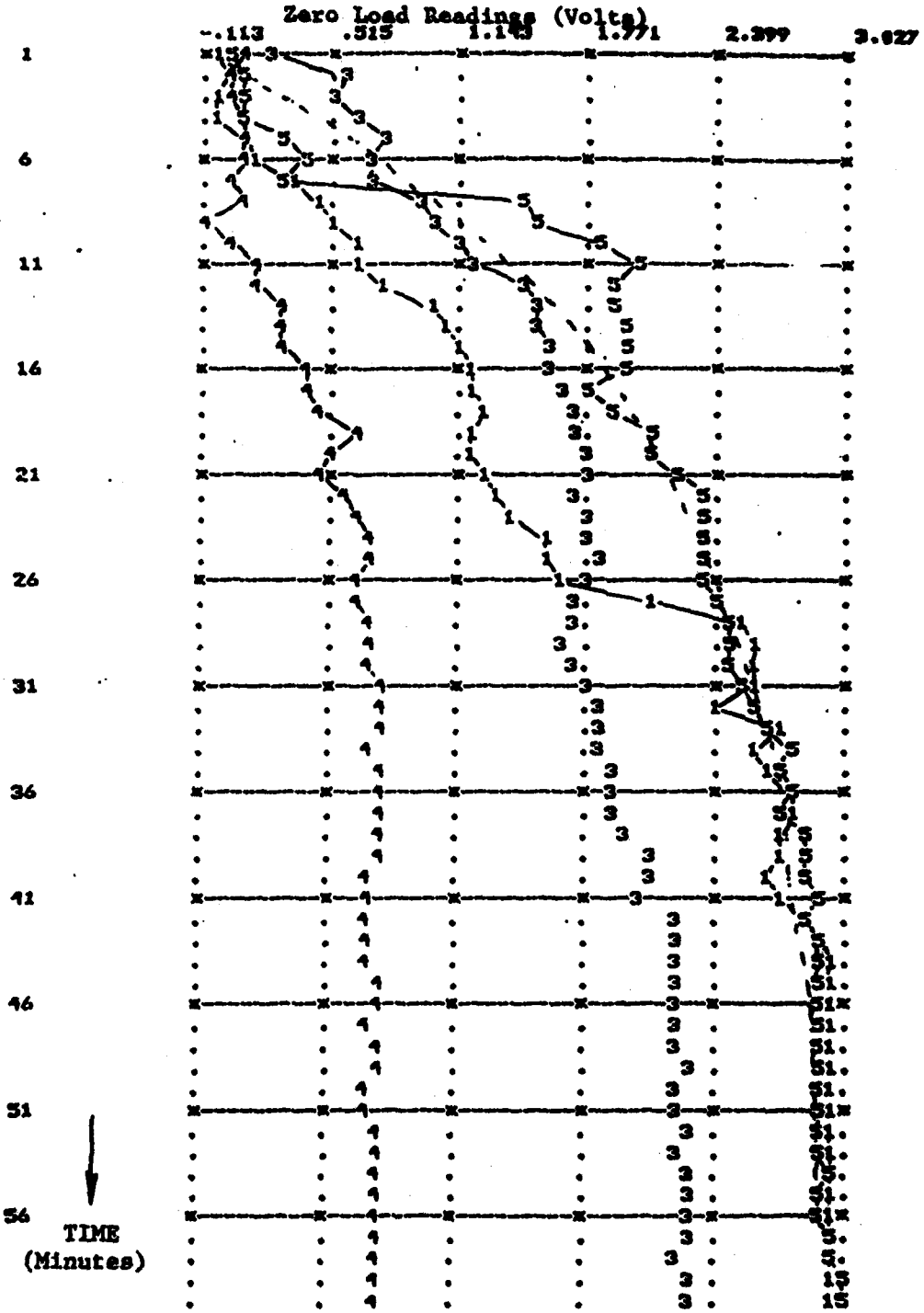

Figure 2.16 Drift Curves for all of the operational right seat backrest sensors are plotted together. Backrest sensor 2 was not functional and is not shown. The dashed line shows and exponential curve with a 15 minute time constant.

2.2.4 Video System

Video cameras were installed behind each seat in the simulation cockpit to record head movement, and the camera field of view as shown in Figure 2.17. The video signals were combined by a screen splitter which accepted only the right half of the right camera field and the left half of the left camera field. A time code generator was used to superimpose a digital time-of-day display on the video image. The resulting combined image was displayed on a monitor at the instrumentation table and recorded on video tape as shown in Figure 2.18. Aircraft intercom conversation and an event mark tone were also recorded on the video tape audio track. The video recordings, made on a Sony Model V01800, are EIJA format compatible.

In order to easily track head position and orientation, each subject wore a helmet liner fitted with two small lightbulbs and powered by a 9 volt battery carried in the flight suit breast pocket. The helmet liner system is diagrammed in Figure 2.19 and can also be seen in Figure 2.20. Video camera f-stop and the helmet lamp intensities were adjusted so that the two position lights were the brightest objects in the video field. The helmet lamp system was designed to allow automatic tracking of the position lights from the video recordings and conversion to digital position versus time data; however, automatic reduction of the video data was not a part of the present study.

2.3 Digital Recording System

All analog data was first passed through a second order prefilter and then sampled and recorded at 100 samples/second. The prefilter, required to reduce aliasing errors, had a corner frequency of 17.5 Hz and a damping ratio of .9. (For a more detailed description of the onboard digital recording apparatus, see Reynolds, et. al., 1972.)

The 58 channels of recorded data are specified on the digital recording list in Appendix B. These include outputs from the seat pressure sensors; output from the pointer/meter device; EMG RMS amplitude and frequency signals; aircraft inertial state; airspeed; and time of day.

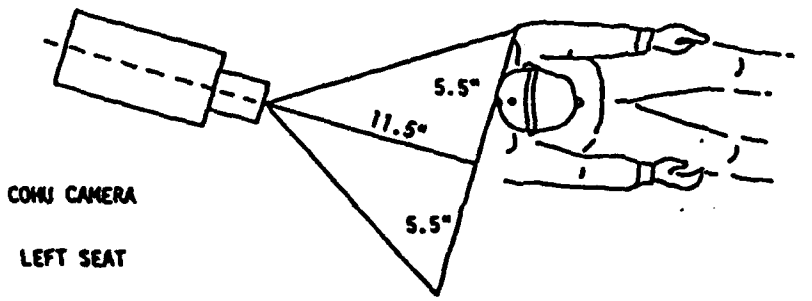

(VIEW FROM TOP)

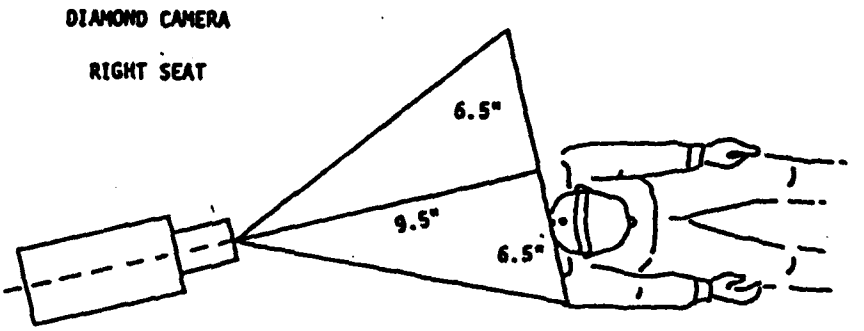

Figure 2.17 TV Camera Field of View

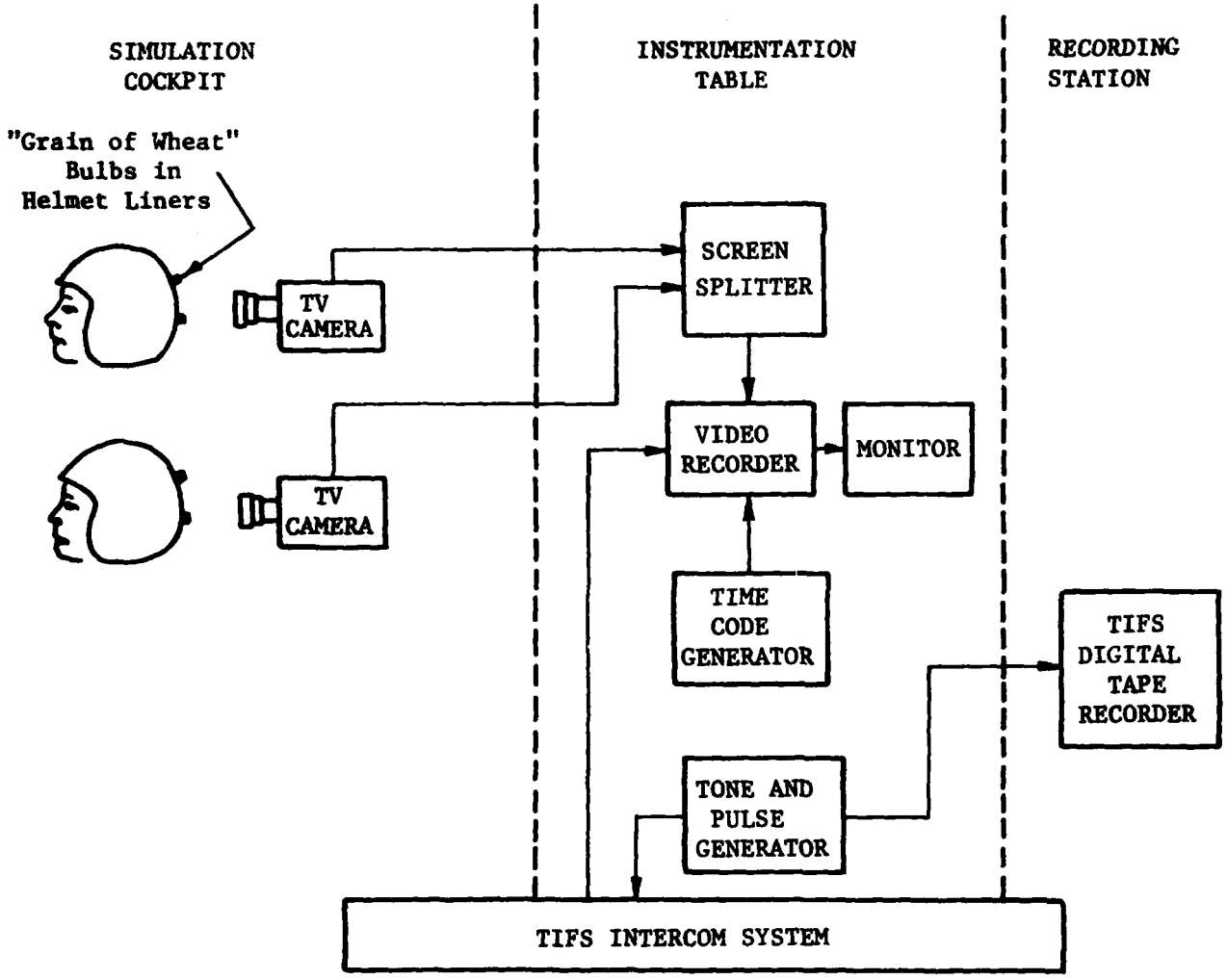

Figure 2.18 Video System Configuration

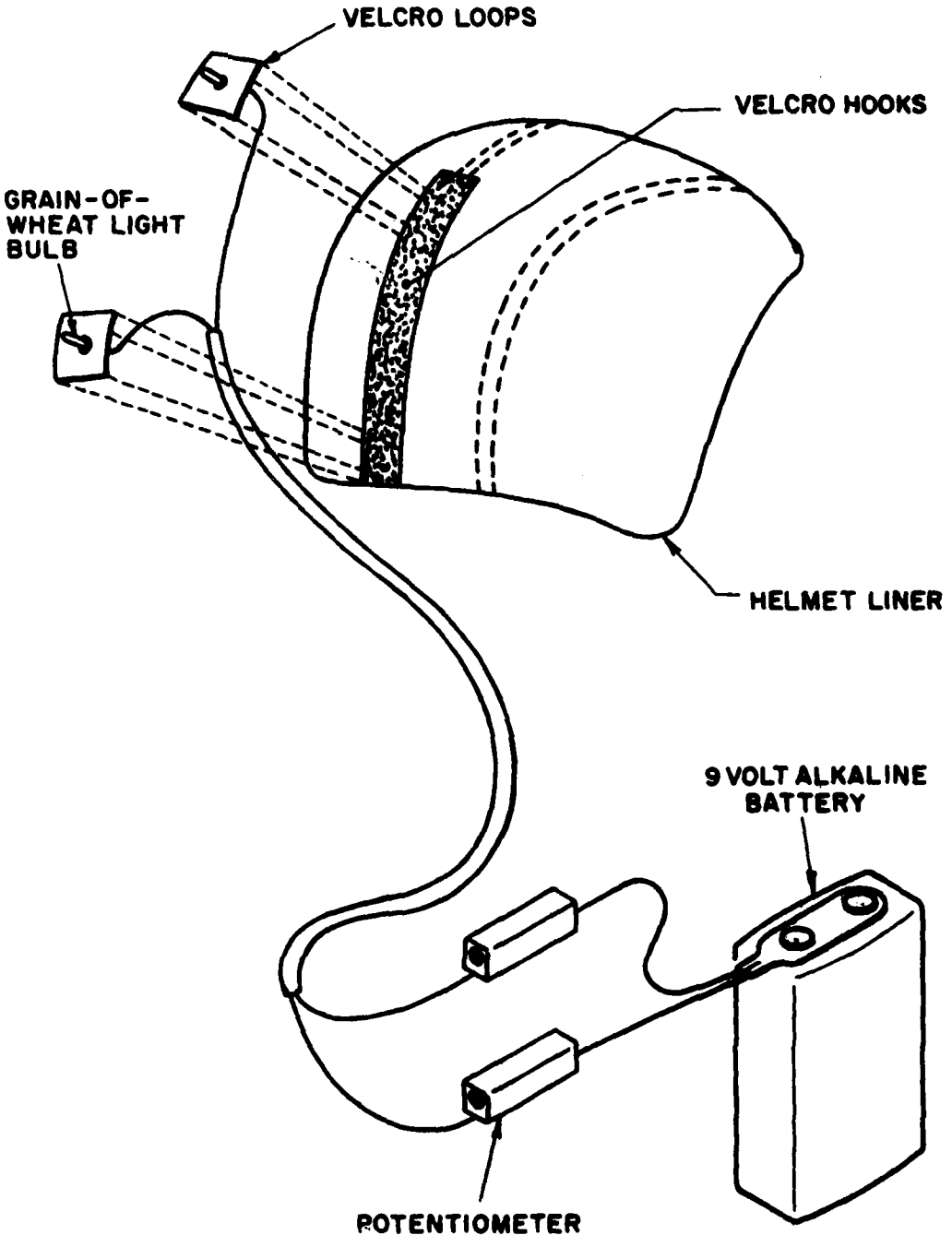

Figure 2.19 Helmet Lamp System (Head Position Lights)

The event mark signal was also recorded both as a pulse on digital tape and as a tone on the video tapes (see Figure 2.18) and was used to synchronize the video and digital data during data analysis.

2.4 Subjects

The left seat subject, sometimes referred to as the pilot subject, was a Calspan test pilot who flew the aircraft from the evaluation cockpit during selected data runs. Since his task required some practice as well as coordination with the command pilots and test engineers, one individual served as the pilot-subject on all flights.

Right seat subjects, sometimes referred to as passive subjects, were selected from a group of Calspan employees who had filled out motion sickness and health questionaires. The questionnaire was used to limit the group to those who were unlikely to become motion sick during the flight and had no medical problems affecting their sense of balance or orientation. Because of potential damage to the pressure sensing seat pads, people weighing over 180 lb. were excluded. An attempt was made to choose people with varying amounts of aircraft experience ranging from test pilots to non-pilots.

The final group consisted of six men and one woman, all between the ages of 20 and 45. They are identified in this report by subject numbers 1 thru 7. Subject 5 was a student pilot, subject 7 was a private pilot instructor and subject 4 was a professional test pilot. Of the remaining four subjects, all of whom were non-pilots, two were engineers, one was a mechanic and one was a secretary.

The health and motion sickness questionnaire is reproduced in Appendix C. Section B of the questionaire is from the MSQ2 form developed by Lentz and Collins (1977) and is scored by assigning numbers 0 through 4 to categories A through E, respectively, and averaging. ("No experience" answers are not included in the average.) Based on the large data sample ($n > 1000$) collected by Lentz and Collins, scores greater than 1.0 indicate far greater than average susceptibility to motion sickness, while scores of less than .01 indicate below average susceptibility. The subjects who participated in this study all scored under .01. An "informed consent" form also reproduced in Appendix C was signed by all subjects.

2.5 Subject Tasks

2.5.1 Left Seat Pilot Subject Tasks

The pilot subject flew the aircraft during selected maneuvers and was a passenger during all other maneuvers. He wore EMG electrodes and a helmet liner containing position lights so that his head motion could be compared to that of the right seat subject. His seat was also equipped with pressure sensing seat pads. It should be noted that even when not flying the aircraft, the left seat subject, unlike the right seat subject, had an out-the-window view, full cockpit instrumentation, and foreknowledge of the maneuver to be performed.

2.5.2 Right Seat Passive Subject Tasks

The right seat subjects also wore EMG neck electrodes, as well as a helmet liner with position lights, and sat on pressure sensing pads. They had no out-the-window view, no access to aircraft instrumentation, and no foreknowledge of maneuvers. Right seat subjects peformed three different tasks during each flight. The tasks, all involving the pointing device and meter described in Section 2.2.1, were each performed during a different part of the flight.

2.5.2.1 Down Tracking Task

During the first part of each flight, the right seat subject used the pointing device to continuously track perceived earth vertical, thus providing a measure of subjective pitch and roll orientation angles. The meter was obscured from the subject's view with a black cover during this phase of the experiment. Instructions to the subject were similar to the following:

> "When you are told to begin tracking, keep your head stationary (avoiding unnecessary head movements), continue to use the seat backrest, and keep your gaze directed at the pointer device. You may operate the device with either hand, rotating it both fore and aft (pitch) and from side to side (roll) by holding either the top or

bottom halves of the pointer rod. You may find it most comfortable to rest your elbow on the armrest as you manipulate the pointer. Your task is to keep the pointer (thin rubber tipped rod) aligned with what you perceive as vertical with respect to the ground. In other words, keep the red tip pointing directly down to the center of the earth and the white tip pointing directly up and away from the ground. The aircraft may undergo various tilting, turning and accelerating motions. Do not try to "out-guess" the experiment. Indicate your "gut" feeling of vertical, even if you can logically deduce that it may be incorrect."

2.5.2.2 Roll Velocity Magnitude Estimation Task

During the second part of each flight, the meter was uncovered (See Figure 2.20) and could be controlled by moving the roll axis of the pointer. The subject's only task was to continuously track the sensation of roll velocity by moving the meter needle to a setting proportional to that velocity. The estimation was made by comparison to a standard rolling motion (modulus) experienced just before each run. The modulus was an uncoordinated 5 degrees/sec roll between left and right 10 degree bank angles. Instructions to the subject were similar to the following:

"Continue, as much as possible, to refrain from changing position in your seat or making unnecessary head motions. Keep your gaze directed at the meter scale. The meter needle can be moved by "rolling" the pointer and will maintain a position proportional to the pointer roll angle. During this part of the experiment, the only purpose of the pointer is to control the meter needle; do not attempt to align the pointer with vertical as you did previously. Try to concentrate on your sensation of roll rate or velocity (roll is rotation about the long axis of the aircraft). You will be given a rolling motion called the 'modulus' and your maximum sensation of roll rate during this motion should correspond to 5 on the meter. Subsequent motions should be rated proportionally; for example, a roll rate that feels twice as fast as the modulus should be 10 on the meter. If you feel that you are rolling to the right your indication should be on the right half of the meter scale and vice versa."

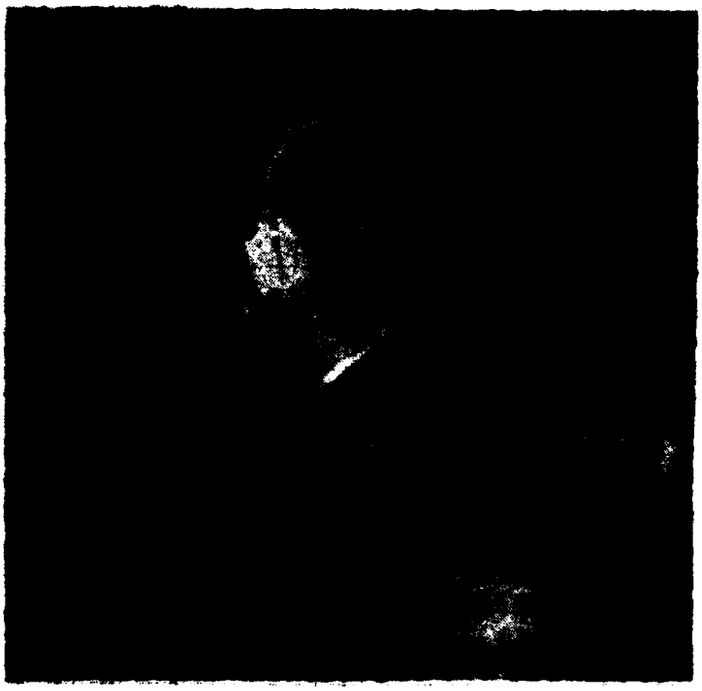

Figure 2.20 Right Seat Station in TIFS evaluation cockpit showing subject wearing helmet liner with position lights.

2.5.2.3 Forward Acceleration Magnitude Estimation

During the last part of each flight, the meter was controlled by fore-aft motion (pitch) of the pointing device and was used by the subject to indicate estimated forward acceleration. Estimates were once again made by comparison to a standard, or modulus, administered before every second run. The modulus was a .1g deceleration. (Instructions to the subjects were the same as for roll-rate estimation, substituting "pointer pitch angle" for references to "pointer roll-angle" and substituting "acceleration" for references to "roll-rate.") Since only two of the seven flights were able to continue long enough to include this part of the protocol, very few data of this type were actually gathered.

2.6 Maneuvers

Six basic maneuvers were used for TIFS data runs:

1. Coordinated turn.
2. Uncoordinated roll.
3. Uncoordinated pitch.
4. Roller coaster (parabolic flight paths)
5. Forward acceleration and deceleration
6. Lateral acceleration.

Many of the maneuvers were flown with several different magnitude variations; these are shown schematically by Figure 2.21.

All but two of the maneuvers result in forces or combinations of forces that are difficult or impossible to produce on the ground. The only exceptions are uncoordinated roll and pitch maneuvers which were used to provide points of comparison with ground base data and to provide a modulus for the roll-rate magnitude estimation task. All data runs began and ended with several seconds of straight-and-level flight. Since most of the runs were controlled from the analog computer, the profiles were

COORDINATED TURN

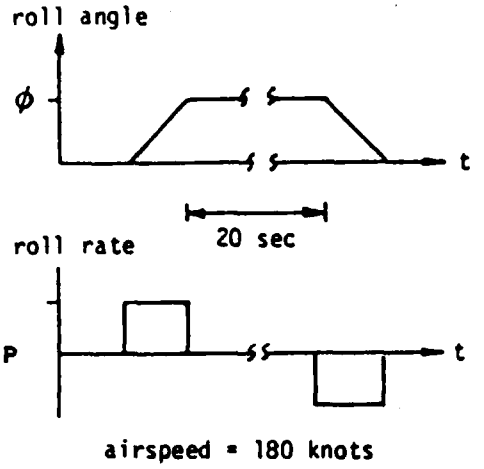

airspeed = 180 knots

6 combinations of ϕ + P

P \ ϕ	10^0	20^0	30^0
3^0/s	X	X	
6^0/s		X	X
10^0/s		X	X

UNCOORDINATED ROLL SEQUENCE

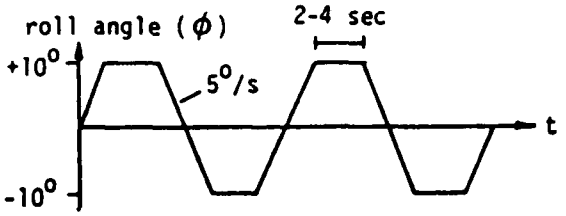

UNCOORDINATED PITCH SEQUENCE

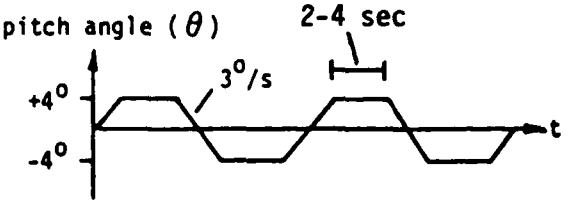

"ROLLER COASTER" SEQUENCE

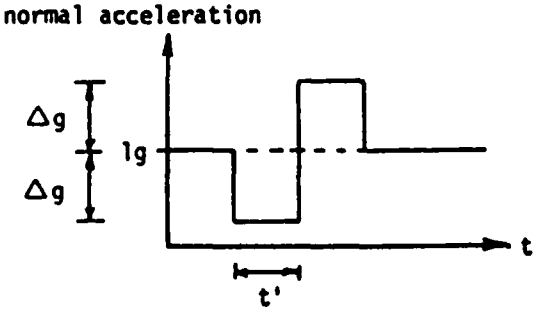

$\Delta g = \begin{cases} \approx 0.9\ g \\ 0.6\ g \\ 0.3\ g \end{cases}$

t' = 7-10 sec

Figure 2.21a Maneuvers

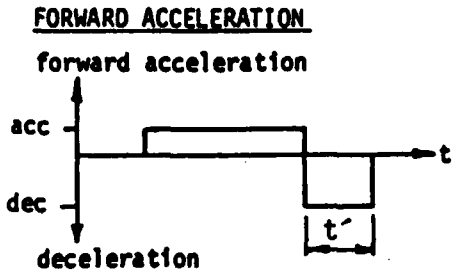

acc = max attainable ($\approx$1 g)

dec = { max attainable ($\approx$.2 g); 1/2 max ($\approx$.1 g); 1/4 max ($\approx$.05 g) }

t' = 7-10 sec

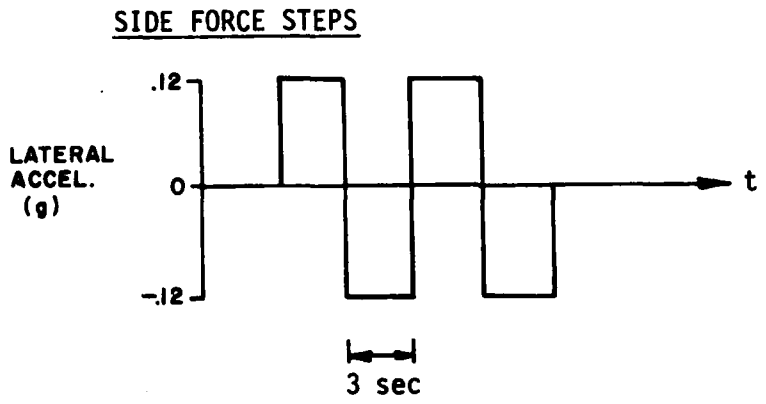

Figure 2.21b Maneuvers

quite repeatable. Implementation details can be found in Dittenhauser (1979). Some selected runs of each maneuver were flown by the pilot subject to obtain active pilot data.

2.6.1 Coordinated Turn

The coordinated turn maneuvers were intended primarily to gather subjective orientation data. Tilting motions during which the subject feels angular velocity, but no change in the direction of specific force, as in a coordinated turn, cannot be easily reproduced on the ground.

As shown in Figure 2.21, six different combinations of bank angle (ϕ) and roll-rate (p) were used, all at a constant 180 knot indicated airspeed.

2.6.2 Uncoordinated Roll

The uncoordinated roll maneuver consisted of a series of 11° banks to both sides during which yaw rate remains zero and side force was $g \sin\phi$, as though a ground base chair were being tilted from side to side. The moveable side force surfaces enable TIFS to perform this rather unusual aircraft maneuver. The purpose of the maneuver was to provide points of comparison with ground base data and to provide a standard or modulus for subjective roll-rate magnitude estimates.

2.6.3 Uncoordinated Pitch

The uncoordinated pitch maneuver was the same as uncoordinated roll except that it was about the pitch axis and had only a 4° excursion in both directions. Its purpose was also as a point of comparison with ground base data.

2.6.4 Roller Coaster

The roller coaster maneuvers produced different levels of z axis specific force by flying parabolic flight paths.

Three different levels were used as shown in Figure 2.21. The motivation for the roller coaster maneuver was to gather body/seat pressure data in response to varying z axis force, and to obtain subjective pitch orientation data in response to z axis force variation.

2.6.5 Forward Acceleration

One level of forward acceleration and three levels of deceleration were used as shown in Figure 2.21. Pitch and roll angles of the aircraft remained nearly unchanged during the forward acceleration sequence. This was the only maneuver that was often flown by the command pilots instead of the computer since it was found to be more expedient and involved little loss of repeatability. The primary purpose of the maneuver was to observe subjective orientation during sustained fore-aft specific force.

2.6.6 Lateral Acceleration

The moveable side force surfaces were used to create pure lateral accelerations of approximately .17g, both to the right and to the left. Acceleration onset was sudden (.3 to .6g/sec) and the accelerations were sustained for 2 to 3 seconds. The purpose of the maneuver was to measure body/seat pressures, head motion, and neck EMG activity under conditions of pure lateral specific force.

2.7 Protocol

Before each flight began, EMG electrodes were applied to both subjects, and the neck muscle EMG signals were calibrated by using a spring scale to apply known lateral forces to each subject's head. The right seat subject performed the down tracking task (see Section 2.5.2.1) for the first part of the flight and data runs were flown in the pseudo-random sequence listed in Table 1. During the second part of the flight, the right seat subject performed the roll rate magnitude estimation task (described in Section 2.5.2.2) and maneuvers were flown in the sequence shown by Table 2. Table 3 shows the maneuver sequence used as the right seat subject performed the acceleration estimation task (described in Section 2.5.2.3) during the

third and last part of the flight.

Approximately one hour was allotted for each flight including takeoff and landing. Minor equipment delays often prevented the protocol from being completed. Thus the three phases of the flight were ordered according to their expected importance and expected data quality.

TABLE I -- SEQUENCE OF MANEUVERS FOR DOWN TRACKING TASK

RUN	MANEUVER
1	Coordinated Turn; 3°/sec, 10°
2	Roller Coaster; .6g
3	Forward Acceleration; .2g
4	Roller Coaster; .3g
5	Uncoordinated Pitch; 3°/sec, 5°
6	Coordinated Turn; 30°, 6°/sec
7	Forward Acceleration; .2 g
8	Uncoordinated Roll; 5°/sec, 10°
9	Coordinated Turn; 10°/sec, 20°
10	Roller Coaster; .9g
11	Coordinated Turn; 3°/sec, 20°
12	Uncoordinated Pitch; 3°/sec, 5°
13	Forward Acceleration; .1g
14	Roller Coaster; .3g
15	Forward Acceleration; .2g
16	Uncoordinated Roll; 5°/sec, 10°
17	Roller Coaster; .9g
18	Coordinated Turn; 10°/sec, 30°
19	Roller Coaster; .6g
20	Coordinated Turn; 6°/sec, 20°

TABLE II -- SEQUENCE OF MANEUVERS FOR ROLL RATE TRACKING TASK

RUN	MANEUVER
1	Uncoordinated Roll; 5°/sec, 10°
2	Uncoordinated Roll; 5°/sec, 10°
3	Coordinated Turn; 3°/sec, 10°
4	Uncoordinated Roll; 5°/sec, 10°
5	Coordinated Turn; 6°/sec, 30°
6	Uncoordinated Roll; 5°/sec, 10°
7	Coordinated Turn; 10°/sec, 20°
8	Uncoordinated Roll; 5°/sec, 10°
9	Uncoordinated Roll; 5°/sec, 10°
10	Uncoordinated Roll; 5°/sec, 10°
11	Coordinated Turn; 3°/sec, 20°
12	Uncoordinated Roll; 5°/sec, 10°
13	Coordinated Turn; 10°/sec, 20°
14	Uncoordinated Roll; 5°/sec, 10°
15	Coordinated Turn; 6°sec, 20°

TABLE III -- SEQUENCE OF MANEUVERS FOR ACCELERATION TRACKING TASK

RUN	MANEUVER
1	Forward Acceleration; .1g
2	Forward Acceleration; .1g
3	Forward Acceleration; .2g
4	Forward Acceleration; .1g
5	Forward Acceleration; .05g
6	Forward Acceleration; .1g
7	Forward Acceleration; .1g
8	Uncoordinated Pitch; 1°/sec, ± 5
9	Forward Acceleration; .05g
10	Forward Acceleration; .1g
11	Forward Acceleration; .2g
12	Forward Acceleration; .1g

3.0 DATA FORMAT

3.1 Digital Data

Fifty-eight channels of data, including signals from the seat pressure pads, pointer/meter device, EMG electrodes, time of day clock, and aircraft inertial package (accelerations, Euler angles, and angular rates) were recorded on the TIFS digital tape system (see Section 2.3). Calspan transferred data from tapes made by the onboard system to multi-file digital tapes. The Air Force Human Resources Laboratory, using computer facilities at Wright-Patterson Air Force Base, plotted data from the multi-file tapes using a large Calcomp plotter.

For each experiment run, all 58 data channels were plotted separately. Every 10th sample was plotted from the 100 sample/sec digital tapes (without further filtering) yielding 10 sample/sec plots. The abscissa of each plot is scaled at 1 inch/sec and the dependent variable on each plot is scaled to utilize the full 2 inch ordinate (i.e., the maximum excursion of the dependent variable during the run corresponds to 2 inches along the ordinate).

Once these Calcomp plots were completed, the Air Force computer facility became unavailable for this project. All data analysis therefore has been performed using only the plots to access the digitally recorded data.

3.2 Video Tapes

Umatic, EIJH format compatible video tapes show the pilot subject and passive subject head position lights on the left and right sides of a split screen picture (see Section 2.2.4) during every run. The video field is dominated by the position lights which appear as bright spots. The head and neck of each subject are only marginally discernible. A digital time code display of hours, minutes, and seconds is superimposed on the video image. The audio channel contains all intercom conversation during each data run as well as a tone actuated by the event mark button and used to synchronize the video and digital data.

3.3 Voice Tapes

All intercom conversation during the flights were recorded by a voice activated system and are preserved on standard audio tape casettes.

4.0 SPATIAL ORIENTATION

4.1 Subjective Role Orientation Results

Subjects in an aircraft who were deprived of visual cues were asked to keep a pointer aligned with earth vertical during coordinated turns and uncoordinated rolling motions. The coordinated turns were flown with bank angles of 10°, 20°, and 30°, and roll rates during roll-in and roll-out of 3°/sec., 6°/sec., and 10°/sec. The subjects were not told what the maneuvers would be. (See Section 2.2.1 for a description of the pointer device and Section 2.5.2.1 for a detailed description of the subject task). By aligning the pointer with perceived earth vertical, each subject, in effect, indicated the subjective tilt with respect to earth vertical.

One of the seven subjects, (No. 3) apparently was unable to master the down tracking task as evidenced by comments to that effect during the flight and seemingly random movements of the pointer. Data from this subject have not been included in the following analysis.

4.1.1 Coordinated Turns

Of the remaining six subjects, all but one responded to coordinated turns by indicating an initial feeling of tilt during roll-in followed by a gradual return toward a feeling of being upright. Roll-out usually produced an illusion of tilt in the opposite direction which then decayed towards zero. The peak magnitudes of the tilting sensations were always much smaller than the actual aircraft bank angle during a steady turn. The profile shown in Figure 4.1 exemplifies this behavior although not all responses conform precisely to the same profile.

Figure 4.2 is a typical response from the only subject (Subject 7) who did not show the same type of response to coordinated turns. Subject 7, a private pilot/instructor, often indicated a subjective bank angle profile with the same shape as the true aircraft profile, but having a much smaller magnitude. The student pilot and test pilot did not differ from the non-pilot subjects in this respect.

Figure 4.3 shows superimposed responses of all subjects to the roll-in part of one coordinated turn profile and Figure 4.4 shows the same subject responses

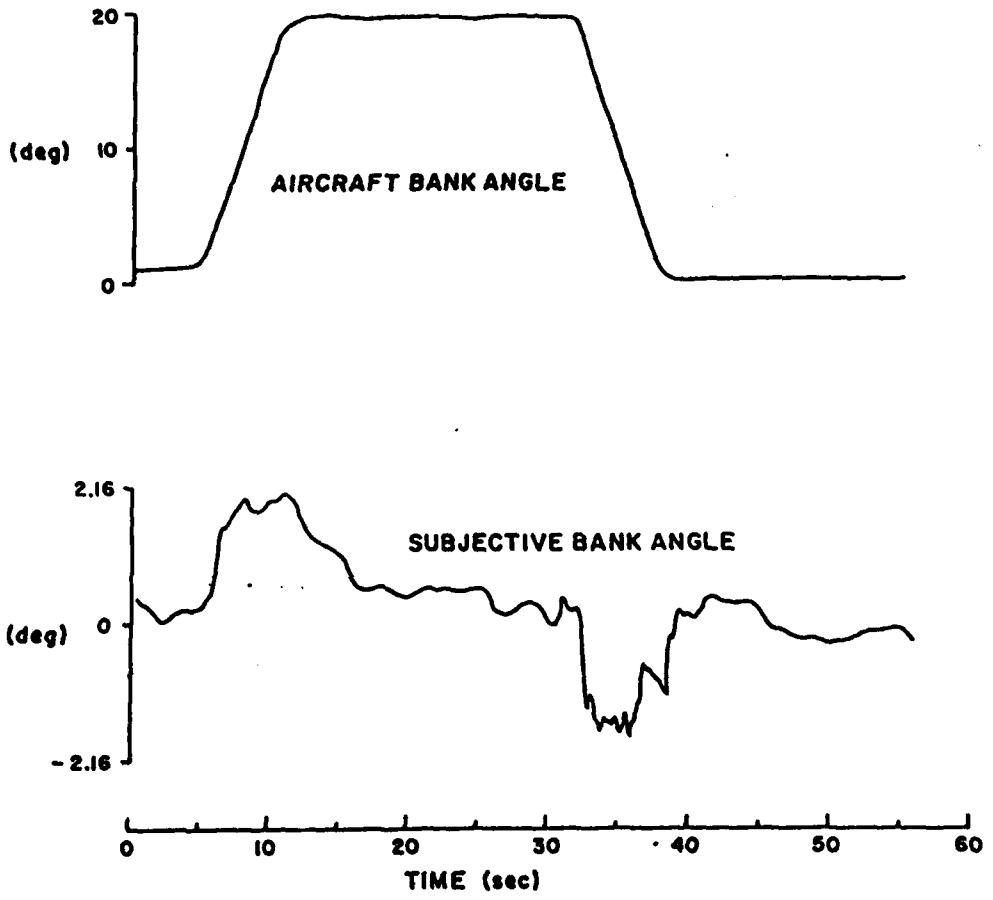

Figure 4.1 Characteristic (typical) bank angle perception during coordinated turn. Initial feeling of tilt during roll-in attenuates during the steady turn.

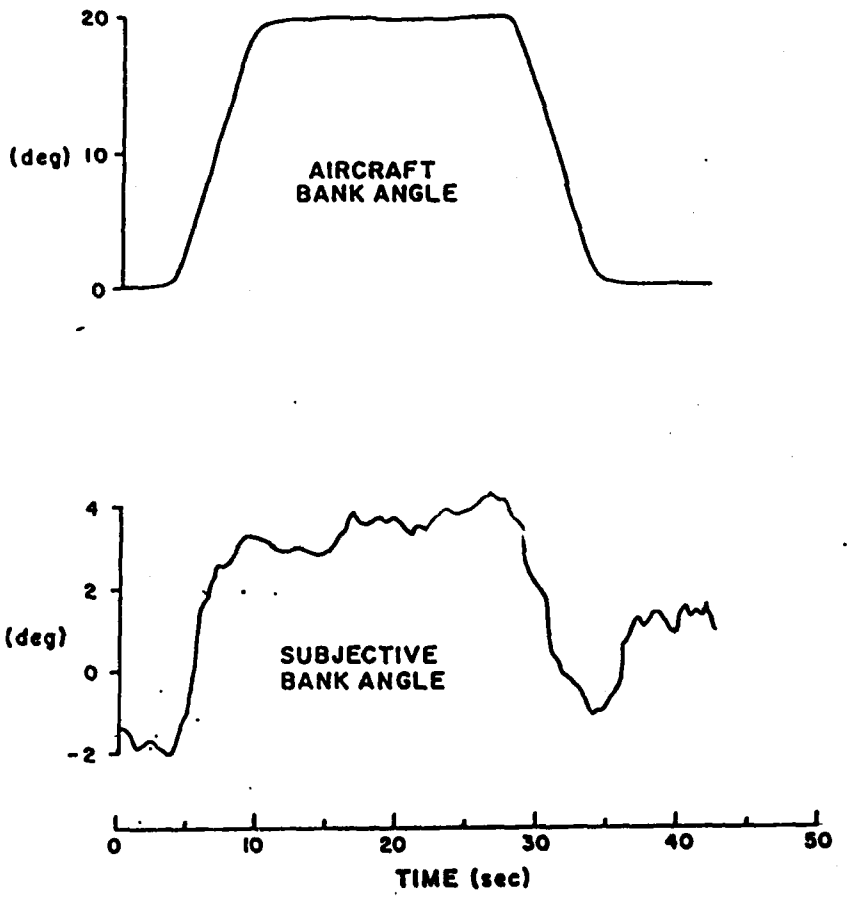

Figure 4.2 Unusual subjective bank angle response during coordinated turn. There is no attenuation of perceived tilt during the steady turn.

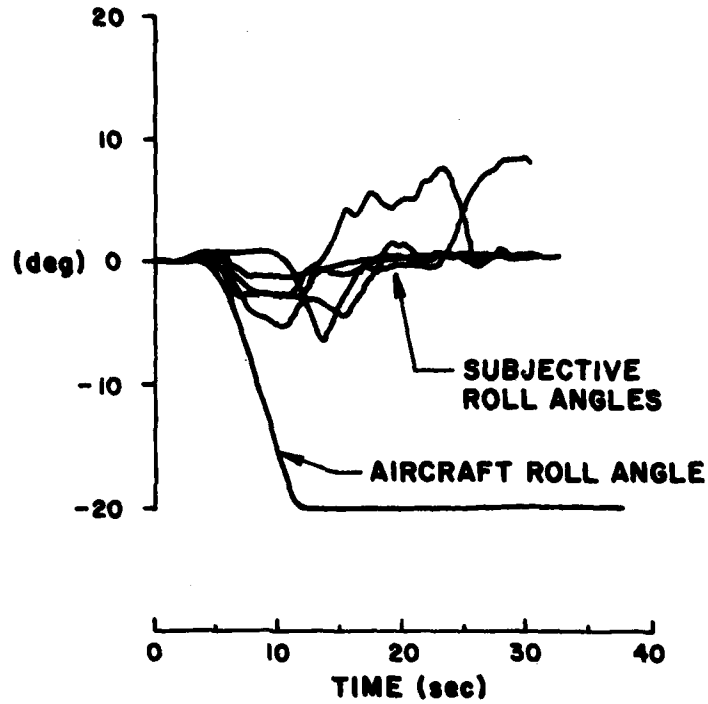

Figure 4.3 Superimposed subjective roll angle responses from five subjects during 20° bank angle, 3°/sec roll-in coordinated turn

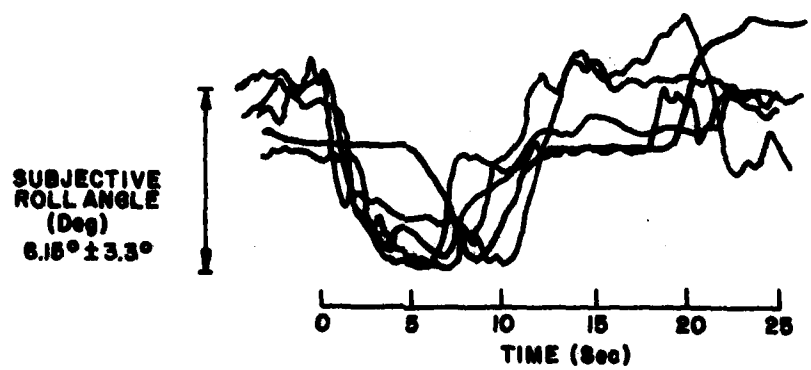

Figure 4.4 Subjective roll angle curves of Figure 4.3, normalized to have the same maximum excursions. (The normalization was done over the entire run, so not all curves have precisely the same excursions during the roll-in portion shown here.)

normalized so that they all have an equal maximum range. The 20°, 3°/sec. turn shown is the one for which the most data runs were successfully recorded.

4.1.2 Uncoordinated Rolls

Uncoordinated rolling motions, resembling the motion of a ground based chair being tilted from side to side, were used as a reference point to the wider data base from ground experiments. All uncoordinated rolls had a magnitude of 11° to each side. Ground based data indicate that in a 1g environment people are able to track the dynamics of their orientation fairly accurately during low frequency rolling motions (Borah, 1976), and this is also demonstrated by the TIFS data. Figure 4.5 shows a typical subjective roll profile in response to uncoordinated aircraft roll.

Steady state perception of a 10° tilt angle in a 1g environment was found by Schöne (1964) to be about 8.5° with a standard deviation of about 1.5°. This is compared, in Figure 4.6 with the data from the TIFS uncoordinated rolls. The TIFS data points were computed by taking the average perceived bank angle over each 3 to 4 second period of constant aircraft bank angle. Subject 3 is not included for reasons previously explained. Responses from other subjects, except for Subject 5, are comparable to the ground base data. Subject 5 data points are over two standard deviations away from both the other TIFS data and ground base data and therefore will be considered "outliers." Subject 5 (student pilot) may simply have an unusually large bias in perceiving tilt. Alternatively, he may have overreacted to side forces that were much larger than those he was used to feeling in a cockpit.

4.1.3 Relation Between Uncoordinated Roll and Coordinated Turn

Figure 4.7 shows the TIFS uncoordinated roll data, ground based tilt perception data from Schöne, and peak subjective roll during TIFS coordinated turns. The TIFS data represent five subjects and excludes subjects 3 and 5 for the reasons previously explained. The uncoordinated roll means and standard deviations were calculated by pooling data points from the five subjects. The amount of coordinated turn data was different for different subjects

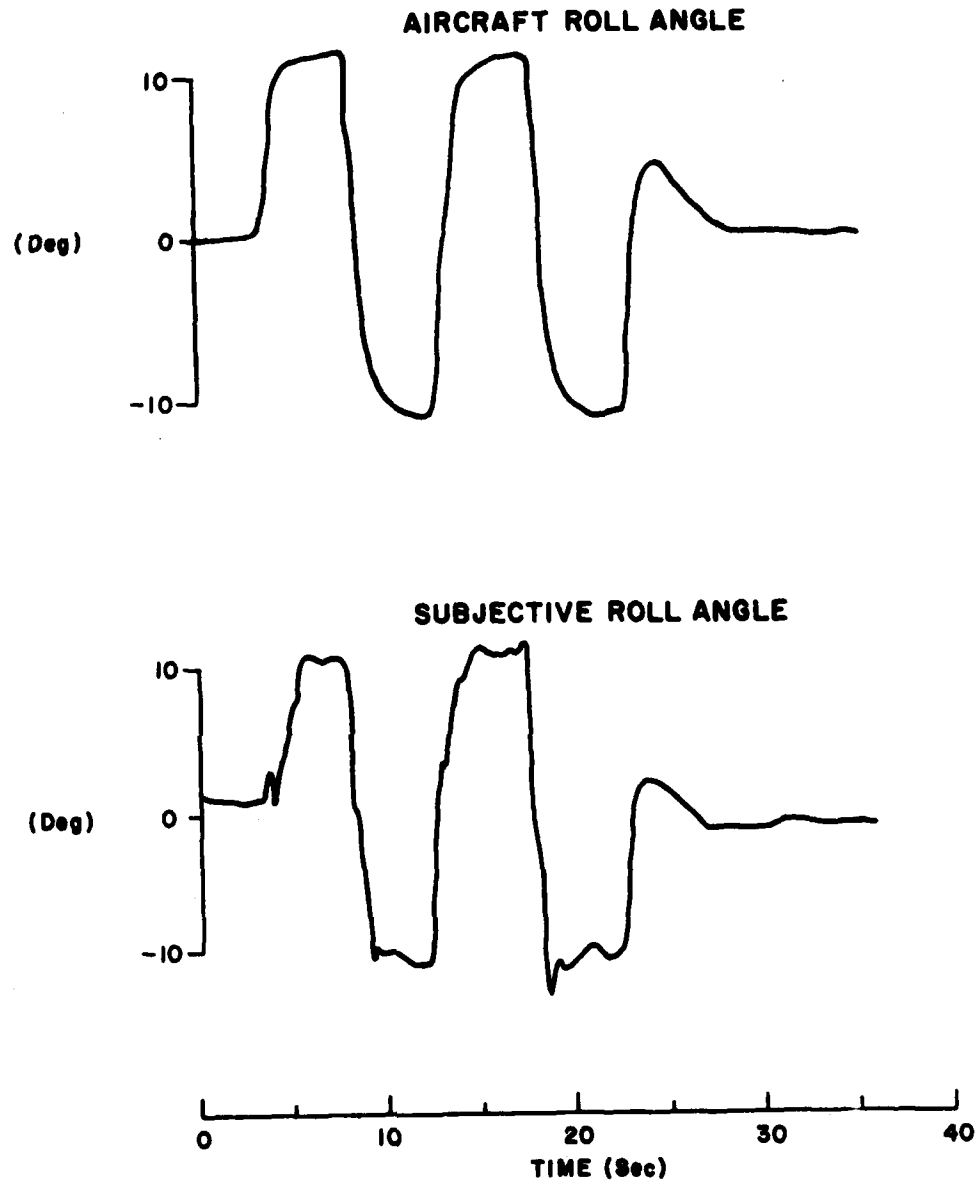

Figure 4.5 Typical subjective roll angle response during uncoordinated roll maneuver.

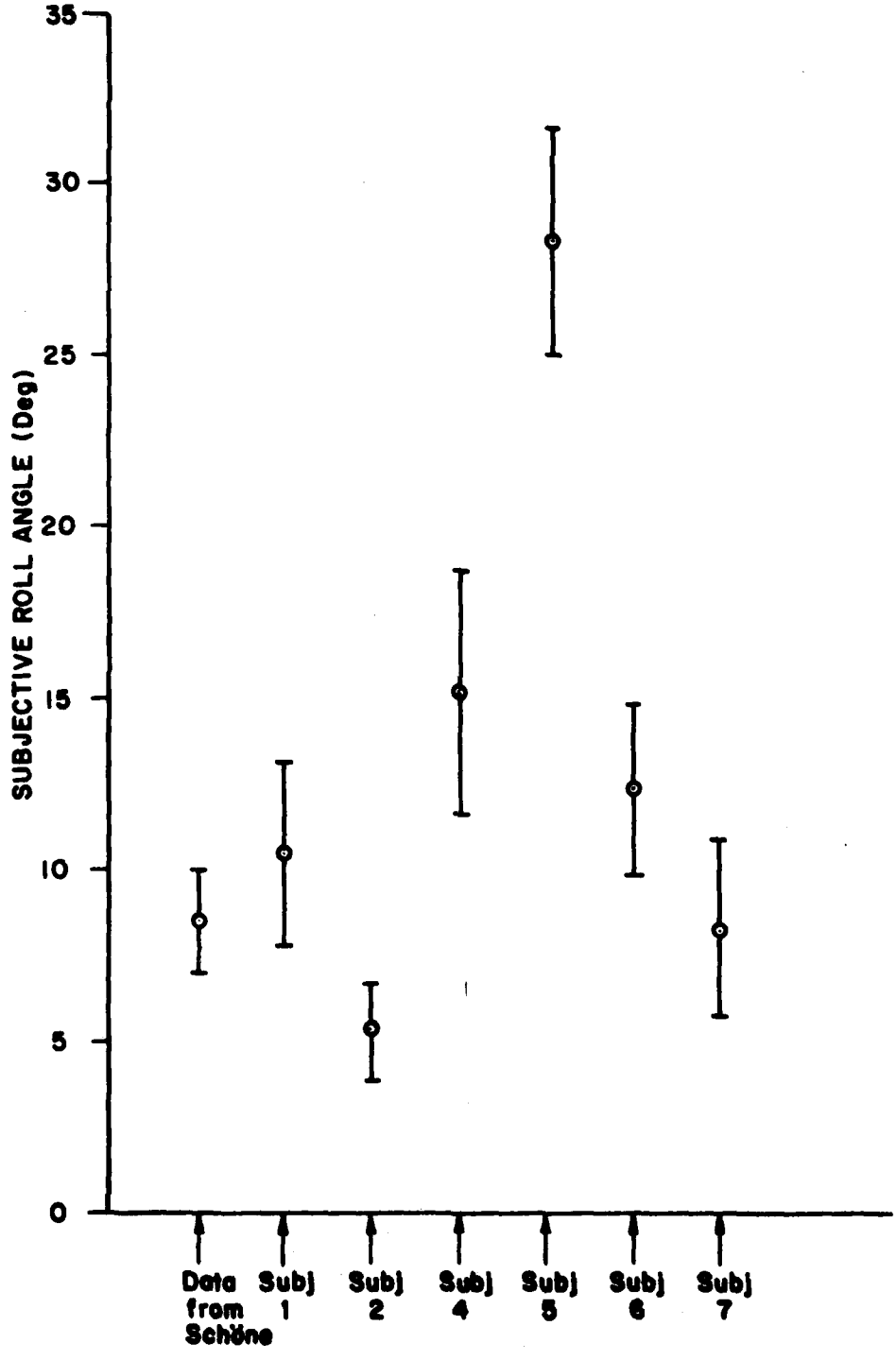

Figure 4.6 Subjective Tilt Angle During 10° Tilt Stimulus

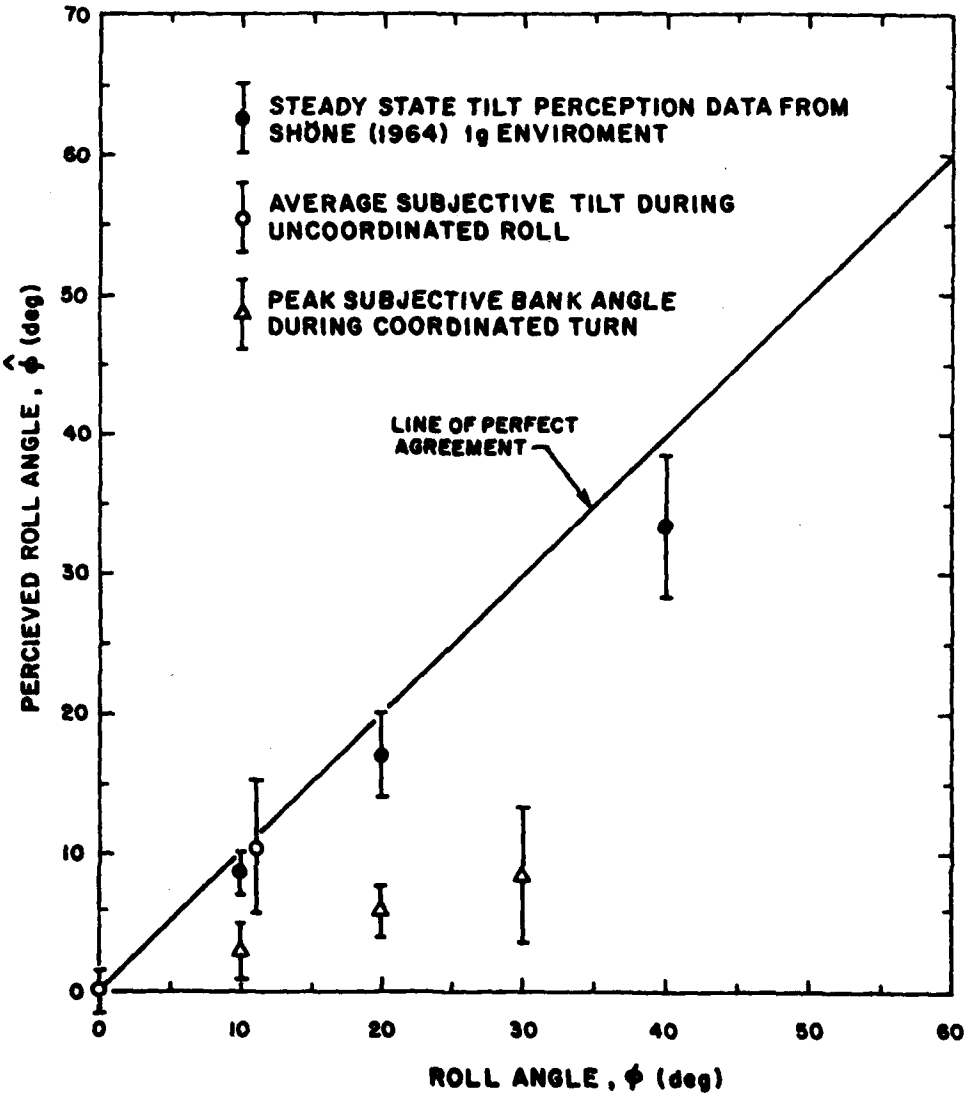

Figure 4.7 Comparison of subjective tilt angles induced by coordinated and uncoordinated roll motion. The Schone data ia for ground based tilts and is comparable to data from the TIFS uncoordinated roll maneuver.

because the digital recorder malfunctioned during several runs. In order to avoid giving unequal weights to different subjects, individual means were calculated for each subject and then were used to caculate the group means shown in Figure 4.7. Since there was no statistical difference between responses to the different roll rates used for coordinated turn roll-in and roll-out, the various roll rates were pooled.

Figure 4.7 clearly shows that when the specific force vector rotates along with the subject as it does in a coordinated turn, even the peak bank angle sensation felt during the rolling motion is substantially smaller than that perceived when the specific force vector is inertially fixed.

4.2 Subjective Roll Velocity Results

During a set of coordinated turns and uncoordinated roll maneuvers, the same group of subjects made continuous magnitude estimates of their roll rate. The task was a standard subjective estimation paradigm in which a person makes estimates by comparison to a standard or modulus. It is based on work by Stevens (1966), Poulton (1968), and others. In this case, estimates were made continuously by controlling an indicator needle. Details of the task and equipment can be found in Section 2.5.2.1 and Section 2.2.1.

A typical subjective response during a coordinated turn is shown in Figure 4.8 and has roughly the same shape as true roll rate. Note that if perceived roll rate were the derivative of perceived bank angle, roll rate perceptions would look like the middle curve in the descriptive illustration of Figure 4.9. In fact, roll rate perception usually resembles the bottom curve of Figure 4.9, and sensations of angular velocity are not really consistent with sensations of orientation angle. For most subjects it appears that an initial perception of tilt during coordinated turn roll-in usually begins to attenuate without any corresponding feeling of angular velocity.

Although subjects seemed able to indicate the profile of their roll rate sensation, they were not consistent in estimating velocity magnitudes. Consistent magnitude estimates of this type usually require some practice on the part of the subject, and practice time was not available during the experiment flights. As a result, it is not

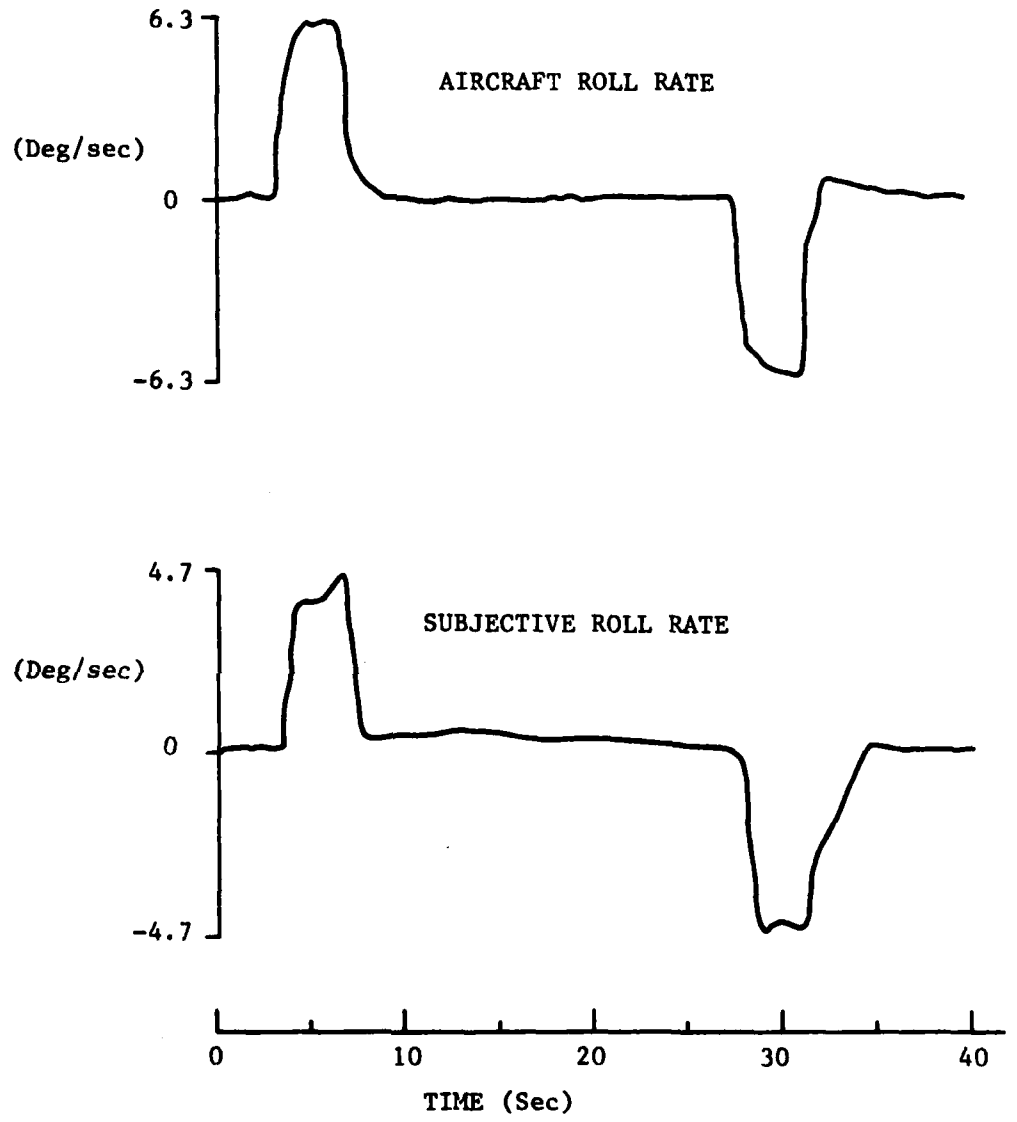

Figure 4.8 Typical roll rate magnitude estimation response during coordinated turn roll-in and roll-out.

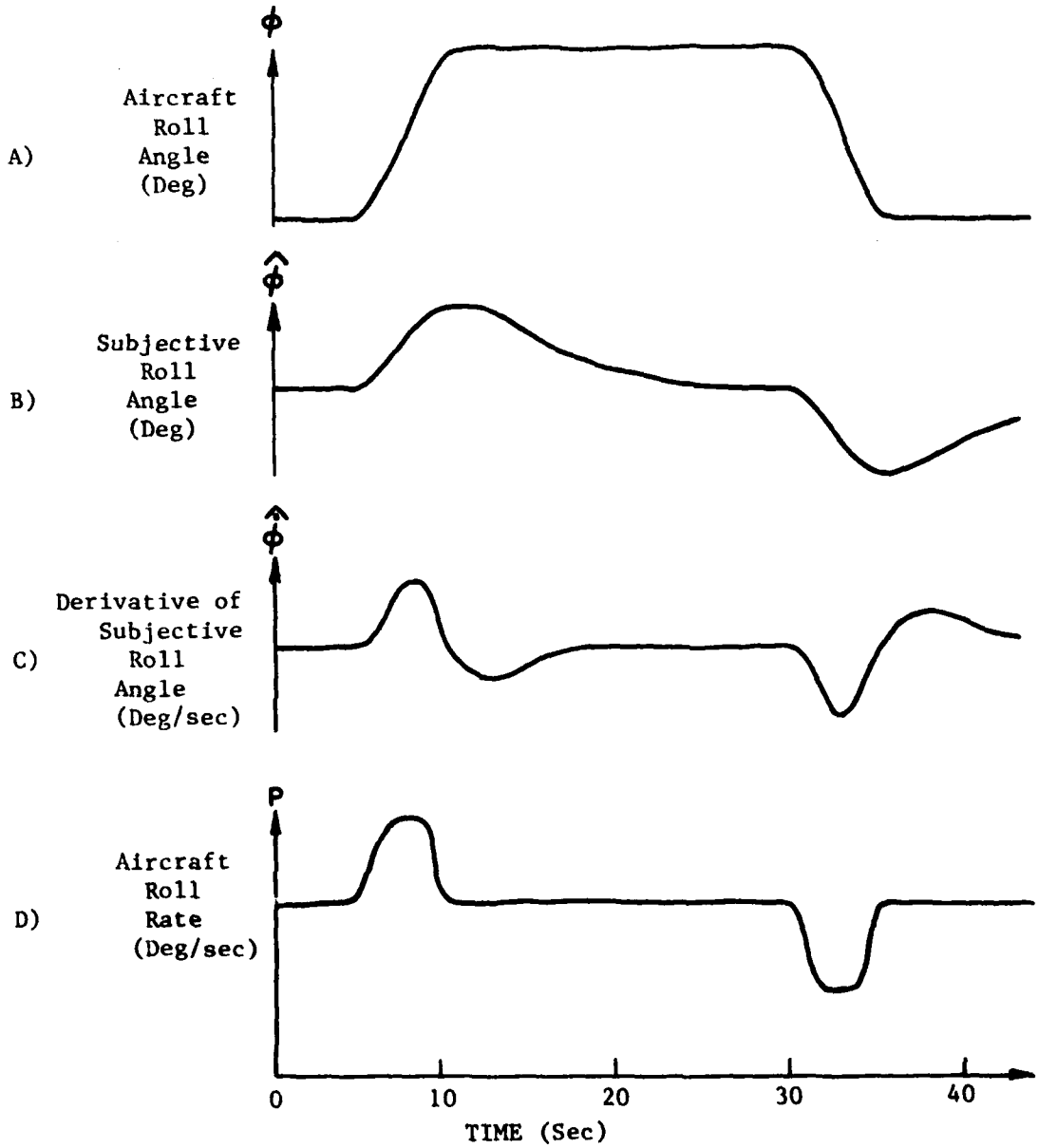

Figure 4.9 Sketch showing the difference between the derivative of subjective roll angle and true aircraft roll angle.

possible to determine the magnitude of perceived roll rates from these data.

4.3 Physiology of Roll Orientation

Although only five subjects were studied extensively, certain generalizations concerning their orientation sensation appear valid. The results described by Sections 4.1 and 4.2 can be summarized as follows:

1. During uncoordinated rolling motions, in the absence of visual cues, subjects indicated fairly accurate perceptions of their orientation and angular velocity profiles.

2. During a coordinated turn, in the absence of visual cues, most subjects felt an attenuated initial tilt sensation during roll-in which gradually decayed and was followed by an illusion of tilt in the opposite direction during roll-out.

3. Feelings of roll angular velocity, during the coordinated turn, matched the aircraft angular velocity profile rather than the derivative of roll orientation perception.

These results are a logical consequence of vestibular system dynamics. The vestibular sensors, which form the body's "inertial guidance system," are located in the non-auditory labyrinthine structure within in each inner ear. The semicircular canals are the rotation sensing component of the vestibular system and respond to angular acceleration as would a heavily damped torsion pendulum with some additional rate sensitivity and adaptation (Young & Oman, 1969; Goldberg & Fernandez, 1971; Ormsby, 1974; Young, 1974). Over frequencies from 0.1 Hz to 1 Hz, semicircular canal output resembles an angular velocity signal, and in fact the semicircular canals seem to be used by the central nervous system as high frequency rate indicators. The otolith organs, which form the other component of the vestibular system, sense gravito-inertial force much like linear accelerometers (Fernandez & Goldberg, 1976; Young & Meiry, 1968).

The semicircular canals signal angular velocity and cause a feeling of tilt during roll-in to a coordinated turn, but provide no steady state information during the steady turn. Otolith organs, on the other hand, continue to

indicate a cockpit-vertical specific force vector which, in the absence of new canal or visual information, is gradually accepted by the central nervous system as "down"; thus, there is a gradual return to a feeling of being upright. Roll-out from the turn causes a similar phenomenon in the opposite direction.

When tilting motions are not "coordinated" and the specific force vector remains aligned with gravity, the otoliths are able to detect steady state tilt. People can sense their orientation fairly accurately under these conditions so long as the tilts are relatively small. As roll angles increase from 10° to 90°, in a 1g environment, people do tend to underestimate their orientation angle by larger and larger amounts. This phenomenon, whose physiological cause is still a subject of research, is called the Aubert effect and can be seen from the Schöne (1964) data in Figure 4.7. Predictions from a previously developed model of the human motion and orientation sensing mechanisms are compared to the experimental data in Section 7.0.

4.4 Subjective Pitch Orientation

In addition to the coordinated turns and uncoordinated rolls discussed in the previous two sections, the same subjects were exposed to uncoordinated pitching motions, roller coaster type motions which produced varying z axis forces, and fore-aft accelerations (See Section 2.6 for details). The subjects had no visual cues during these maneuvers and had the task of keeping an instrumented pointer aligned with what they perceived as earth vertical. Since the pointer was a two degree-of-freedom device, the results indicate perceived pitch as well as perceived roll orientation.

Because the pointer was located directly in front of the subject, visual pitch alignment involved some depth perception and was a more difficult task than was roll alignment. This probably accounts for the greater variance in the pitch data. Figure 4.10 is an example of a typical subjective response to uncoordinated pitch, a motion comparable to that of a ground based rocking chair. Average subjective pitch during the 4 seconds of 4° sustained aircraft pitch angle was 4.12° with a standard deviation of 3.6°. Data from Subject 3, who had a great deal of trouble with the tracking task, have again been excluded. Ground based experiments indicate fairly accurate perception of

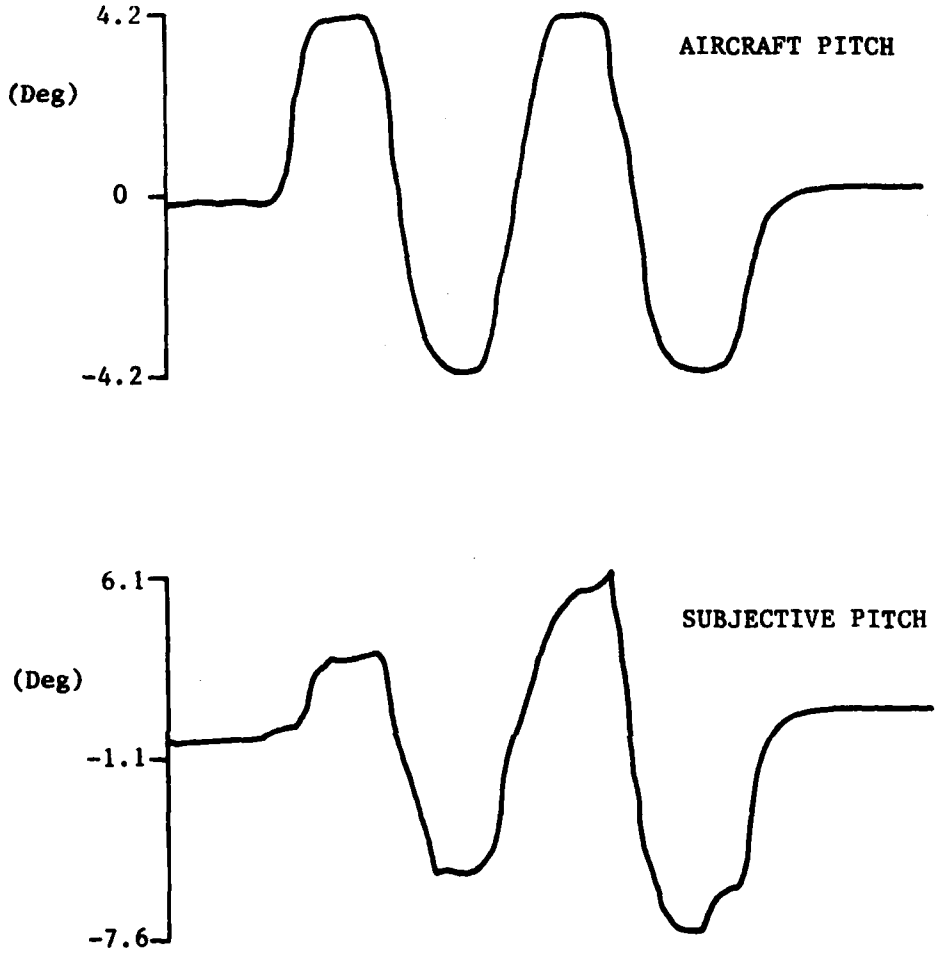

Figure 4.10 Example of subjective response to uncoordinated pitch. Aircraft pitch angle in nominal trim condition (at beginning and end of run) is taken as zero and average perceived pitch during the same periods is also taken as zero.

small pitch angles in a 1g environment (Schöne, 1964).

During coordinated turns, a component of the turn rate falls along the aircraft pitch axis because the aircraft is banked. Specifically,

$$Q = \dot{\psi} \sin \phi$$

where Q is angular velocity about the pitch axis, $\dot{\psi}$ is turn rate, and ϕ is bank angle. The human semicircular canals can sense Q and will signal a pitch axis angular velocity during the turn, so a subjective perception of pitch-up might be expected.

Using the criterion of a monotonic increase in subjective pitch during the first 10 to 20 seconds of the turn, followed by a monotonic decrease after roll-out; 50% of the TIFS data follow a similar profile. Because of the large variance in the pitch data however, the existence of a pitch-up illusion during coordinated turns (in the absence of visual cues), can neither be rejected nor accepted conclusively. This issue is discussed further in Chapter 7.

5.0 HEAD/NECK SYSTEM RESPONSE TO LATERAL ACCELERATION

The head/neck system biodynamics may be thought of as an inverted pendulum balanced on the body trunk with the aid of neck muscles and may provide an important spatial orientation cue. Proprioceptive signals provide cues about the inertial environment by signalling head position with respect to the torso and the required neck muscle tension. Some theoretical modeling work has been done concerning this mechanism, and aircraft simulator designers have considered devices to simulate head forces. To the authors' knowledge, no such mechanisms have been implemented. Some experimental data are available concerning the biomechanics of the head/neck system in response to fore-aft accelerations (Schneider, Bowman, & Peck, 1976) but very little is available concerning side forces. Although neck muscle EMG signals have been investigated for possible use in controlling prosthetic devices (Von Renner, 1970), there is a paucity of literature describing neck muscle EMG activity as an individual responds to vehicle accelerations and tilts.

Head motions, as well as EMG neck muscle signals were monitored in the TIFS during rolling motions and side accelerations in order to begin to fill this data gap. The data are needed to validate or improve parts of a multi-cue perception model recently developed (see Section 7.0), and to aid in the development of aircraft simulator cueing devices. The amount of adequate EMG data gathered was limited, but perhaps quite valuable. A great deal of head motion data was gathered on video tape, however only partial analysis of the video data was possible as part of this study.

5.1 EMG Activity

The EMG pulses are electrical signals generated by nerves to stimulate muscle contractions. Raw EMG signals, measured at the skin surface, resembled the output of a noise generator. It has been shown that integrated EMG activity varies monotonically with muscle tension (Bigland, Lippold, & Wrench, 1959; Von Renner, 1970). The frequency of EMG pulses is also related to muscle tension but in a much more complex manner.

EMG electrodes were placed over the sternocleido-mastoideus muscles on either side of the neck during aircraft uncoordinated roll and side acceleration

maneuvers. The uncoordinated roll is an aircraft roll not accompanied by any turning and therefore leaving the specific force vector aligned with gravity. It is much like tilting a ground based chair from side to side. The side force acceleration maneuver is a pure lateral acceleration produced by the special side force control surfaces on TIFS (see Section 2.6 for a detailed description of the maneuvers). A pilot subject, who had instrument as well as visual cues and who sometimes controlled the aircraft, was monitored in this way as were the seven passive subjects, who had no visual cues. Each EMG signal was processed to produce one signal proportional to RMS amplitude and another proportional to EMG frequency (See Section 2.2.2 for details). Because of its more straightforward relation to muscle tension, only the RMS amplitude data are used in the subsequent analysis. EMG signals were calibrated before each flight by asking subjects to resist lateral pull on a headband at about ear level, and comparing the EMG signal with the lateral force measured on a spring scale.

Outputs from the EMG RMS and frequency circuits were much more noisy during the experimental flights than they had been in the lab, probably due to a noisy environment in the aircraft and high temperatures which caused the subjects to sweat. The noise level varied from subject to subject, with softer, less calloused skin usually yielding better conduction (lower noise). For many subjects, background noise obscured all but the most extreme neck muscle tension. Only Subject 3 showed an EMG response during uncoordinated rolling motions that is consistently distinguishable from background noise. This subject's EMG responses to lateral acceleration are also the only data of good enough quality for really meaningful comparison with the muscle tension predicted by head/neck system models. The subsequent discussion is based almost entirely on data from Subject 3 and from the pilot subject who often (but not always) showed EMG responses distinguishable from background noise.

Figures 5.1 and 5.2 show calibration curves computed for passive Subject 3 and the pilot subject. Figure 5.3 shows integrated EMG response (RMS circuit) of Subject 3 during the side acceleration maneuver. This response is compared to the response of a head/neck system model in Section 7.0. The scale on the right side of the specific force profile approximates the equivalent side force acting laterally on the head, under the assumption that the head weighs 10 lb. (Gum, 1973). Figure 5.3 shows activity only in the neck muscle which must be contracted to counteract

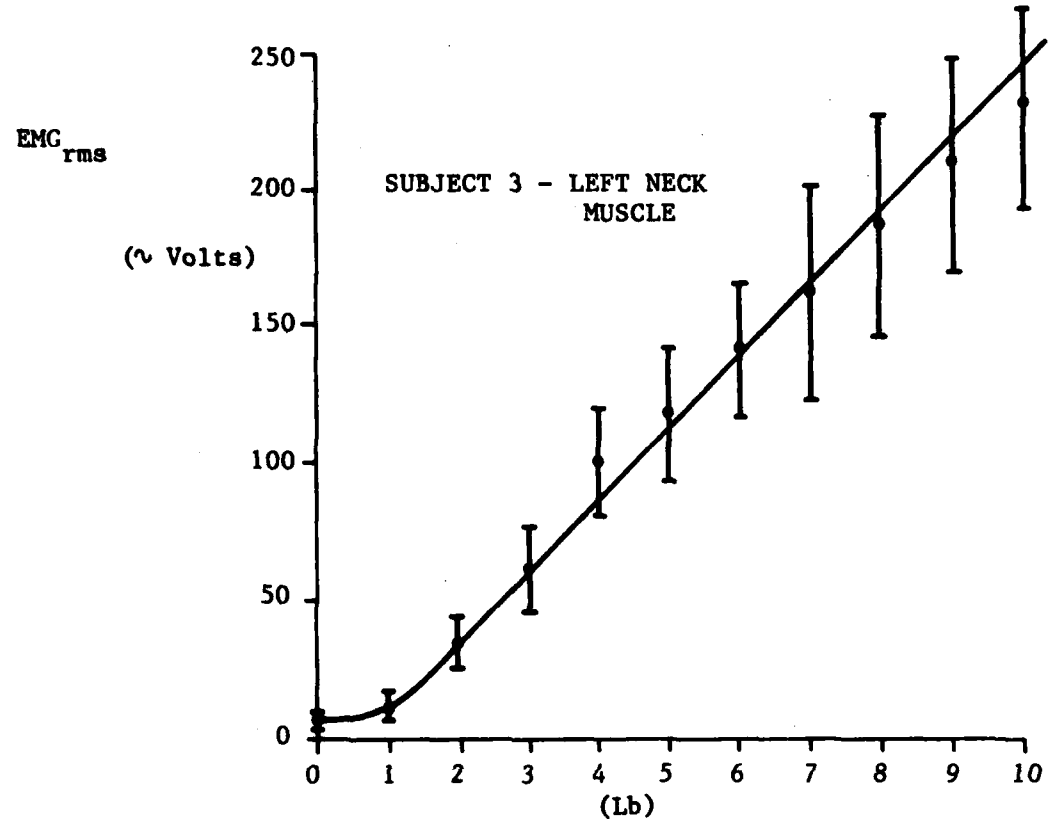

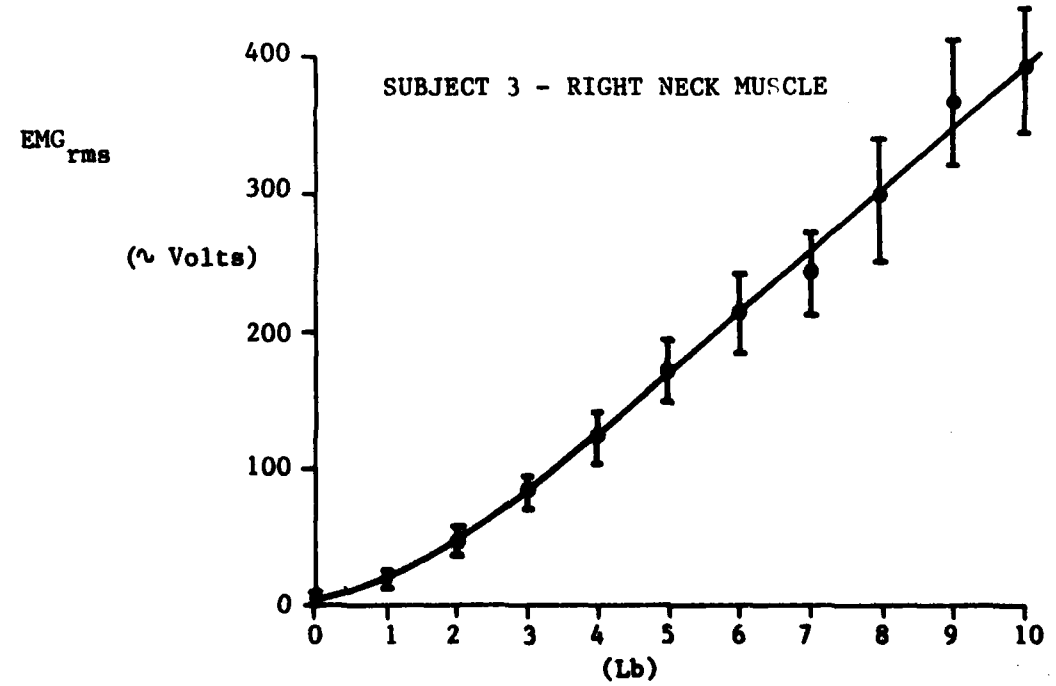

Figure 5.1 Calibrated EMG Signal (rms magnitude) for Subject 3

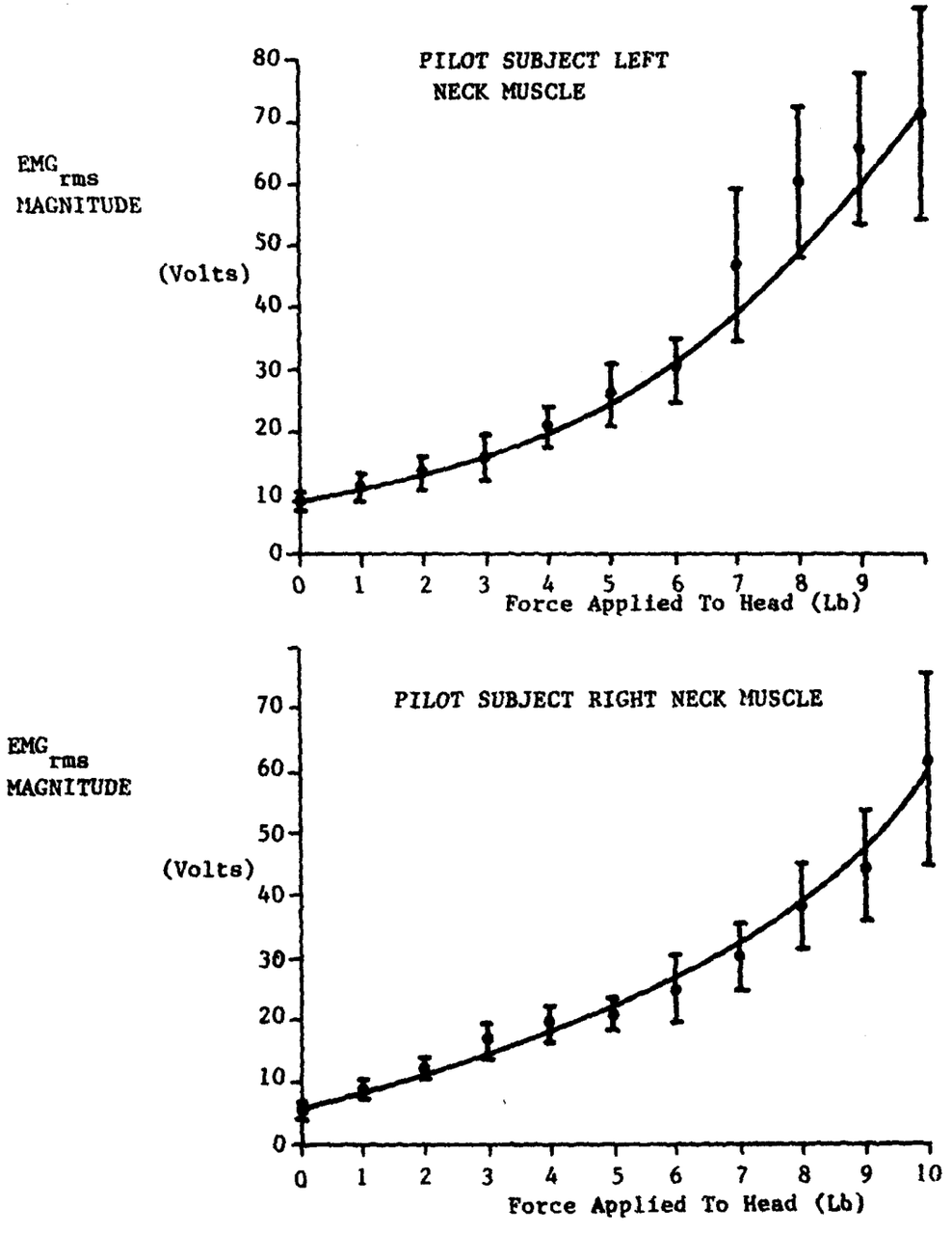

Figure 5.2 Calibrated EMG Signal (rms magnitude) for pilot subject.

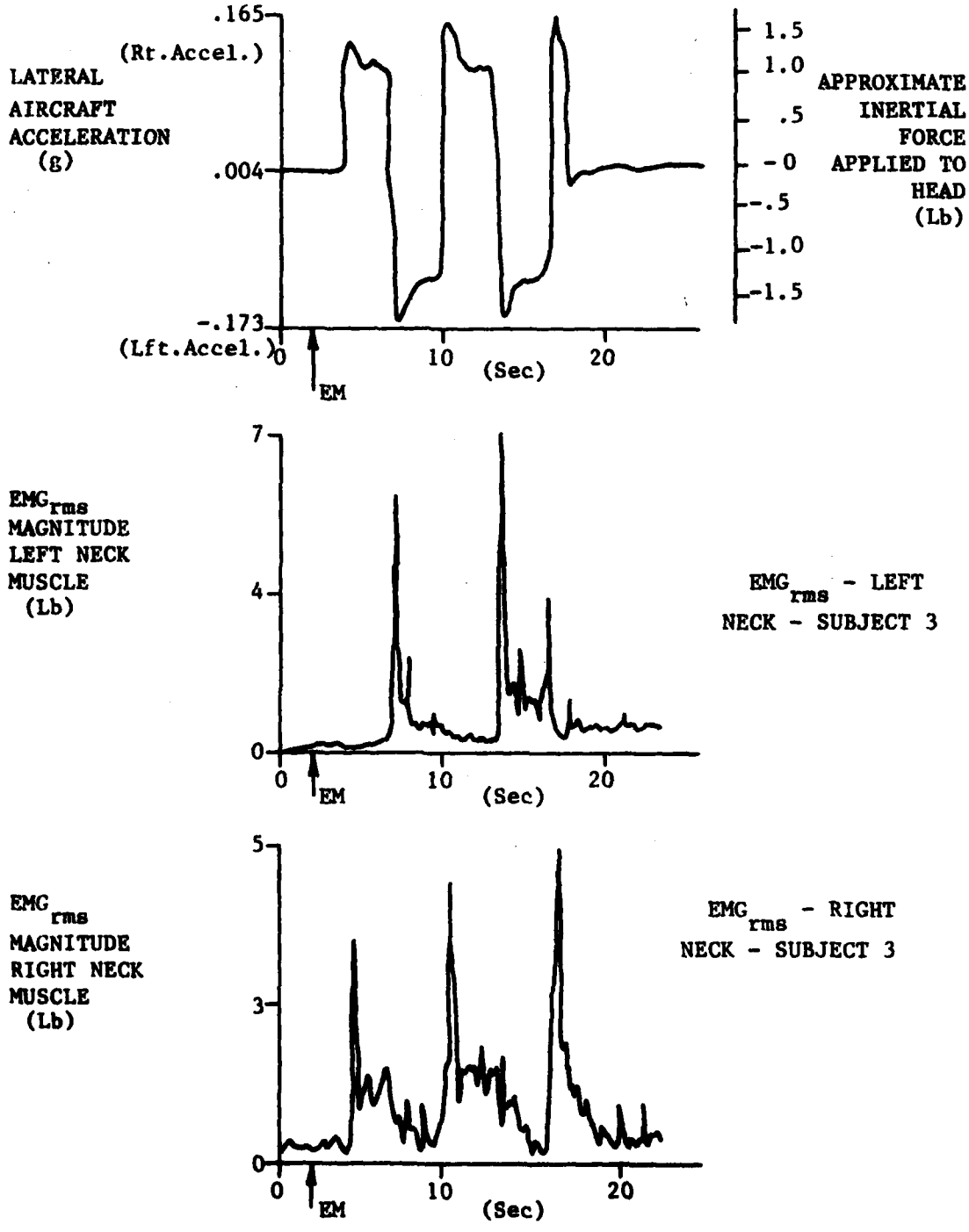

Figure 5.3 EMG neck muscle response from Subject 3 during lateral acceleration maneuver.

inertial forces; thus, the left muscle responds to left acceleration and vice versa. The large response to each acceleration onset is followed by a steady state, or possibly diminishing, signal during the steady acceleration. The apparent rate sensitivity must be due to either head/neck system dynamics, postural adjustment of the body trunk, or both. This is discussed further in the next section in connection with head motion.

Figure 5.4A shows integrated EMG activity (RMS circuit output) from Subject 3 in response to an uncoordinated roll maneuver. Note that the EMG magnitudes involved are near the lower end of the calibration chart (Figure 5.2) and, even though these are the best quality data among the subjects, this signal is partially buried in background noise. Computer processing was not available during this phase of data analysis; so, to clarify the signal, high frequencies were low pass filtered "by hand" as shown by the heavy line in Figure 5.4B.

Figures 5.5 and 5.6 show the "hand filtered" RMS signals from neck muscles of both the pilot and passive subject (Subject 3) along with lateral specific forces measured by aircraft inertial sensors. Note that this maneuver generates side forces that are comparable to those during the side acceleration maneuver (Figure 5.3), but with a slower more gradual onset. The aircraft was being controlled by the pilot subject during this run. The passive subject, again, contracts just the set of muscles needed to overcome presently felt inertial forces. The muscle pair acts in an agonist-antagonist fashion. In contrast, the pilot stiffens his neck by simultaneously contracting both left and right neck muscles. The pilot's stiffening response does not seem to anticipate the maneuver, but rather occurs gradually as the maneuver begins. This behavior on the part of the pilot subject is seen often (but not always) during runs in which he controlled the aircraft.

Figure 5.7 shows the EMG RMS record ("hand filtered") as the same pilot responds to a similar uncoordinated roll sequence being flown by the on-board computer. In this instance, the pilot is a passive subject during the run although he still can look at instruments and see out the cockpit window. His neck muscle response is now qualitatively the same as that of the passive subject in Figure 5.5.

The amount and quality of data do not allow any generalization in terms of pilot versus non-pilot behavior,

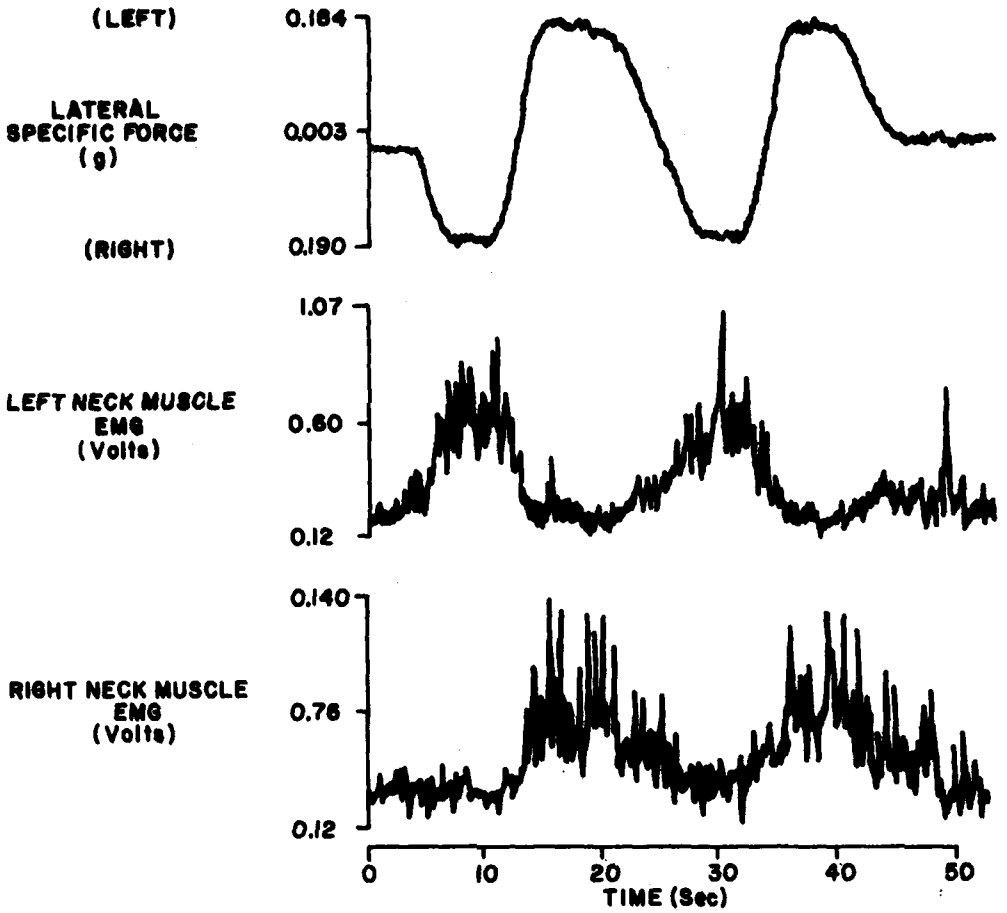

Figure 5.4a Integrated EMG during uncoordinated roll maneuver.

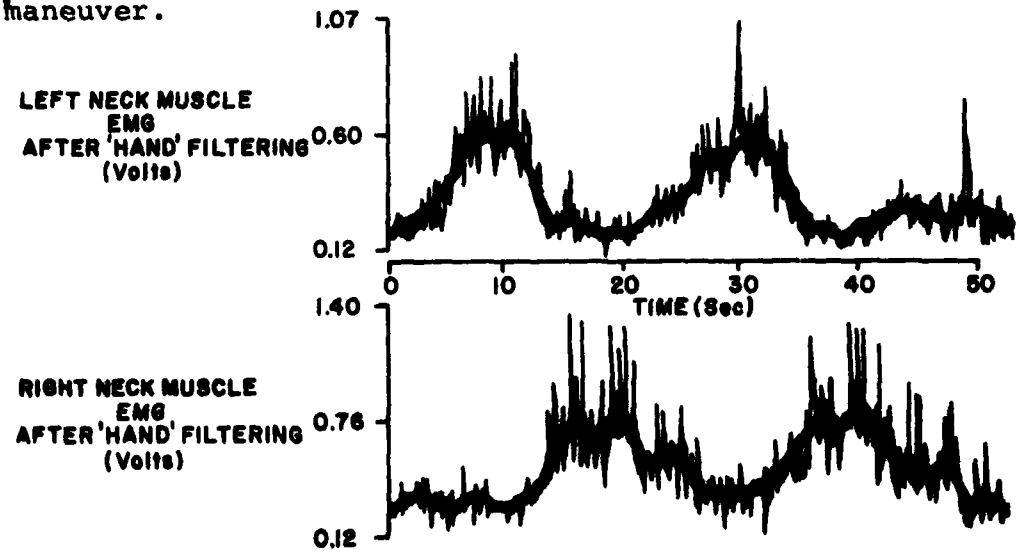

Figure 5.4B "Hand" filtering of EMG output from Figure 5.4a

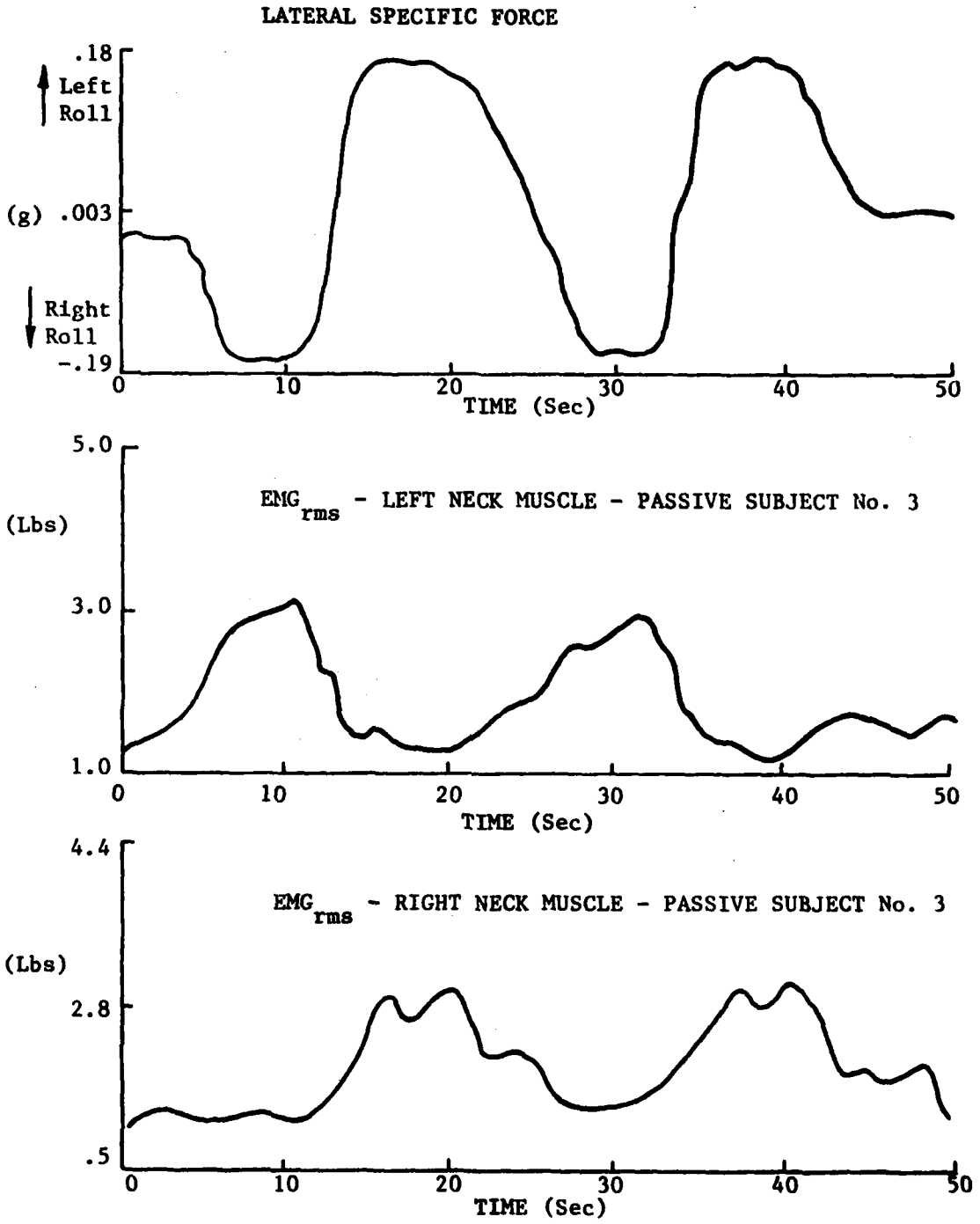

Figure 5.5 Integrated (rms magnitude) EMG response from passive subject during uncoordinated roll maneuver showing reciprocal activation of muscles to oppose head roll.

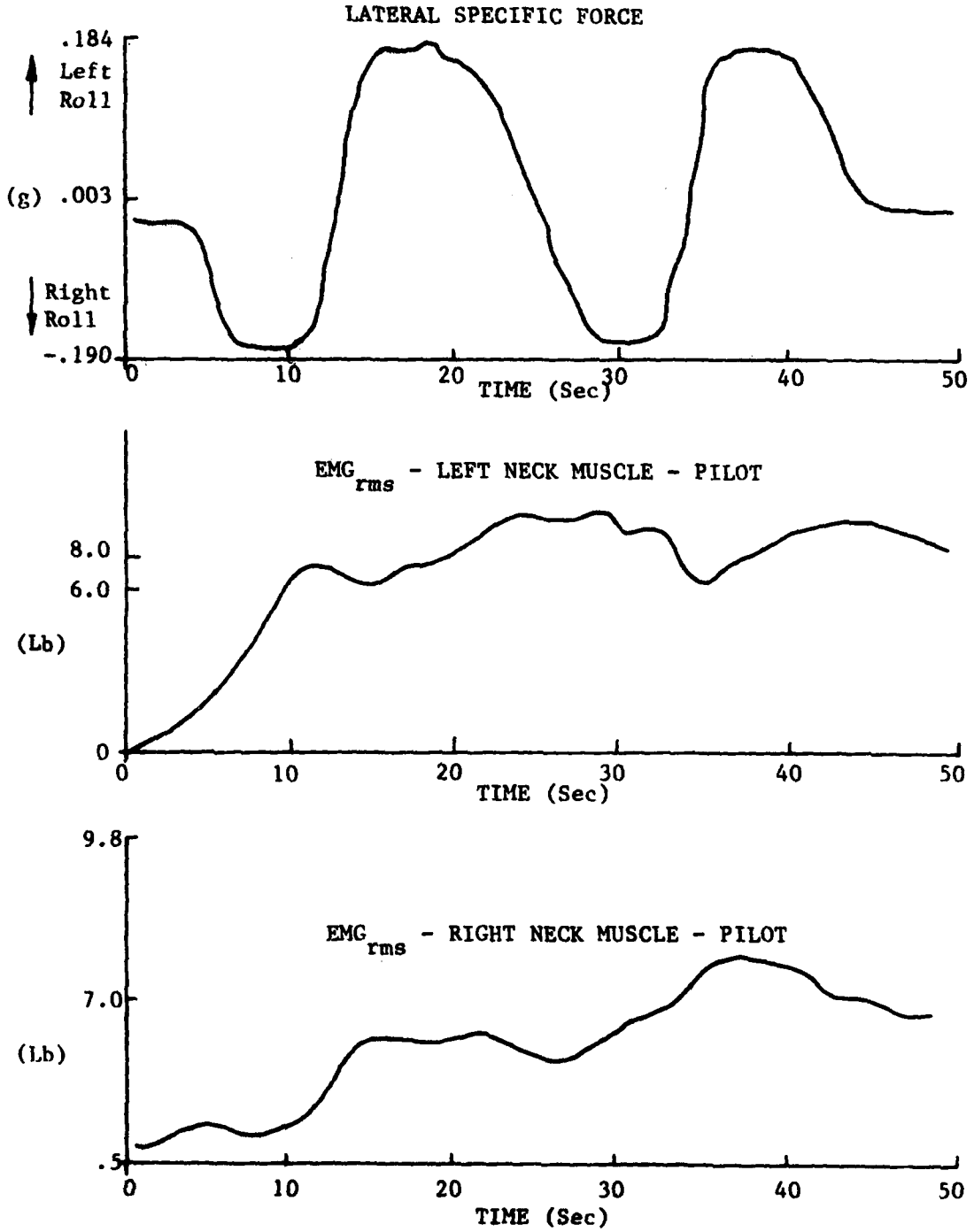

Figure 5.6 Integrated EMG response from pilot subject as he flew uncoordinated roll maneuver, showing co-contraction to stiffen the neck musculature.

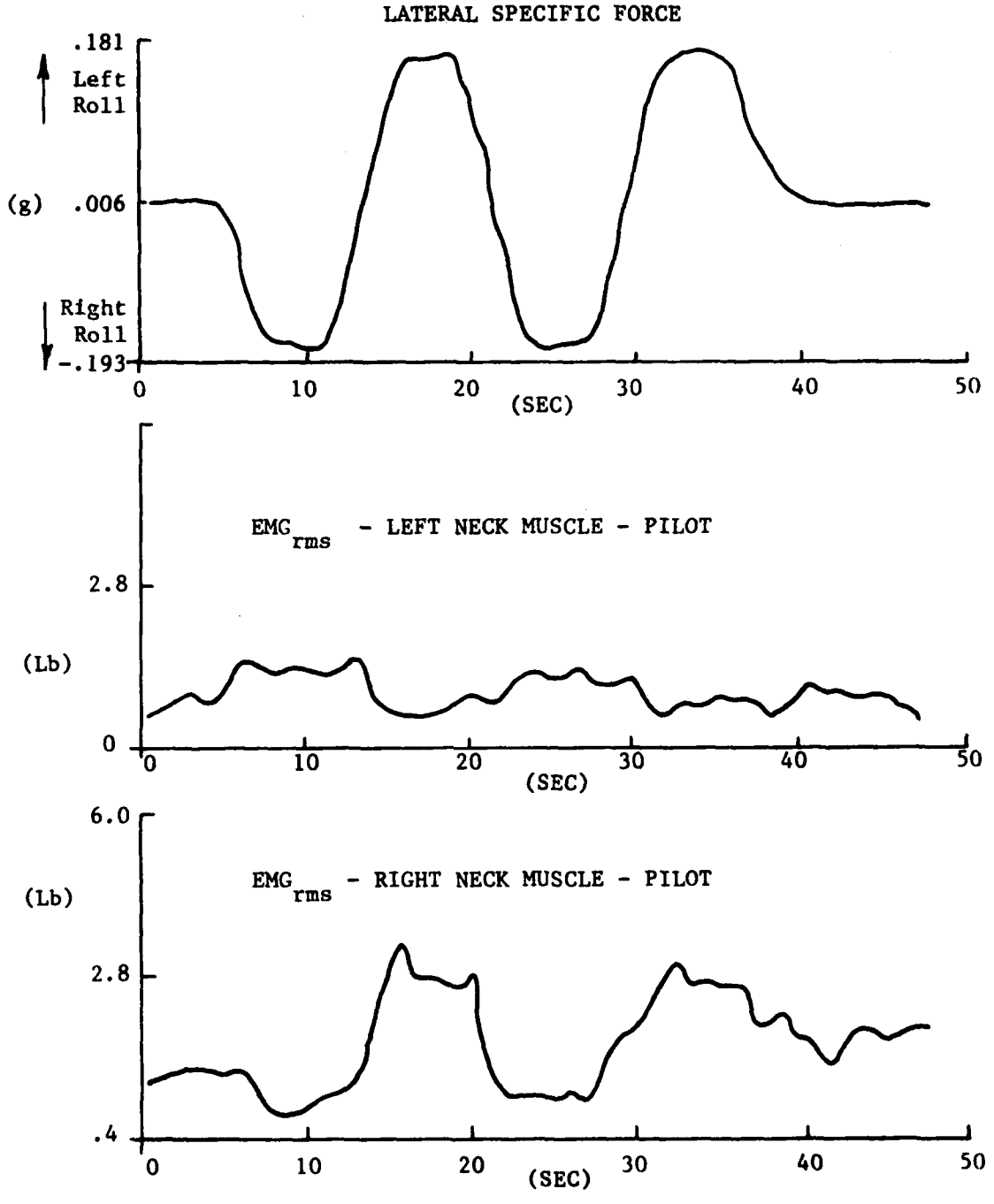

Figure 5.7 Integrated EMG response from pilot subject during computer controlled uncoordinated roll maneuver.

but two different types of behavior are shown.

5.2 Head Motion Response to Lateral Acceleration

Both the pilot (left seat) and passive (right seat) subjects' lateral head motions were monitored with video cameras during uncoordinated roll and side force maneuvers. Small light bulbs attached to helmet liners served as head position indicators and produced the type of split screen video picture shown schematically by Figure 5.8. A detailed description of video camera placement and the position light system can be found in Section 2.2.4.

When a person is seated, the head can move laterally if the neck and torso bend about the pivot points shown in Figure 5.9. This is an oversimplification since neither the neck nor the torso bend about a single pivot, but it is, nonetheless, a useful model. The location of the lower position light is very near the upper pivot point in Figure 5.9, but the position of the lower pivot cannot be determined from the video data.

Figure 5.10 shows the three basic modes of possible lateral motion from an aircraft seat. Since subjects wore snug shoulder harnesses, it was anticipated that most lateral motion would be head/neck motion only (type a in Figure 5.10) allowing unambiguous evaluation from the helmet light positions alone.

Figures 5.11 to 5.14 are examples showing motion of just the top position light, and therefore, illustrate total lateral head motion without specifying orientation. Head motion is shown for both the right seat passive subject and the left seat pilot subject. The passive subject's head is pushed from side to side by an amount roughly proportional to the lateral force during the uncoordinated rolls in Figures 5.11 to 5.13. This is consistent with the vehicle passenger behavior observed by Fukada (1975). The side force steps shown in Figure 5.14 have a very rapid acceleration onset (jerk) which causes some head motion overshoot.

In contrast, the pilot subject shows a response to uncoordinated roll that is not at all proportional to the lateral force profile. The magnitude of the pilot's lateral head motion is generally smaller than that of the passive right-seat subject especially during the latter part of the profile. After an initial motion in the

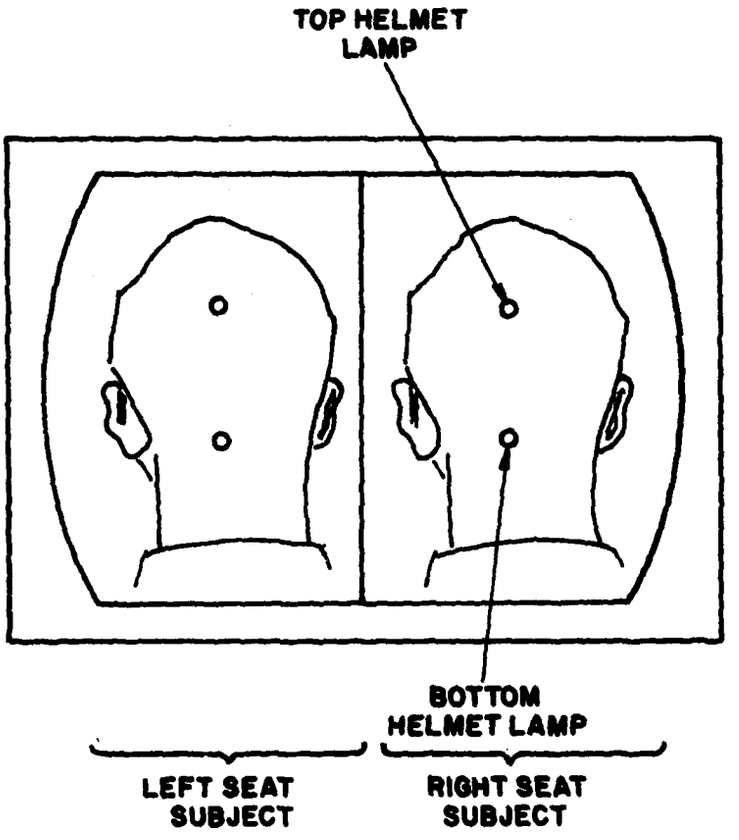

Figure 5.8 Schematic showing split screem image on video monitor.

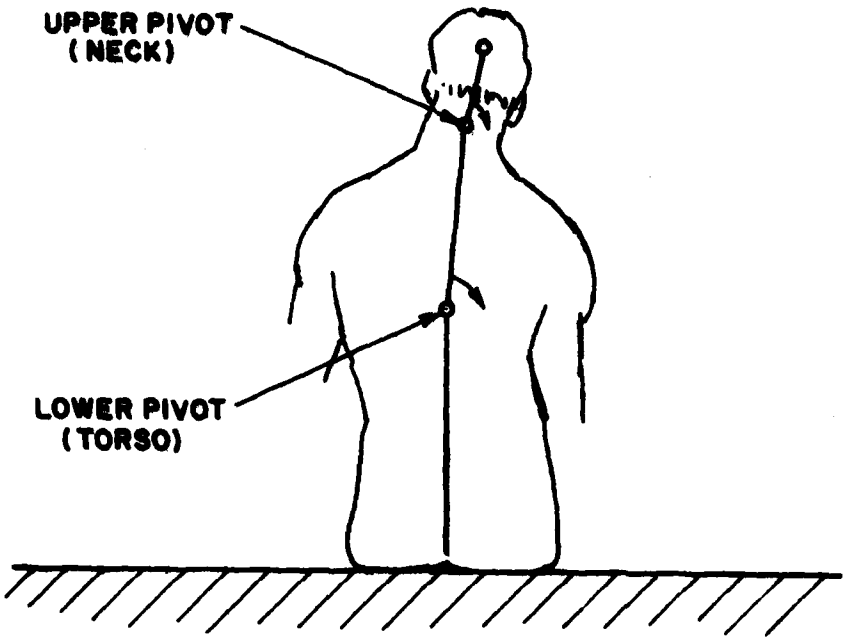

Figure 5.9 Simple model of lateral head motion from a seated subject.

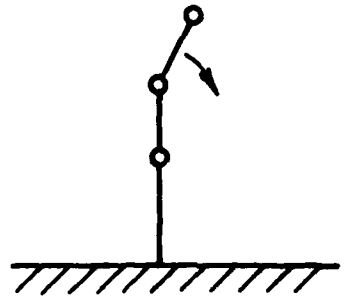

a) Movement About Only the Upper Pivot (Neck)

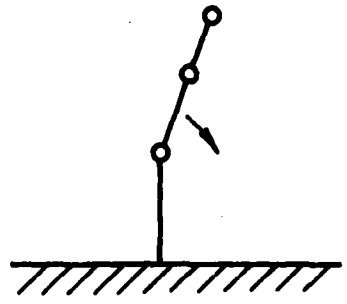

b) Movement About Only the Lower Pivot (Spine)

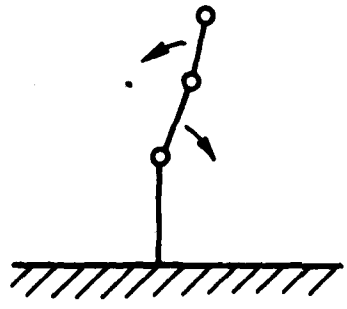

c) Movement of Both Neck and Spine

Figure 5.10 Simplified model showing three basic modes of lateral head motion from a seated position.

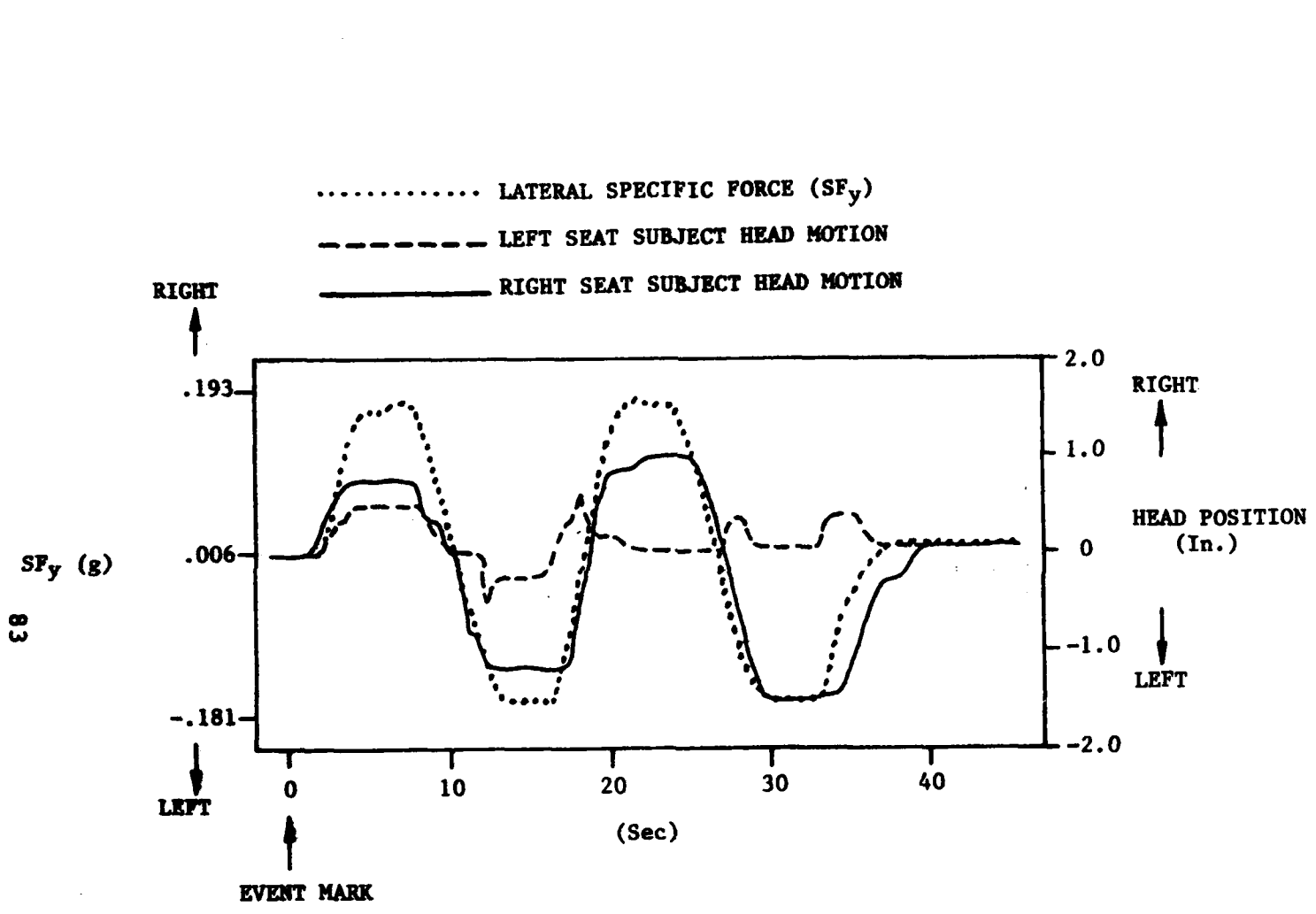

Figure 5.11 Lateral specific force and subject head motion profiles during uncoordinated roll maneuver. The aircraft was flown by computer during this run and the left seat pilot subject was inactive. He did, however, have access to instruments, and out-of-the-window view, and fore-knowledge of the maneuver.

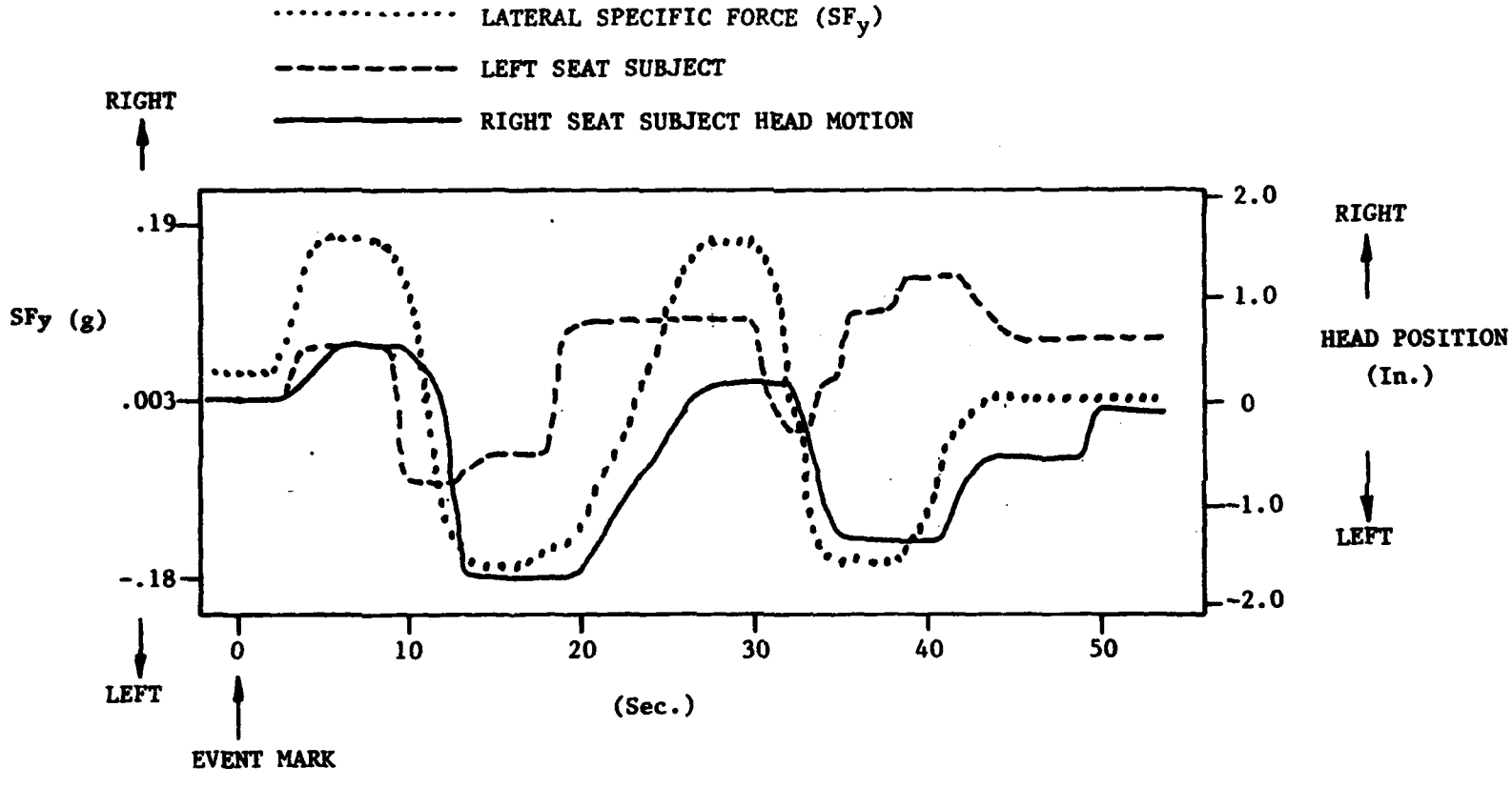

Figure 5.12 Lateral specific force and subject head motion profiles during uncoordinated roll maneuver. The left seat subject was controlling the aircraft.

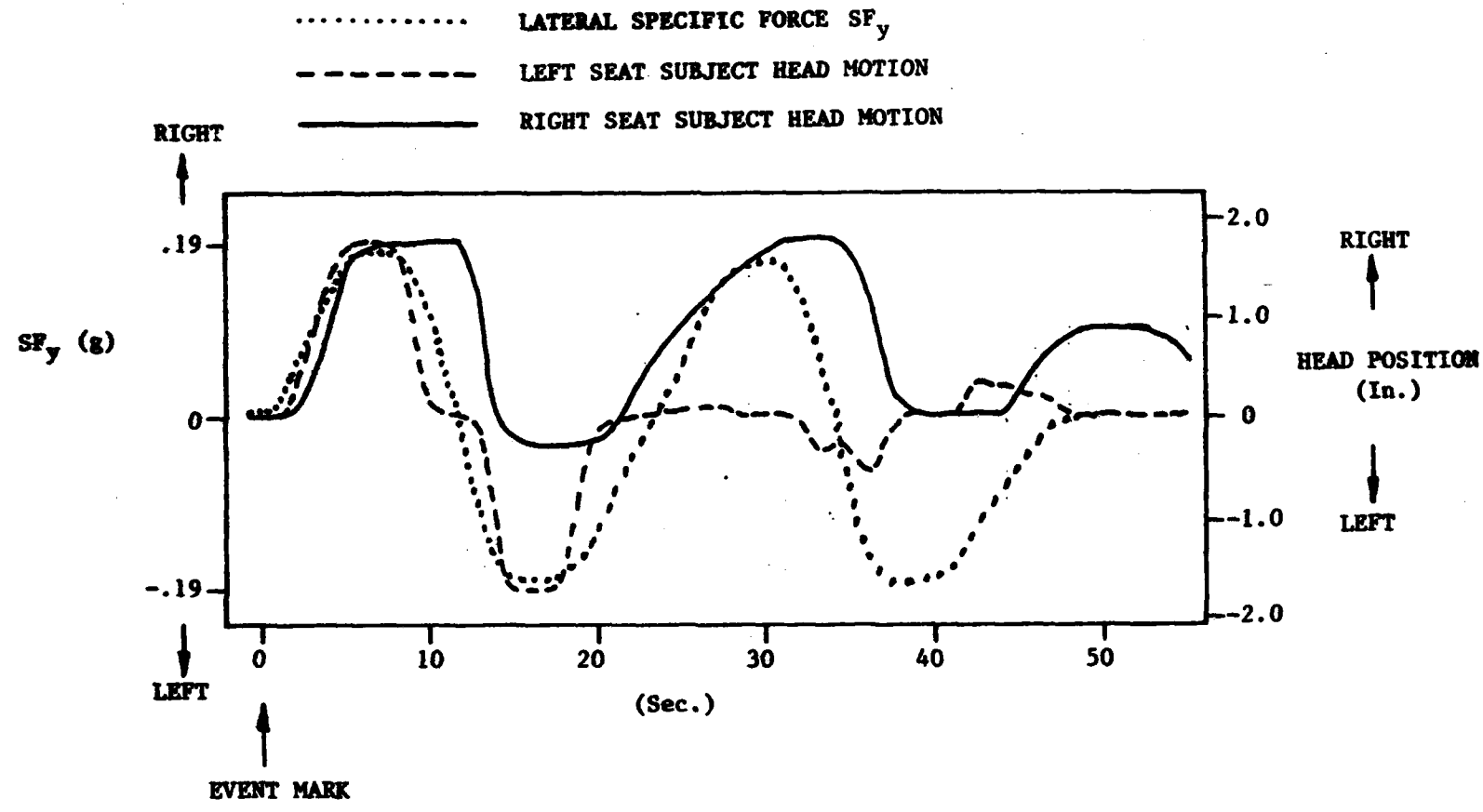

Figure 5.13 Another run of the uncoordinated roll maneuver during which the left seat subject controlled the aircraft. The right seat subject is not the same individual as in Figures 5.11 and 5.12.

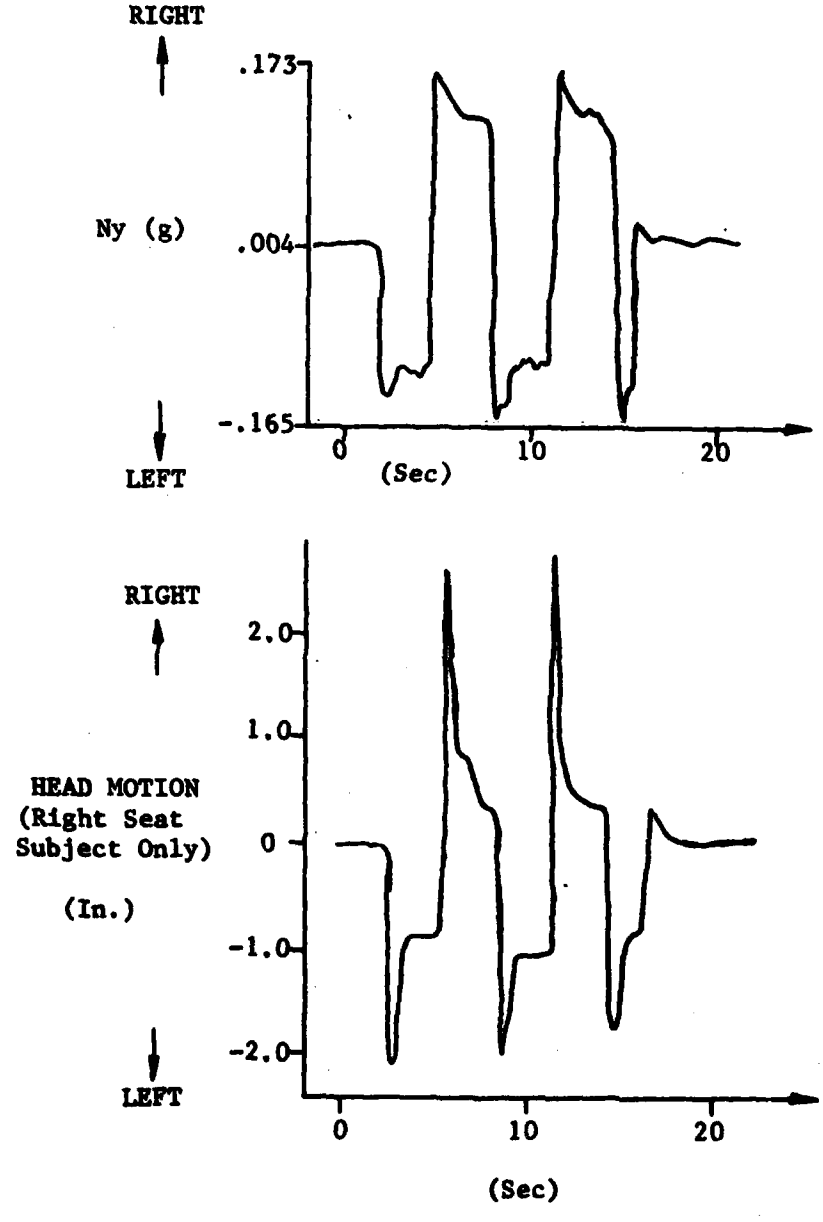

Figure 5.14 Lateral specific force and head motion profile during the pure side force maneuver. Head motion is shown only for the right seat subject.

direction of the lateral force, the pilot-subject unlike the passive subject, often moves his head back toward upright. Note, however, that the pilot does not usually anticipate by moving in a direction opposite to the upcoming lateral force during initiation of the maneuver (180 phase lead). Thus, the extreme anticipatory behavior of the driver observed by Fukada (1975) in buses is not demonstrated.

The relative positions of the two helmet lamps determines lateral head orientation in space. Orientation of the torso cannot be uniquely determined since the location of the lower pivot (see Figure 5.9) is not known, but some inferences can be made. Figures 5.15 to 5.18 show the positions of both top and bottom helmet lights during some of the runs discussed previously. During the uncoordinated roll in Figure 5.15, the right seat passive subject exhibits head motion about an apparent pivot that is approximately 6 to 9 inches below the lower position light. This would be compatible, for instance, with motion about a pivot point at the level of the shoulder blades and no neck motion (Figure 5.10B). In contrast, the pilot subject, in Figure 5.16, is using his neck to compensate for torso motion and to maintain his head in a constant orientation with respect to the cockpit (see Figure 5.10C). When the pilot subject actually flew the aircraft, Figure 5.17 shows that he began by using his neck to compensate for torso motion (as in Figure 5.16), but as the run progressed, he used less neck motion and kept his head more rigidly aligned with his upper torso. EMG Activity (Figure 5.6) shows a corresponding tensing of both neck muscles to stiffen the neck.

The sudden acceleration onset (jerk) of the lateral acceleration maneuver probably causes a combination of neck and torso motion in the direction of the specific force (see Figure 5.18). Figure 5.19 illustrates a motion sequence that would fit the data in the previous figure, although this solution is not unique.

5.3 Discussion of Head and Neck System Results

Even when shoulder straps are used, the torso as well as the neck undergoes considerable lateral motion during rolling and side force maneuvers. In fact, people may often tend to let only the torso move, keeping the head rigidly aligned with the upper torso. This should be considered by any future modeling efforts as well as any

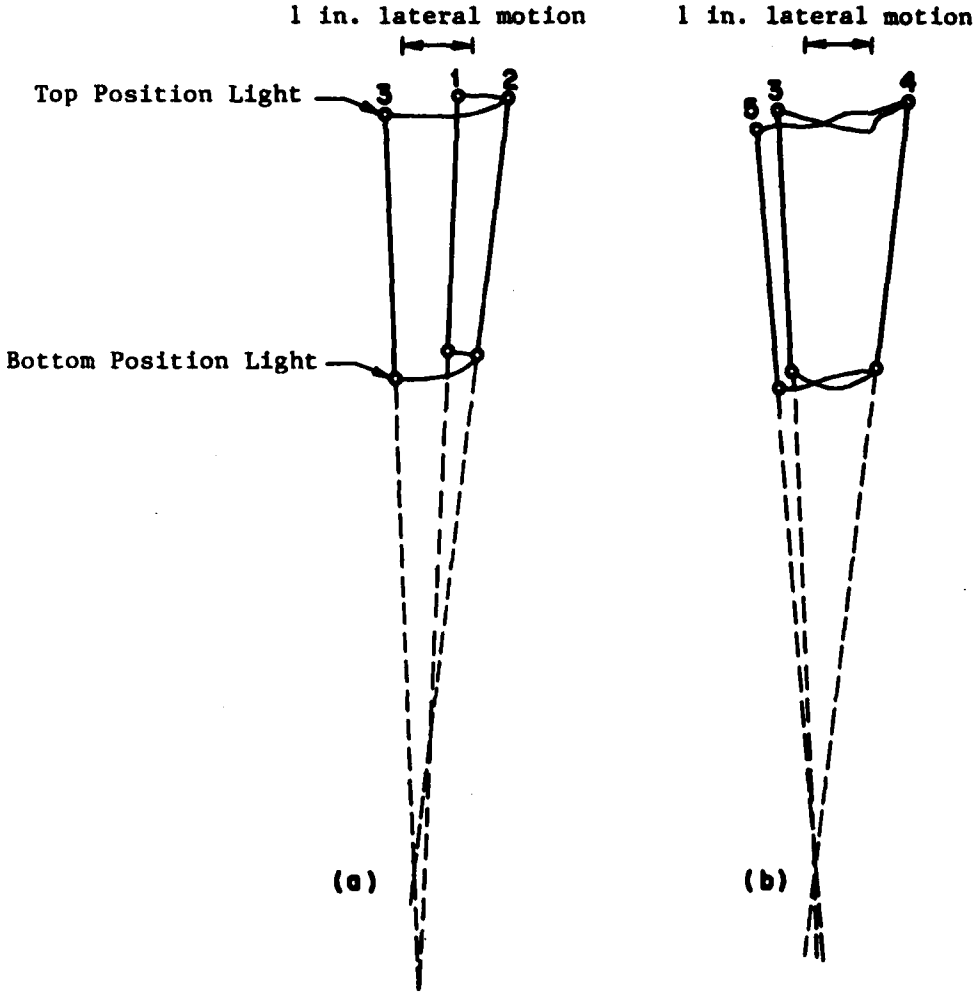

POSITION	TIME (Sec)	LATERAL ACCELERATION (g)
1	0	0
2	4	-.2
3	12	.2
4	22	-.2
5	30	.2

Figure 5.15 Motion of head position lights for passive Subject 3 during uncoordinated roll maneuver (same run as shown in Figure 5.11).

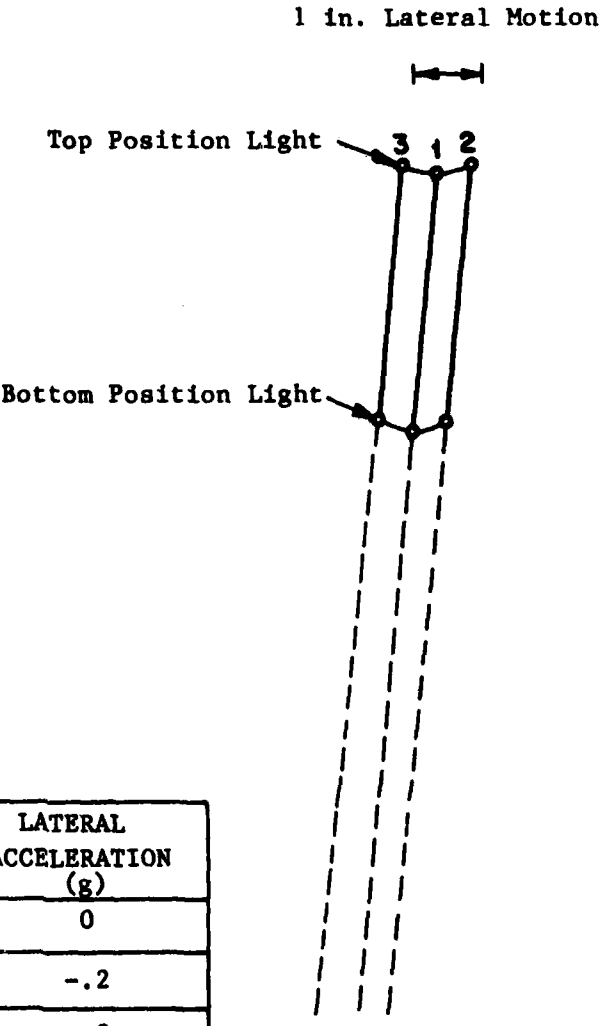

POSITION	TIME (Sec)	LATERAL ACCELERATION (g)
1	0	0
2	4	-.2
3	12	.2

Figure 5.16 Motion of position lights for left seat pilot subject during uncoordinated roll maneuver. The pilot subject did not control the aircraft during this run (same run shown in Figure 5.11). Only 3 positions are shown because others are simply superimposed on these.

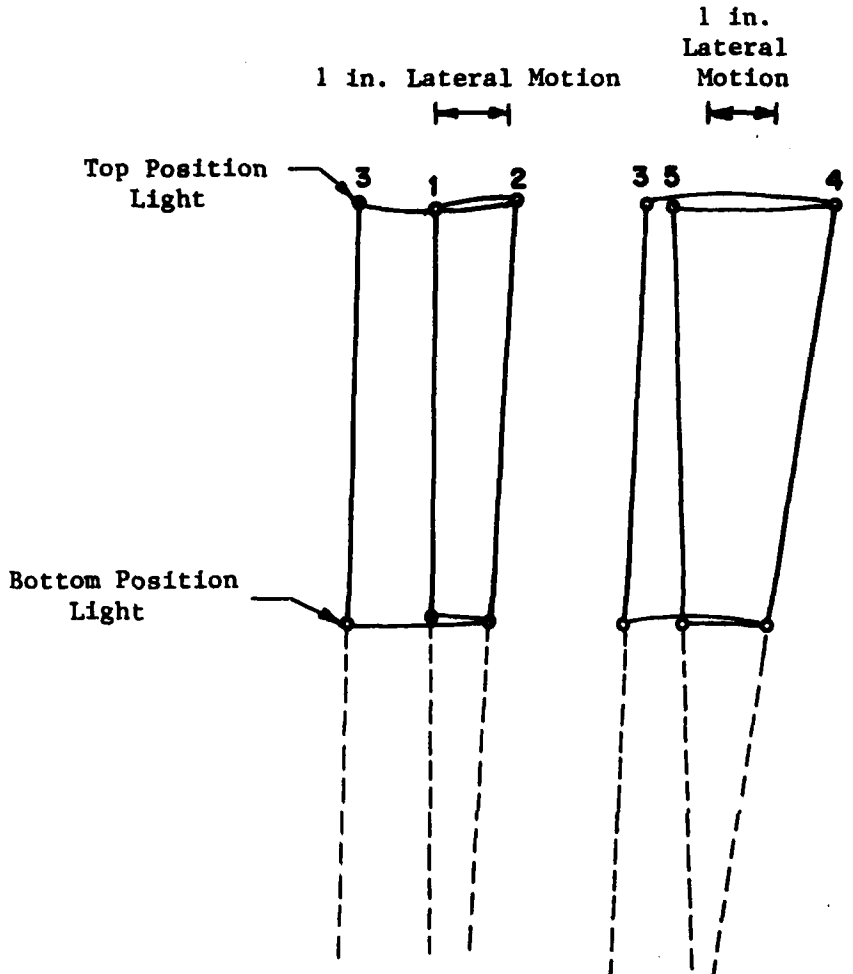

POSITION	TIME (Sec)	LATERAL ACCELERATION (g)
1	0	0
2	4	.17
3	10	.10
4	20	-.11
5	32	-.02

Figure 5.17 Motion of position lights for pilot subject during uncoordinated roll maneuver. The pilot subject was controlling the aircraft during this run. (Same run shown in Figure 5.12.

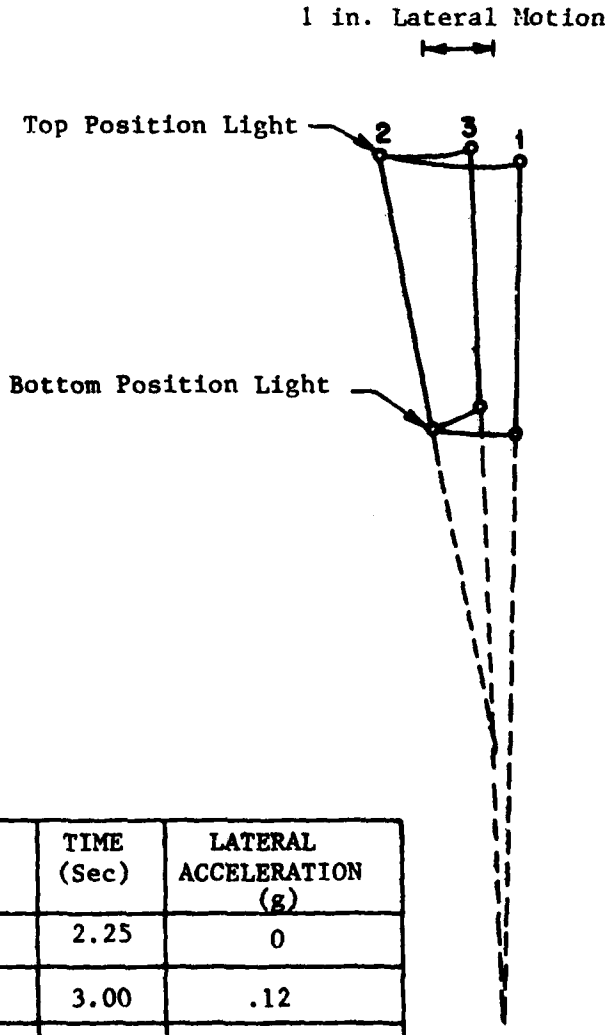

POSITION	TIME (Sec)	LATERAL ACCELERATION (g)
1	2.25	0
2	3.00	.12
3	4.00	.12

Figure 5.18 Motion of head position lights for passive Subject 3 during a single lateral acceleration (compare to Figure 5.14).

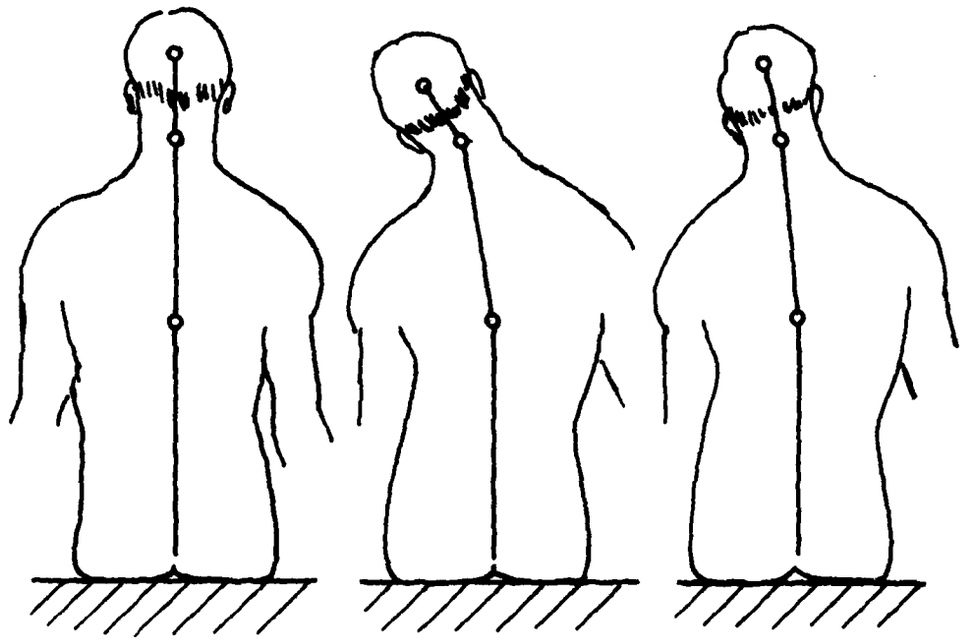

Figure 5.19 Possible head/trunk motion in response to 0.12 g step-in lateral acceleration. The sequence is consistent with data in Figures 5.18 and 5.14.

AD-A129 391 SPATIAL ORIENTATION AND MOTION CUE ENVIRONMENT STUDY IN THE TOTAL IN-FLIG..(U) GULF AND WESTERN APPLIED SCIENCE LABS WALTHAM MA J BORAH ET AL. JUN 83 AFHRL-TP-82-28 2/2

UNCLASSIFIED F33615-78-C-0062 F/G 5/9 NL

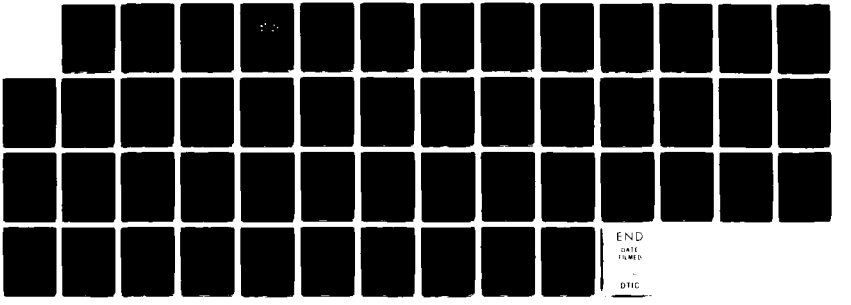

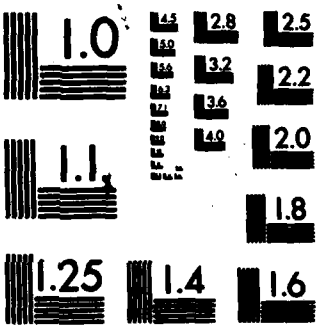

MICROCOPY RESOLUTION TEST CHART
NATIONAL BUREAU OF STANDARDS-1963-A

efforts to simulate "head forces" on ground based aircraft simulators.

Passive subject behavior in aircraft is probably similar to that described by Fukada (1975) for bus passengers. Specifically, passive subjects allow themselves to be pushed from side to side by lateral forces. Some different behaviors are also apparent, especially in the case of the pilot subject, but no clear pattern can be discerned from a limited amount of "hand reduced" data.

The "hand reduction" analysis does demonstrate that information can be successfully extracted from the video tapes. It is strongly recommended that all of the video data showing the head position lights be reduced to X-Y position versus time profiles in an automated fashion. This reduction can be accomplished with existing equipment designed to track high resolution elements in video signals. The data would be made substantially more valuable by a brief study to determine the most usual mode of lateral torso motion when people are seated in a chair with a low backrest (similar to the TIFS cockpit seats). Such a study would eliminate much of the ambiguity from the head position data.

Although only a small amount of the EMG data is of good quality, it is enough to allow comparison with the head-neck system model (see Section 7.0) and to reveal a common response to lateral forces, at least among some passive subjects in aircraft.

6.0 BODY/SEAT PRESSURE

6.1 Output from Pressure Sensing Seat Pads

Special seat pads, each equipped with an array of load cells, were used to measure body-seat pressure dynamics during coordinated turns, uncoordinated rolls, lateral accelerations, and roller coaster maneuvers. (A detailed description of the seat pads can be found in Section 2.2.3 and a description of the maneuvers can be found in Section 2.6.) Measurements were made with seven different passive subjects, who had no visual cues or foreknowledge of the maneuvers, and one pilot subject, who sometimes flew the aircraft.

Because of a warm-up drift problem, the static pressure values at the start of each experiment run cannot be precisely determined, even after making corrections for drift. However, excursions from these static values during the 0.5 to 1.5 minute runs can be determined quite accurately. The position of each load cell in the seat pan and backrest sensor arrays is given in Figure 2.15.

Pressures against the seat backrest were very small (less than 0.5 psi) and pressure changes due to inertial forces are sometimes hard to distinguish from those caused by postural adjustments, sensor noise, or other artifacts. Most of the analysis in this section, therefore, concerns the seat pan.

Even allowing for uncertainties introduced by the warm-up drift problem, static pressure distributions appear to be more even than those found by Hertzberg (1955) and Kron (1975) (See Figures 2.12 and 2.13), probably due to the soft seats used in TIFS. The values shown in Figure 6.1 were calculated from only the last run of each flight to minimize warm-up drift effects, and represent the average and standard deviations during straight and level flight.

Roller coaster maneuvers and coordinated turns produced, respectively, large and small changes in the total z axis specific force. Both maneuvers produced low frequency changes in specific force without any large components of jerk (the derivative of acceleration) and body-seat pressure dynamics simply follow the specific force profile. This is illustrated by the examples shown in Figure 6.2 and 6.3 and is consistent with a simple mass

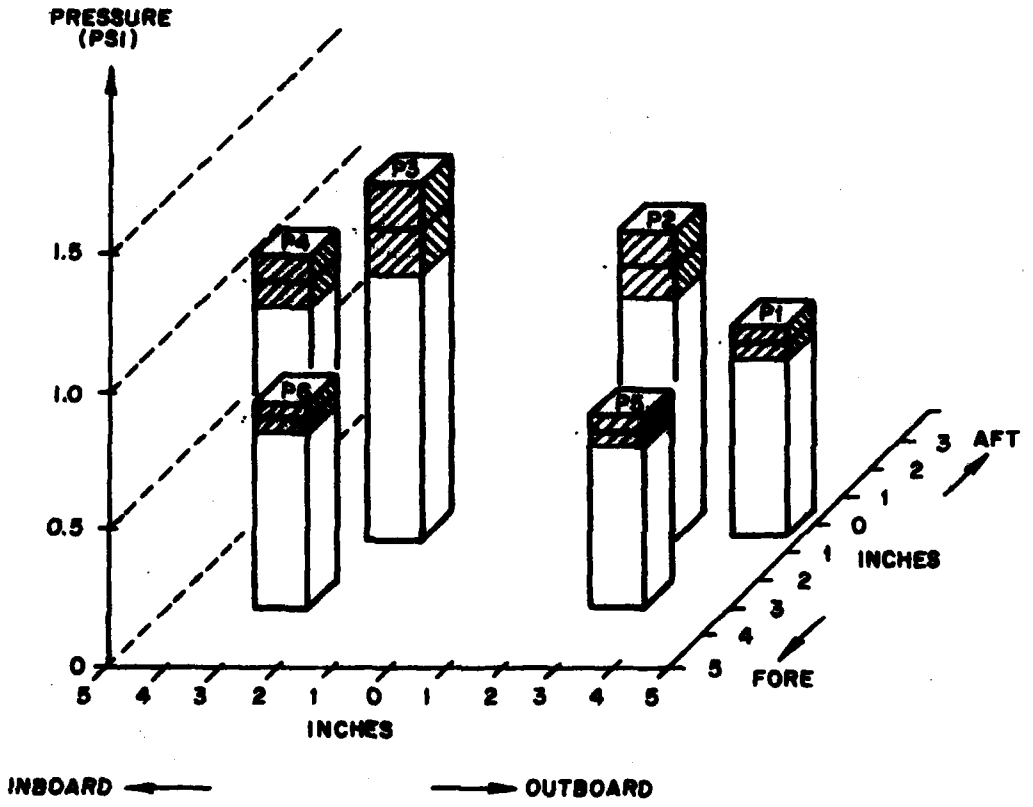

Figure 6.1 Static Pressure Distribution Measured on Left Seat Pan (Pilot-subject) Showing Mean and Standard Deviation for Each Sensor.

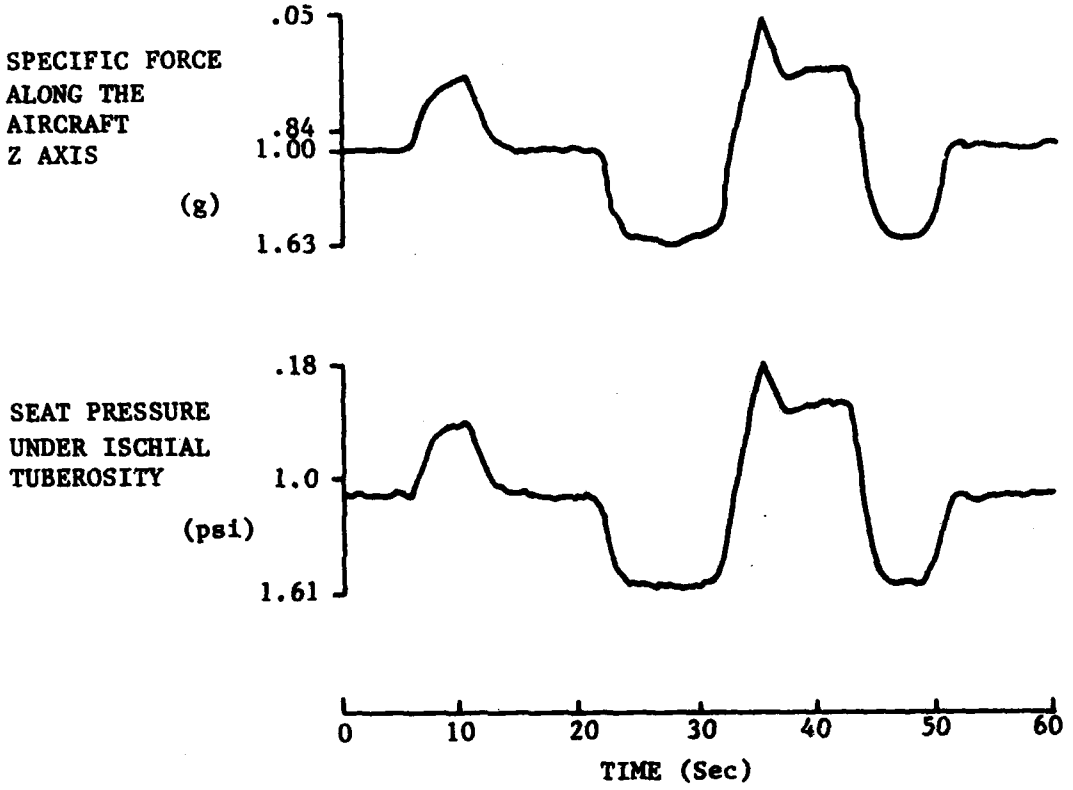

Figure 6.2 Example of seat sensor array output during 0.6 g "roller coaster" maneuver.

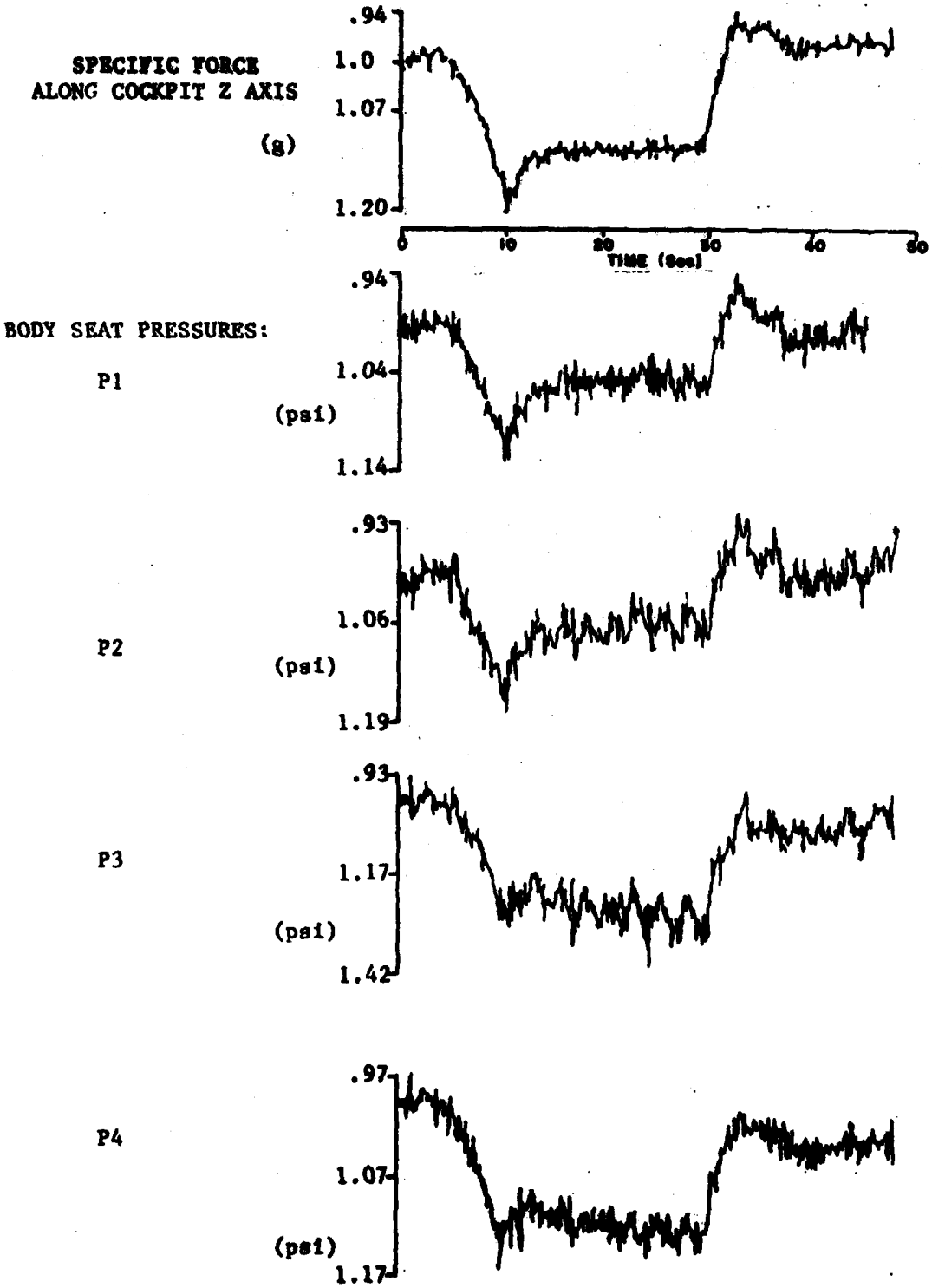

Figure 6.3 Example of seat sensor array output during 30°, 6°/sec coordinated turn

model response.

Lateral forces, produced either by the uncoordinated roll (Figure 6.4) or by the lateral acceleration maneuver (Figure 6.5) increase pressure under one buttock and decrease pressure under the other. During the uncoordinated roll, the dynamics of the pressure profiles once again matched the specific force profile (Figure 6.4). During the lateral acceleration maneuver, some of the seat pressure curves show an overshoot in response to the sudden acceleration onset (Figure 6.5). This may be due to motion of the torso (described in Section 5.2) or may imply some higher order dynamics in the seat cushion/buttocks system.

6.2 Mass Model

For most roll axis motion, the seat pressure data is compatible with the simple, two dimensional, mass model shown in Figure 6.6. The two supports indicated in Figure 6.6 are located at the approximate average position of the ischial tuberosoties (see Figure 2.13). The force under these supports is

$$F_R = \tfrac{1}{2}(I\alpha/\ell + mr\alpha - F_z - \tfrac{d}{\ell}F_y) \qquad (6.1)$$

$$F_L = \tfrac{1}{2}(-I\alpha/\ell + mr\alpha - F_z + \tfrac{d}{\ell}F_y) \qquad (6.2)$$

where,

$$F_z = m(g\cos\phi - N_z) \qquad (6.3)$$

$$F_y = m(g\sin\phi - N_y) \qquad (6.4)$$

The symbol α refers to aircraft angular acceleration (rad/sec^2) about the roll axis. W and N refer to aircraft acceleration along the yaw and pitch axes respectively, and "I" refers to the moment of inertia of the supported part of the subject about an axis perpendicular to plane ab and passing through the center of gravity. Factoring mg from the right side of 6.1 and 6.2 puts these equations in terms of specific forces with units of g's.

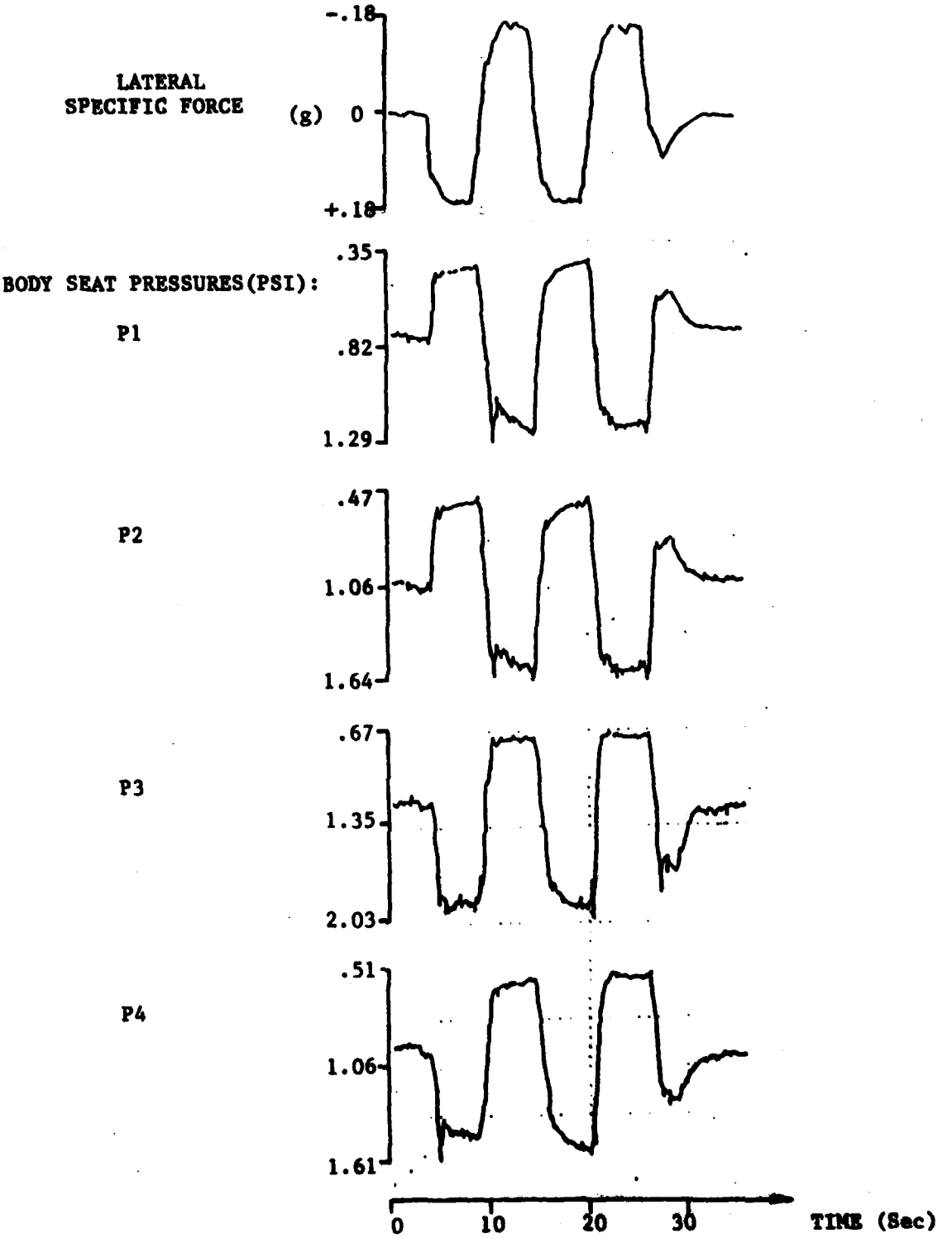

Figure 6.4 Example of seat sensor array output during uncoordinated roll maneuver

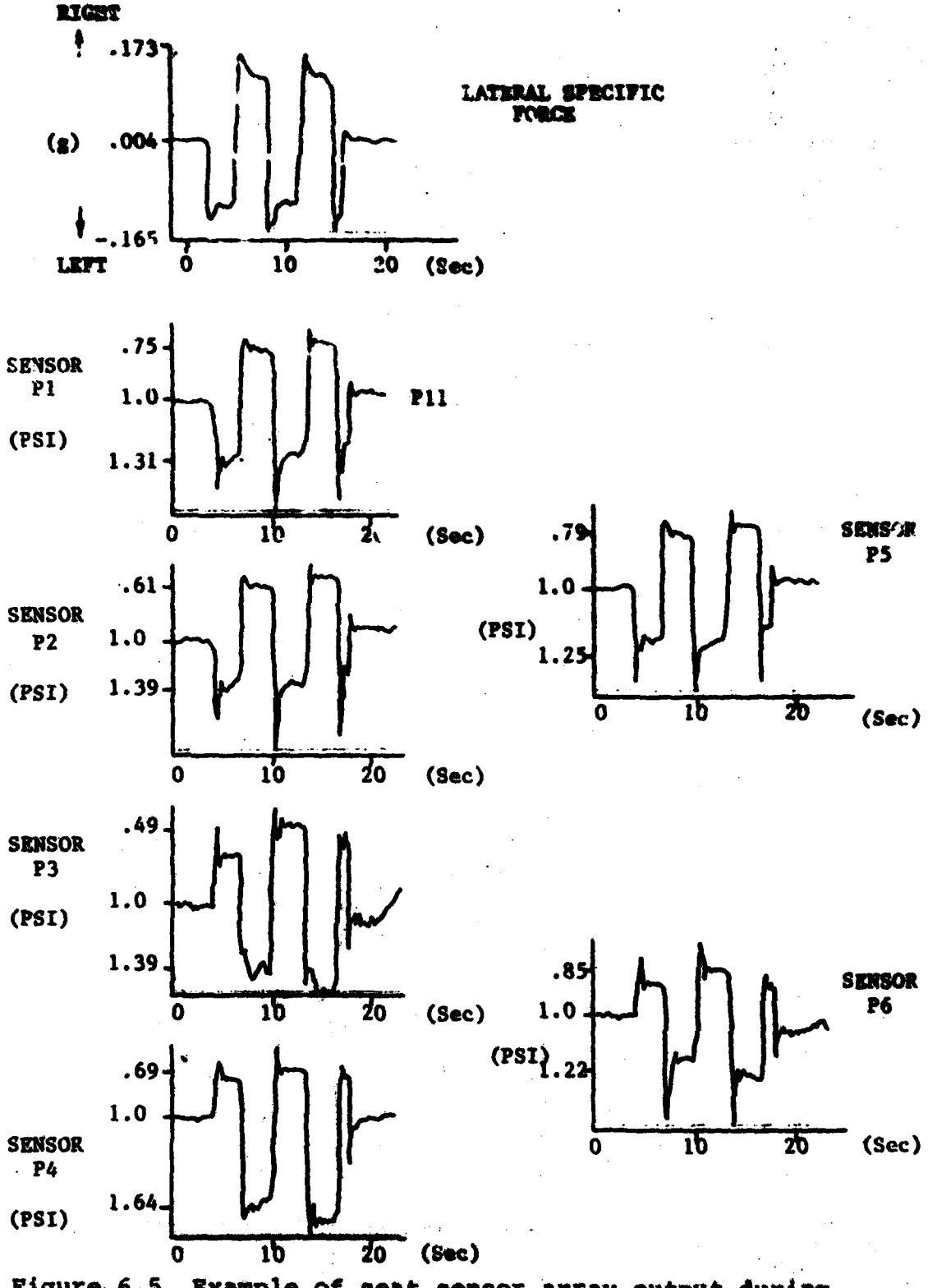

Figure 6.5 Example of seat sensor array output during lateral acceleration maneuver.

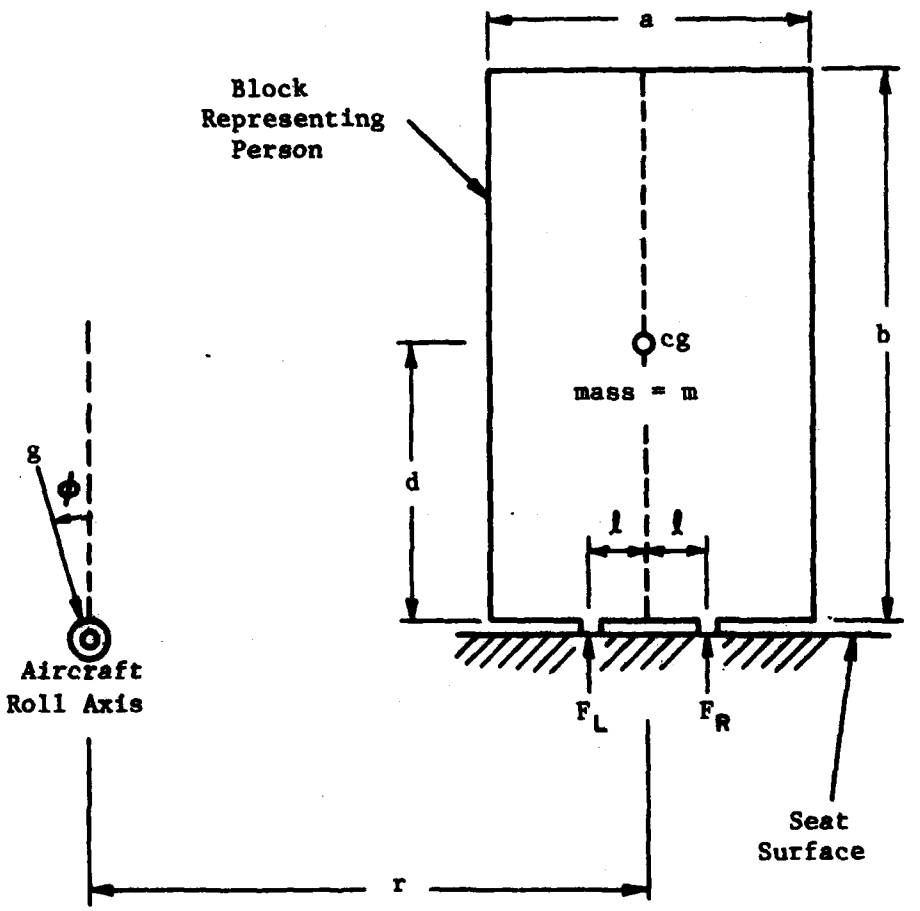

a = 14", b = 25", d = 12.5", ℓ = 2.5", r = 24"

Figure 6.6 Simple mass model for person sitting in aircraft seat.

$$F_R = \frac{mg}{2}(K_\alpha \alpha + \frac{r}{g}\alpha - K_{SF_z} SF_z - K_{SF_y} SF_y) \quad (6.5)$$

$$F_L = \frac{mg}{2}(-K_\alpha \alpha + \frac{r}{g}\alpha - K_{SF_z} SF_z + K_{SF_y} SF_y) \quad (6.6)$$

where,

$$SF_z = F_z/mg \; ; \; SF_y = F_y/mg \quad (6.7)$$

$$K_\alpha = I/mg\ell = (\frac{a^2+b^2}{12\ell})\frac{1}{g} \quad (6.8)$$

$$K_{SF_z} = 1 \quad (6.9)$$

$$K_{SF_y} = d/\ell \quad (6.10)$$

In this form, terms on the right hand side of the equation can be directly related to outputs from aircraft inertial sensors. Thus, when flying straight and level SF_z is 1.0, SF_y is 0, and α is 0; or, for example, when executing the lateral acceleration manuever (during the constant acceleration phase), SF_z is 1.0, SF_y is .17 (magnitude of lateral acceleration in g units), and α is 0.

Using the dimensions listed in Figure 6.6 for a, b, l, r , and D,

$$K = 0.07$$

$$K_{SF_z} = 1.0$$

$$K_{SF_y} = 5.0$$

The precise values of these constants are not very meaningful because of the over-simplified nature of the model, but the analysis clearly suggests that lateral forces will contribute to body/seat pressure with a greater gain than vertical acceleration. Furthermore, it is implied that a very large angular acceleration is required to produce a significant change in body seat pressure. By comparing seat pressure changes measured during roller coaster (pure SF_z) and lateral acceleration (pure SF_y)

maneuvers, an empirical value for K_{SF_y}/K_{SF_z} can be computed. Over the seven passive subjects and the pilot subject, this value ranges from 1 to 4.

6.3 Discussion of Body/Seat Pressure Results

Some advanced aircraft simulators now use g-cueing seats to simulate somatosensory motion cues. Since it is difficult to increase or decrease the total force between the buttocks and seat without real acceleration, g-seat designs usually attempt to vary the pressure under the ischial tuberosities by varying the effective surface area of the seat and/or varying the relative hardness of different parts of the seat's surface.

The results described in the previous two sections suggest that it might be reasonable to strive for pressure profiles under the tuberosities that conform approximately to

$$P_R = K(.1\alpha + \frac{r}{g}\alpha - SF_z - 2SF_y) \qquad (6.11)$$

$$P_L = K(-.1\alpha + \frac{r}{g}\alpha - SF_z + 2SF_y) \qquad (6.12)$$

where P_R and P_L are pressures under the right and left tuberosities, α is the roll angular velocity to be simulated, SF_z and SF_y are simulated specific forces due to gravity and accelerations along the model aircraft's yaw and pitch axes, and K is a proportionality constant.

The data gathered in the TIFS Study can be adequately fit with unity dynamics between the specific force and body-seat pressure profiles, keeping in mind that most manuevers had very little jerk (rate of change of acceleration). Where some rate sensitivity was observed, during the lateral acceleration manuever, it is unclear whether higher order seat-cushion/buttocks dynamics or the effects of upper torso motion are the cause.

The following future work is suggested in order to further define the "seat-of-the-pants" cues received by aircraft pilots and to refine g-seat drive algorithms:

1. Perform experiments similar to the present study using harder, fighter aircraft type seats, rather than the soft transport seats now on TIFS. The drift problem in the pressure sensing pads should be resolved sufficiently to measure static values accurately.

2. Install the pressure sensing pads on a G-seat, use the G-seat drive to simulate the TIFS manuevers, and compare pressure profiles with those found during the current study and in suggestion 1.

3. Install a G-seat with pressure sensing pads on TIFS. Compare the effect of real and simulated motions. At the same time, use psychophysical tracking and magnitude estimation tasks to compare subjective motion and orientation perceptions during real and g-seat simulated motions. Since mental set is very important to spatial orientation, the psychophysical experiment should be performed in an environment, like TIFS, that permits subjects to believe that motion is possible.

4. Using the TIFS aircraft, equipped with a g-seat and pressure sensing pads, investigate the use of combined inertial onset cues and g-seat cues. Compare pressure profiles as well as psychophysical orientation results for combined inertial and g-seat cues, g-seat cues alone, and motion alone.

As of this writing, the pressure sensing seat pads are being used in a study at the Air Force Aerospace Medicine Laboratory, under the direction of Drs. Grant McMillan (AMRL/HEF) and Ed Martin (ASD/SNETS), to compare pressure profiles on a roll axis motion device with those produced by the Advanced Low-Cost g-cueing System (ALCOGS).

7.0 COMPARISON OF DATA WITH SPATIAL ORIENTATION MODEL

A model has been developed to predict human dynamic spatial orientation in response to multi-sensory stimuli. Motion stimuli, corresponding to aircraft or simulator motion, are first processed by dynamic models of the visual, vestibular, tactile, and proprioceptive sensors. Central nervous system function then is modeled as an optimal estimator (specifically a Kalman Filter) which, using information from the various sensors, estimates state variables corresponding to perception of motion and spatial orientation. Where necessary, non-linear elements have been used to preprocess input to the central estimator in order to reflect more accurately some non-linear human response characteristics. The basic structure of the model is shown in Figure 7.1 and is implemented as a FORTRAN computer program. It was developed under the sponsorship of the Air Force Human Resources Laboratory and is described in detail by Borah, Young, and Curry (1977), and Borah, Young, and Curry (in press).

Relying primarily on visual and vestibular components (tactile and proprioceptive components need further validation and development), the model has shown substantial agreement with subjective data for several basic patterns of motion. In the following sections subjective orientation data gathered during the TIFS study are compared to output from the model central processor (see Figure 7.1). The model is configured to assume that no visual cues are available (to represent the passive, right seat subjects on the TIFS flights) and all model parameters are exactly those specified in Borah, Young, and Curry (in press). The proprioceptive component of the model (see Figure 7.1), consisting of a head-neck system biodynamics model, is individually compared with head motion and EMG data from the TIFS study in Section 7.3.

7.1 MODEL SPATIAL ORIENTATION ESTIMATES

7.1.1 Roll Orientation

Figure 7.2 shows model predictions of roll orientation and roll rate perception during a 20 bank, 3 /sec roll-in coordinated turn. The inertial stimulus profile used as input to the model closely matches the profiles recorded by TIFS inertial sensors during the same maneuver (aircraft bank angle and roll rate stimulus profiles are also shown

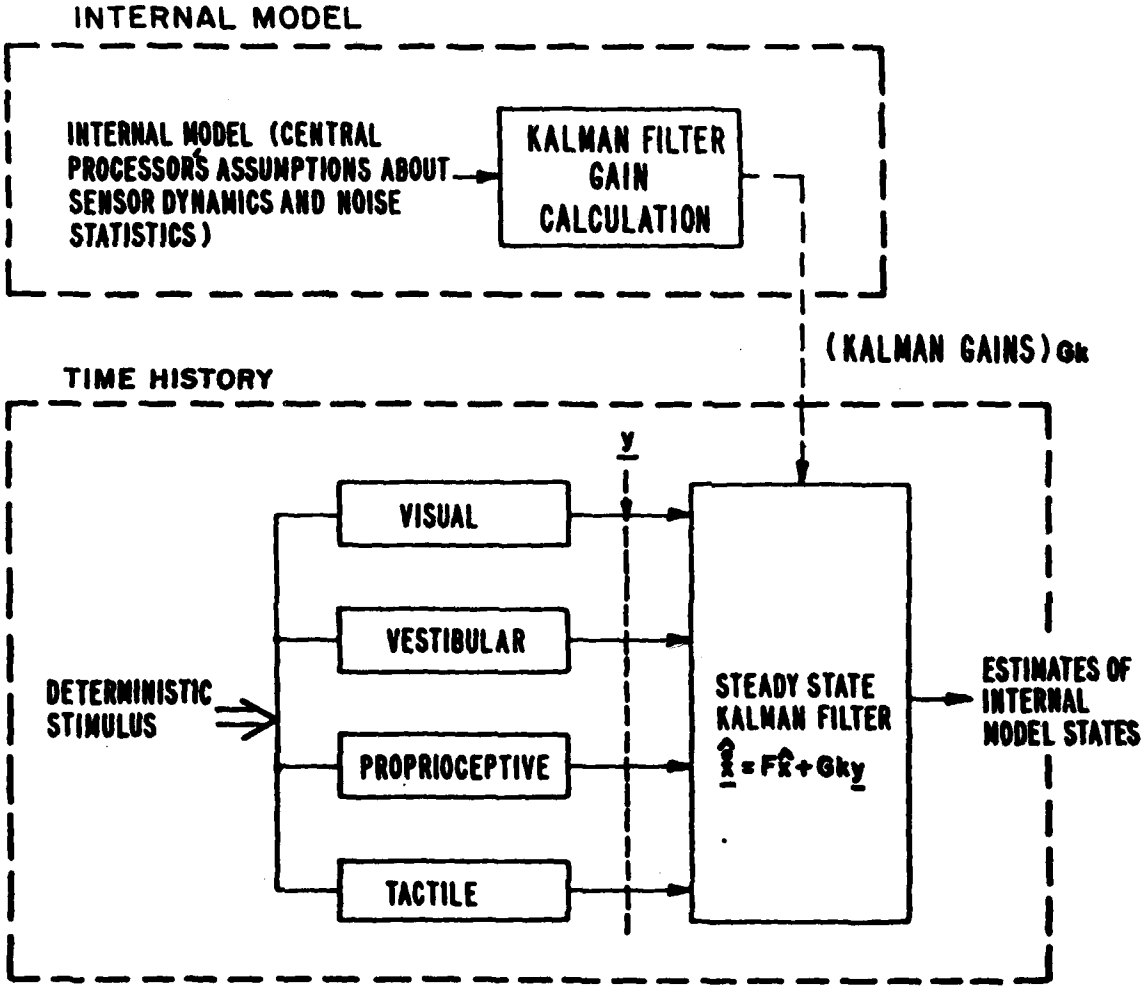

Figure 7.1 Optimal estimator model for human spatial orientation.

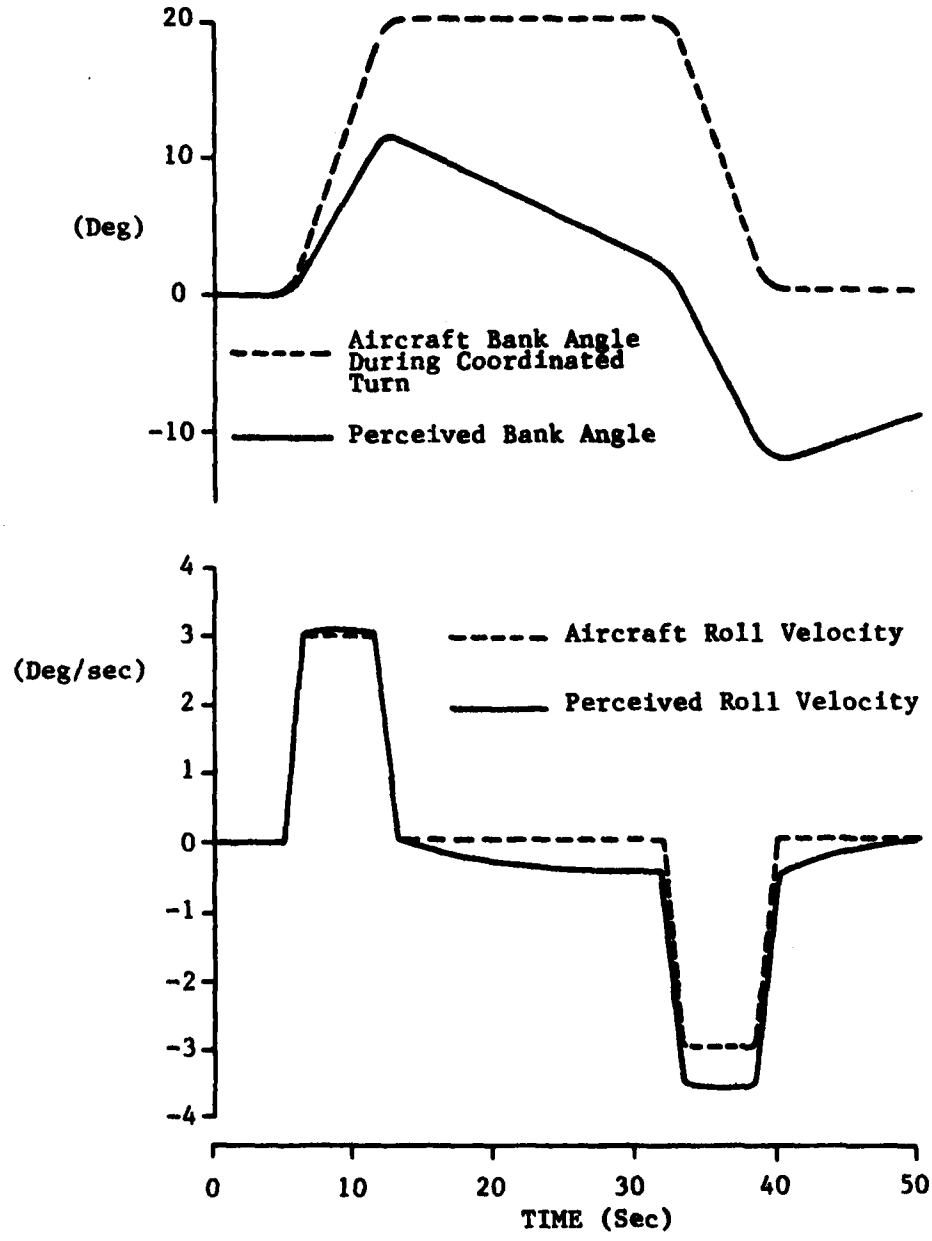

Figure 7.2 Model predictions of subjective bank angle and roll velocity during a 20° bank, 3°/sec roll rate coordinated turn.

in the figure). In Figure 7.3 the same roll orientation prediction is compared to subjective data from the TIFS study (see Sections 4.1 and 4.2). Model response is qualitatively the same as most subjective data, showing an initial tilt sensation during roll-in that begins to attenuate during the steady turn. The model, however, predicts a somewhat higher peak bank angle sensation and slower decay than are shown by the data.

As illustrated by Figure 7.4, the perception model predicts a slightly larger peak roll angle sensation as stimulus angular velocities become larger. The difference is substantially smaller than the variance in the experimental data and the data do not, in fact, show any significant difference as a function of roll velocity.

In Figure 7.5, model predictions are superimposed on the roll perception data as presented in Figure 4.7. Model predictions of tilt sensation during uncoordinated roll are compared to both the TIFS uncoordinated roll data and the data from Schöne. Predicted peak roll sensations during coordinated turns are indeed smaller than the predicted sensations during uncoordinated roll, but the difference is not as great as that found experimentally.

Referring to Figure 7.1, note that the only significant roll information reaching the central processor comes from the semicircular canal model. Remember that the semicircular canals are the rotation (angular velocity) sensing component of the human vestibular system (see Section 4.2) and are sensitive primarily to high frequencies. The comparison with experimental data implies that the model central processor gives more weight to unconfirmed semicircular canal input then does the human system, and the optimal estimator probably should be adjusted to decrease the weight placed on semicircular canal input and to place relatively more weight on the otolith inputs.

7.1.2 Pitch Orientation

Since an aircraft is banked during a coordinated turn, a component of the turn rate falls along the pitch axis. As explained in Section 4.3, this stimulates the human semicircular canals and might be integrated by the central nervous system to form a feeling of increasing pitch angle. The semicircular canals are high pass filters of angular velocity (they have no static sensitivity), so the effect

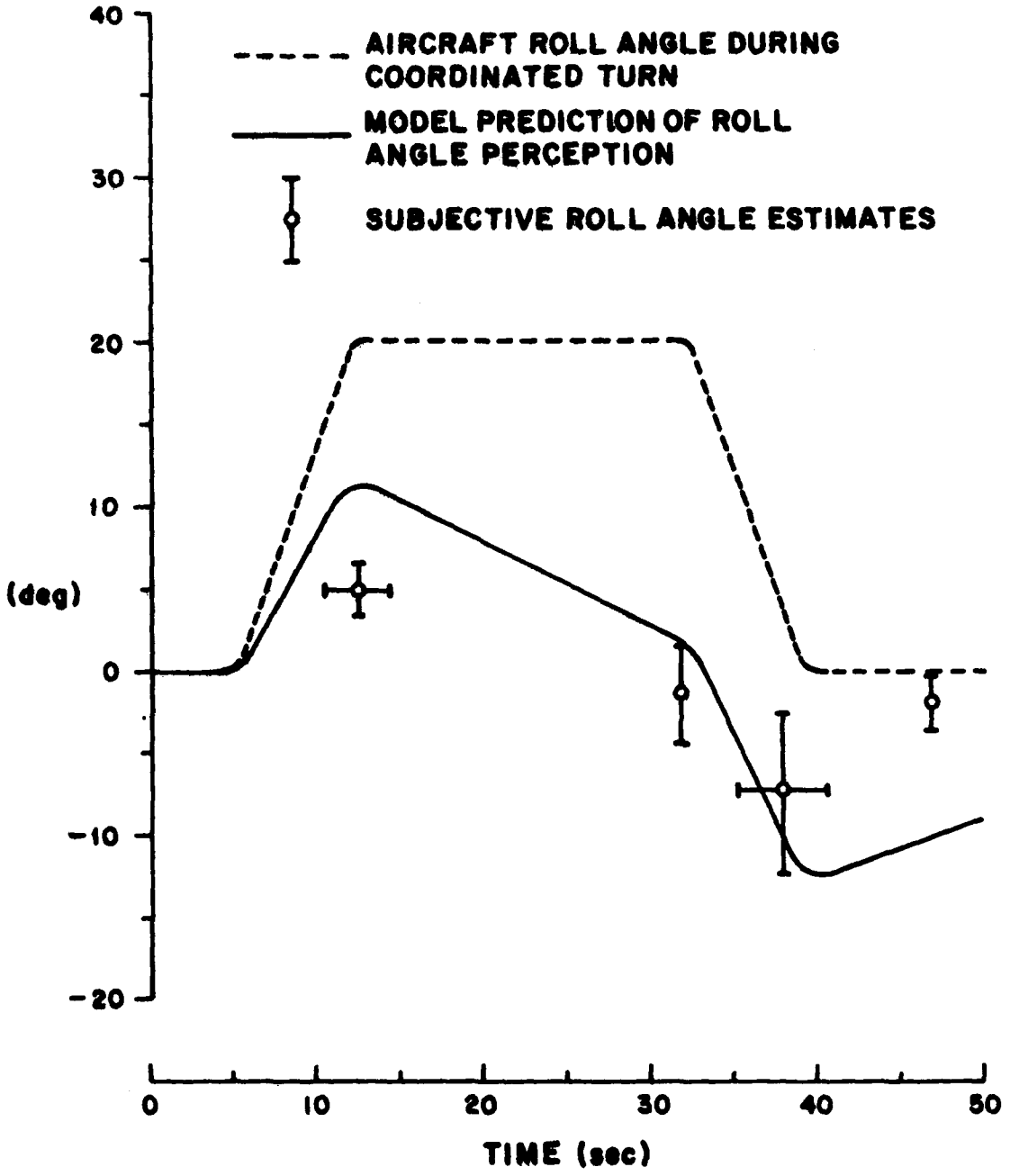

Figure 7.3 Model prediction of roll angle perception compared to TIFS data for 20°, 3°/sec coordinated turn. The experiment data points show mean peak subjective roll angle during roll-in and roll-out (the horizontal standard deviation bars indicate that peaks did not always occur at the same time) as well as mean values at the onset of roll-out, and 10 seconds after straight and level flight had been resumed.

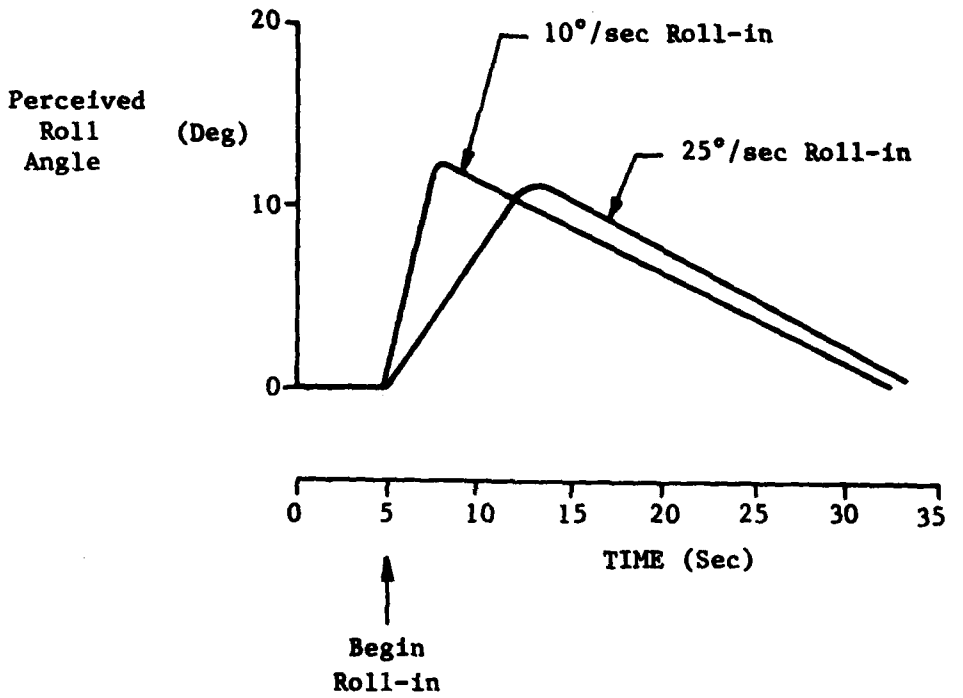

Figure 7.4 Model prediction of perceived roll angle during 20° bank angle, coordinated turns.

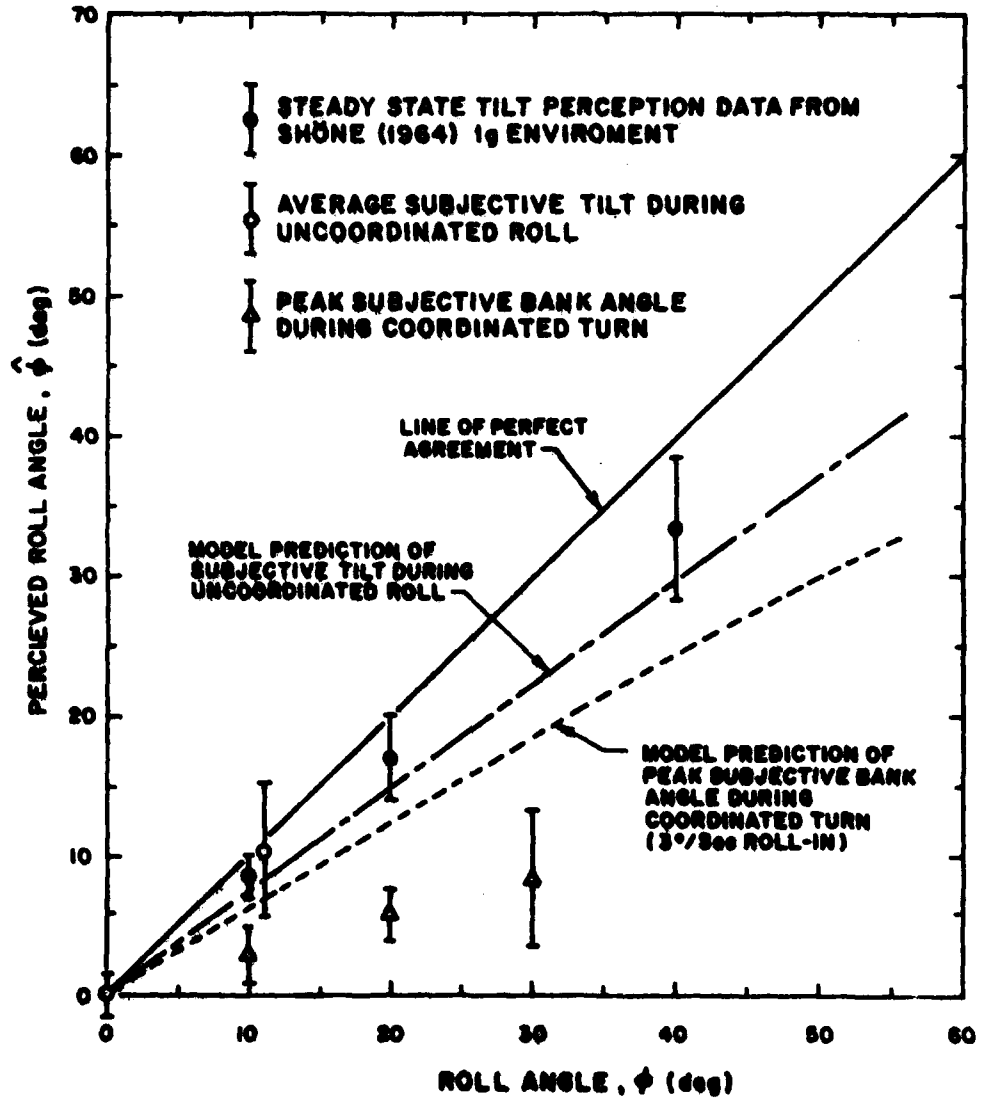

Figure 7.5 Model prediction of subjective tilt during uncoordinated roll and peak subjective bank angle compared to experimental data.

can be expected to diminish with time and to reverse during roll-out from the turn. The spatial orientation model behaves in just this way, as shown by Figures 7.6. Some (50%), but not all, subjective data show profiles having the same basic shape as that in Figure 7.6; the best such example is shown in Figure 7.7. The magnitude of the pitch-up sensation, however, is usually less than that predicted by the model. Using only those data showing a subjective pitch profile similar to Figure 7.6 (fairly monotonic increase in subjective pitch during the steady turn), the subjective pitch-up sensation averaged over the last 5 seconds of the steady turn was 7.87° $\pm$7.8°. The decrease in weight given by the central processor to unconfirmed semicircular canal input, suggested in the previous section on the basis of roll orientation data, would also have the desired effect of reducing model pitch estimates.

7.2 HEAD-NECK SYSTEM MODEL

The head, an inverted pendulum balanced on the body trunk with the aid of neck muscles, may be an important proprioceptive cue in determining spatial orientation. The head/neck system model shown in Figure 7.8 represents an initial attempt to include proprioception in the multi-sensory spatial orientation model and occupies the "proprioceptive system" block in Figure 7.1. The model considers muscle spindle (length sensor) response to lateral gravito-inertial force and assumes that the torso is stationary.

Figure 7.9 shows the head-neck model predictions of muscle torque compared to the best quality (least noisy) data from the TIFS lateral acceleration maneuver. The TIFS EMG data were converted to units of specific torque (torque/moment-of-inertia) by first using the spring scale calibration to convert to an equivalent force as in Section 6.1, and then using the approximate mass moment-of-inertia, and lever arm (r) values in Figure 7.8 to convert to specific torque.

The steady state values during each acceleration are comparable, but the large transient response to the sudden acceleration onset seen in the EMG data does not appear in the model response. The discrepancy might be accounted for by the large torso motion apparent in the experimental data (see Section 6.2) but not considered by the model; or, a discrepancy in the basic head-neck proprioceptive dynamics

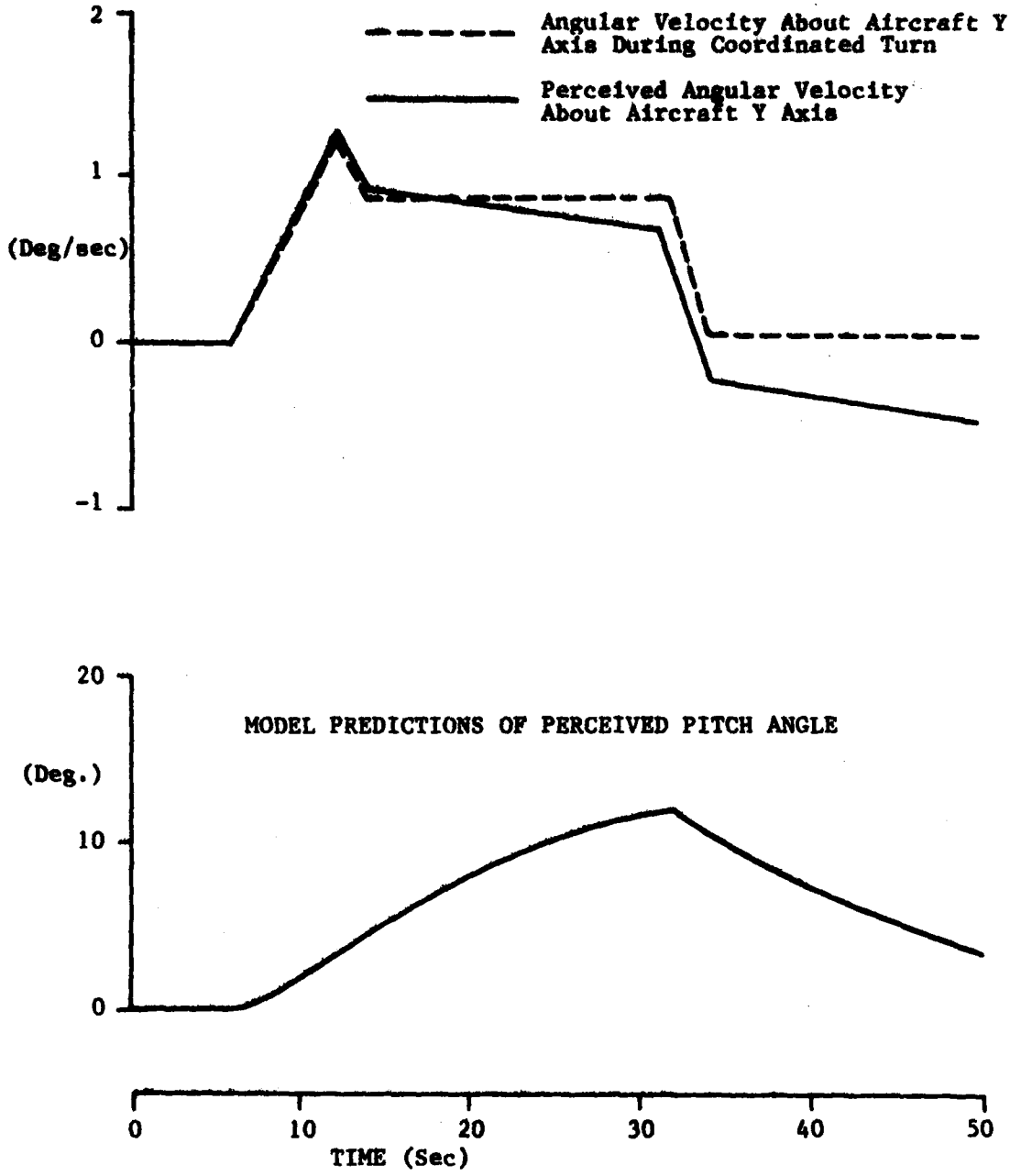

Figure 7.6 Model predictions of subjective pitch during a 20°, 3°/sec coordinated turn.

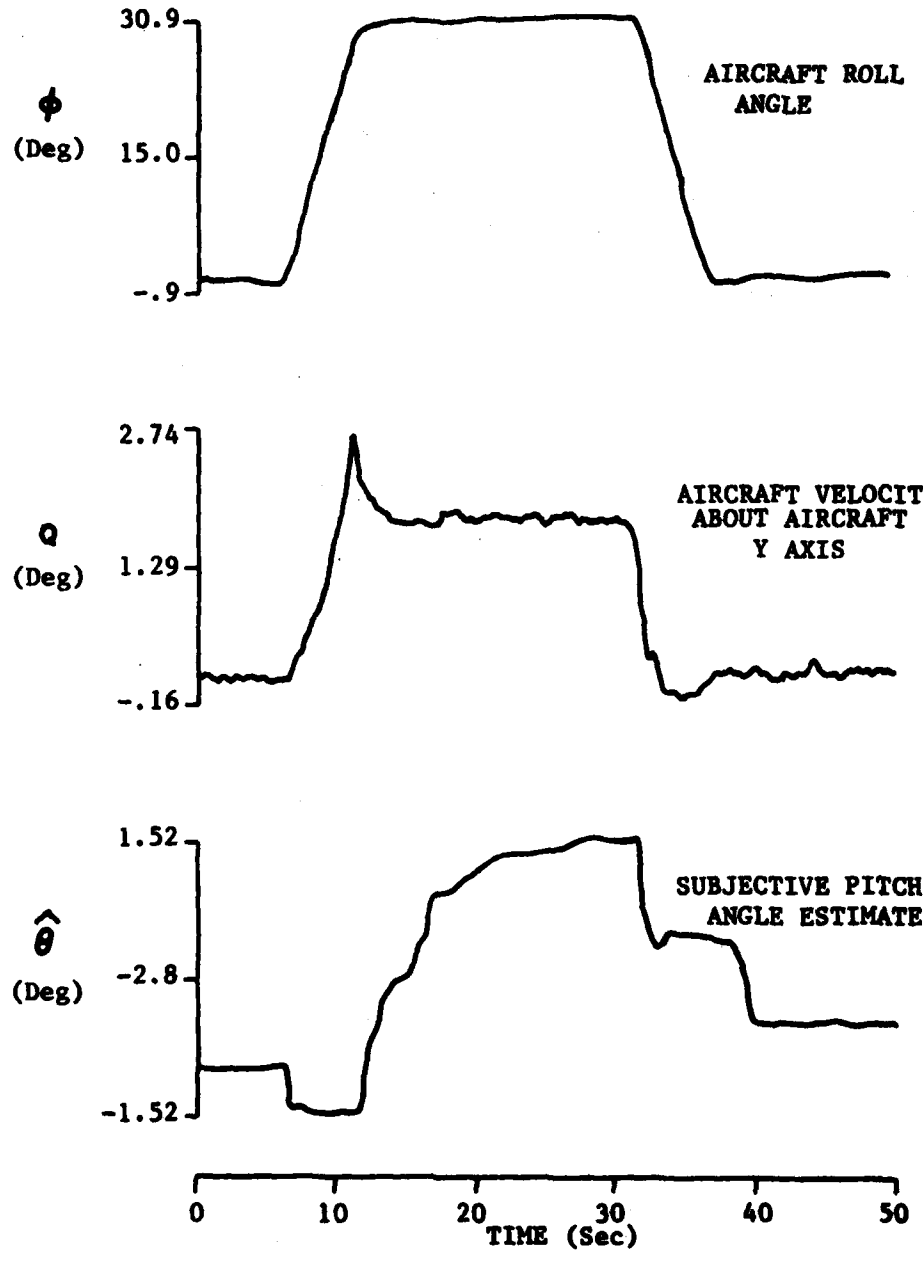

Figure 7.7 Example of subjective pitch indication during coordinated turn at TIFS.

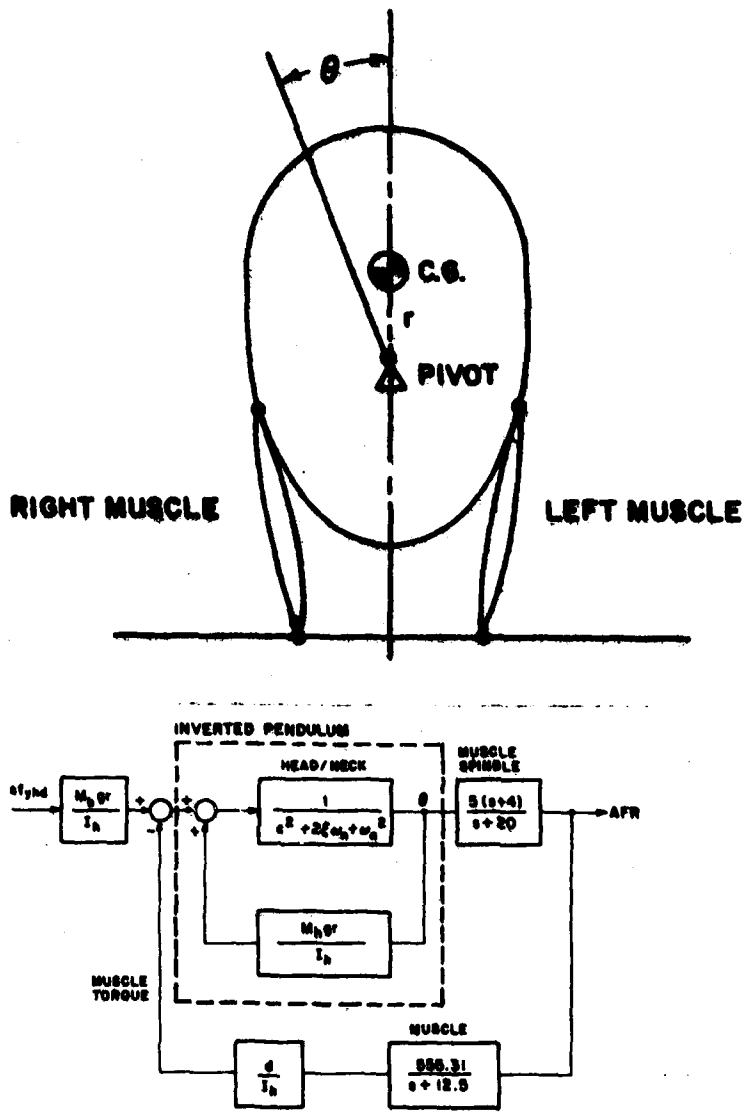

$d \equiv$ muscle lever arm = .075 m

$I_h \equiv$ head moment of inertia = .0304 kg m^2

$M_h \equiv$ head mass = 4.6 kg

$\omega_h \equiv$ 7.81 $\frac{rad}{sec}$

$r \equiv$ inverted pendulum length = .0498 m

$sf_{ghd} \equiv$ specific force parallel to body axis

$sf_{yhd} \equiv$ lateral specific force

$\zeta \equiv$ 0.64

Figure 7.8 Head/neck Proprioception Model (after Gum, 1973)

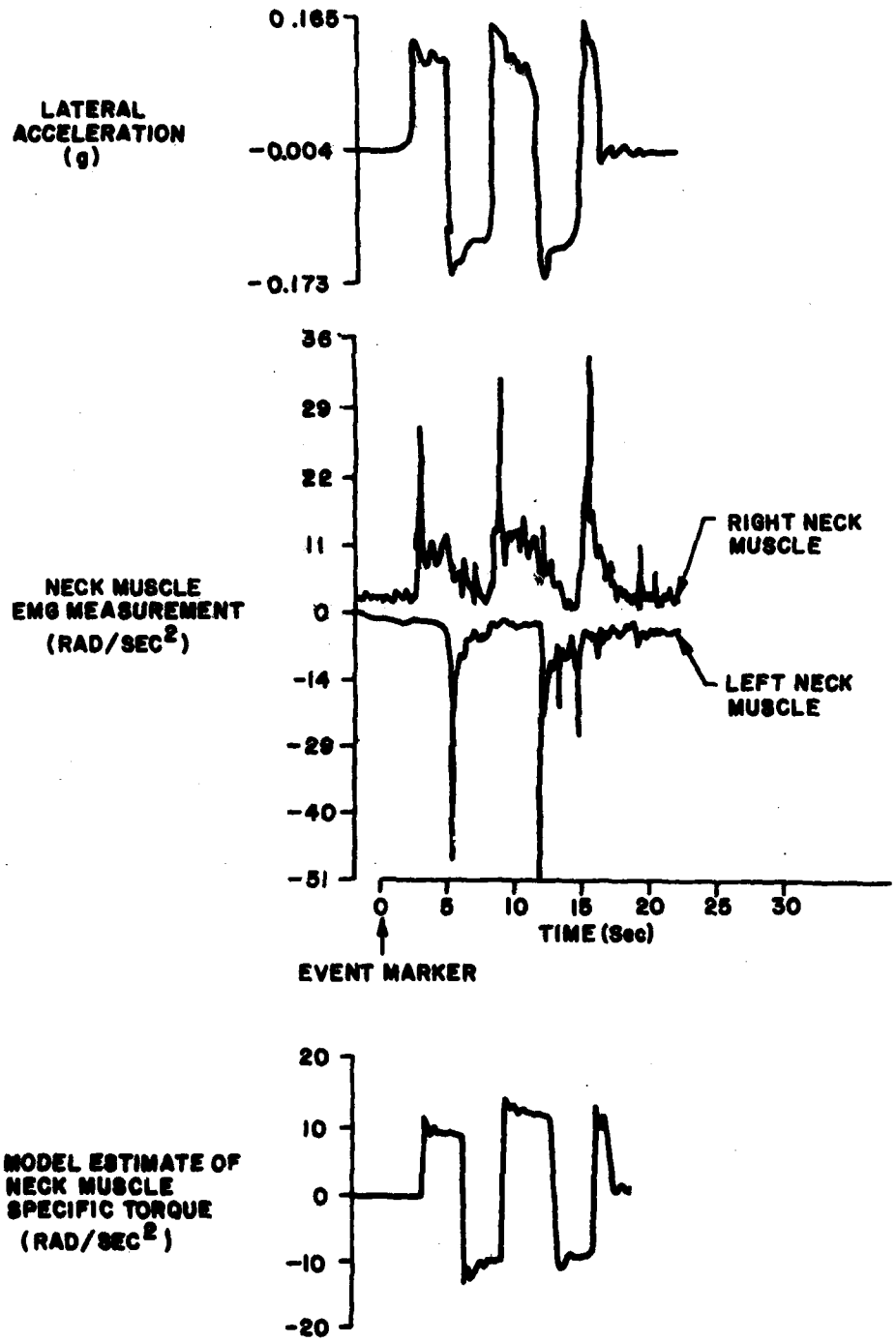

Figure 7.9 Specific Torque (torque/moment-of-inertia) produced by neck muscles during pure lateral acceleration.

might be implied.

Figure 7.10 shows model predictions of head motion during the same maneuver. Since the TIFS video head position data contain not just head-neck motion, but a great deal of torso motion, the two are not directly comparable. If video data are reduced in an automated way, and if a brief study to determine the characteristics of lateral torso motion is performed as suggested in Section 6.3, it should be possible to separate the neck and torso motions in the TIFS data to allow more meaningful model comparisons.

It is further suggested that a more elaborate proprioceptive model, including torso motion, be developed. One could also consider inclusion of Golgi tendon organ dynamics (muscle tension detectors) in the proprioceptive model.

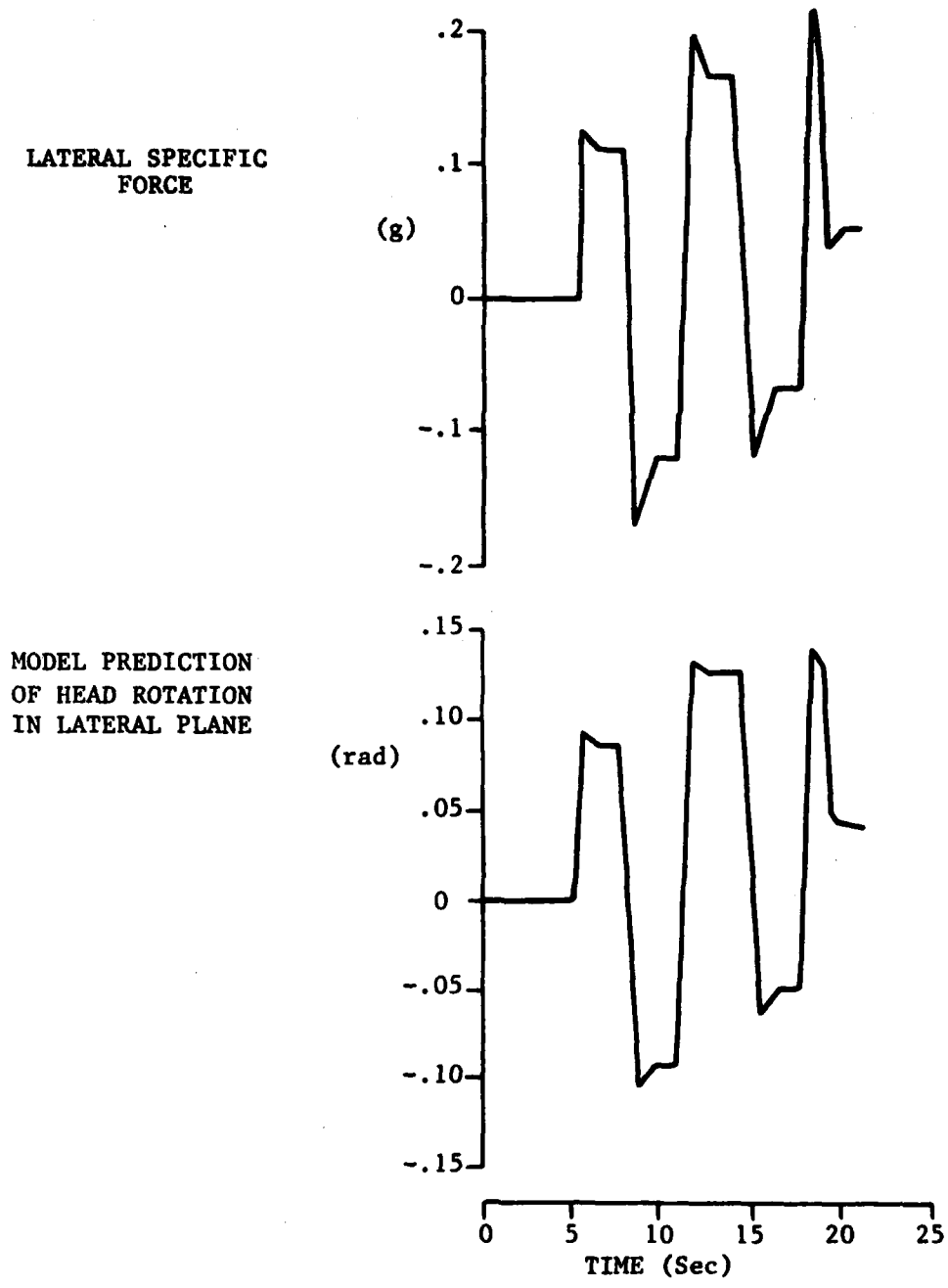

Figure 7.10 Head/neck model (see Figure 7.9) prediction of head motion in response to lateral specific force. Head rotation is θ in Figure 7.8

8.0 CONCLUSION

TIFS was used to make measurements for studies of subjective spatial orientation, head/neck biodynamics, and the tactile cue environment during some specific aircraft maneuvers. Data analysis has yielded useful information in all three areas. It is felt that considerably more information can be extracted from the TIFS data with direct computer processing of the digital data tapes and automated reduction of videotaped data.

Some conclusions from the data analysis are summarized below.

SPATIAL ORIENTATION:

1. As documented in previous ground based studies, the subjects had fairly accurate perceptions of their orientation and angular velocity profiles during uncoordinated rolling motions, in the absence of visual cues.

2. During a coordinated turn, in the absence of visual cues, most subjects felt an initial tilt sensation during roll-in (less than the actual roll), which gradually attenuated and was followed by an illusion of tilt in the opposite direction during roll-out. This well-known illusory profile has been quantified.

3. Perception of roll angular velocity during the coordinated turn tended to match the aircraft angular velocity profile, rather than the derivative of roll orientation perception.

4. The roll orientation results were consistent with knowledge of the physiological mechanisms involved.

5. The predictions of a previously developed model for human spatial orientation are in qualitative agreement with the roll orientation data, but the model seemed to place excessive weight on roll rate from the semicircular canals relative to roll angle cues from the otolith organs.

6. The predicted pitch-up illusion during coordinated turns could be neither confirmed nor rejected by visual examination of the data, due to the large variance in pitch orientation data. Computer analysis of the digital data tapes might allow an effect to be identified.

HEAD/NECK BIODYNAMICS:

1. Lateral inertial forces often caused significant lateral motion in the torso, as well as the neck, of the seated subject, even though the subject wore a shoulder harness.

2. Passive subjects often allowed themselves to be "pulled" in the direction of a lateral gravito-inertial (specific) force as described by Fukada (1975) in reference to bus passengers.

3. The expected tendency to lean into the turn (against the force) as reported by Fukada was not observed in the pilot subject during the TIFS flights.

4. The passive subject usually responded to inertial side forces by contracting only the muscles on one side of the neck (measured with EMG electrodes) as needed to counteract the force.

5. The pilot's neck muscle EMG response was sometimes similar to that of the passive subject and sometimes included a gradual simultaneous tensing of both left and right muscles, presumably stiffening the neck. Anticipatory tensing of neck muscles was not observed.

6. A previously developed head/neck system model (part of a model for human spatial orientation) predicts a steady state muscle torque similar to that indicated by EMG data during .2g lateral accelerations. The model does not predict the same transient response (a very large initial overshoot) seen in the data.

7. A more accurate biodynamics model should consider torso as well as neck motion.

TACTILE CUE ENVIRONMENT:

1. For low frequency acceleration profiles (low component of jerk), body/seat pressure dynamics can be adequately described by a simple mass model.

2. A static model algorithm for driving a g-seat is presented.

3. Body/seat pressure profiles produced by g-cueing seats should be measured by the same or a similar technique and compared to the TIFS data (and/or similar data gathered during real motion).

9.0 REFERENCES

1. Borah, J. Human dynamic orientation model applied to motion simulation. M.S. Thesis, Department of Aeronautics and Astronautics, MIT, 1976.

2. Borah, J., Young, L.R., & Curry, R.E. Optimal Estimator Model for Human Spatial Orientation, IEEE trans on Systems, Man and Cybernetics, in press.

3. Borah, J., Young, L.R., & Curry, R.E. Sensory mechanism modeling, final report. AFHRL-TR-78-83, AD-A069439. Wright-Patterson AFB, Ohio: Advanced Systems Division, Air Force Human Resources Laboratory, February 1979.

4. Bigland, B., Lippold, O.C.J., & Wrench, A.M.. The electrical activity in isotonic contractions of human calf muscles. Journal of Physiology, 1959, 123, 322-325.

5. Cohen, M.M., Crosbie, R.J. & Blackburn, L.H. Disorienting effects of aircraft catapult launchings. Aerospace Medicine. 1973, 44(1): 37-39.

6. Dittenhauser, J.N. Motion perception and related measurements obtained in flight-data report. Calspan Corporation No. 6241-F-4, Contract No. F33615-78-C-3602, Prepared for: U.S. Air Force Human Resources Laboratory, Wright-Patterson AFB, Ohio, December 1979.

7. Fernandez, C. & Goldberg, J.M. Physiology of peripheral neurons innervating otolith organs of the squirrel monkey, I, II, and III. Journal of Neurophysiology, 1976. 39:970-1008.

8. Fukada, T. Postural behavior and motion sickness, Acta Otolaryngol Supplement, 1975. 330:9-14.

9. Goldberg, J.M. & Fernandez, C. Physiology of peripheral neurons innervating semicircular canals of the squirrel monkey, I, II, and III. Journal of Neurophysiology, 1971. 34:661-675.

10. Gum, D.R. Modeling of the human force and motion-sensing mechanisms. AFHRL-TR-72-54, AD-766 444. Wright-Patterson AFB, Ohio: Advanced Systems Division, Air Force Human Resources Laboratory, June 1973.

11. Hertzberg, H.T.E. Some contributions of applied physical anthropology to human engineering," Annals of the New York Academy of Sciences, 1955. 63 (4) 616-629.

12. Kron, G.J. Advanced simulation in undergraduate pilot training; G-Seat development. AFHRL-TR-75-59(III), AD-A017468. Wright-Patterson AFB, Ohio: Advanced Systems Division, Air Force Human Resources Laboratory, October 1975.

13. Lentz, J.M. & Collins., W.E. Motion sickness susceptibility and related behavioral characteristics in men and women. Aviation Space Environment Medicine, 1977. 48(4) 316-322.

14. Lay, W.E. & Fisher, L.C. Riding comfort and cushions. Society of Automotive Engineers Journal (Transactions), 1940, 47(5), 482-496.

15. Ormsby, C. Model of human dynamics orientation. Ph.D. Thesis, Department of Aeronautics and Astronautics, MIT, 1974.

16. Poulton, E.C. The new psychophysics: Six models for magnitude estimation. Psychological Bulletin, January 1968, 69, 1-19.

17. Reynolds, P.A., et.al. Capability of the Total In-Flight Simulator (TIFS). AFFDL-TR-72-39, TB-3020, Wright Patterson AFB, Air Force Flight Dynamics Laboratory, Air Force Systems Command, July 1972.

18. Schneider, C.W., Bowman, B.M., Snyder, R.G. and Peck, L.S. A prediction of response of the head and neck of the U.S. adult military population to dynamic impact acceleration from selected dynamic test subjects. 12 Month Technical Report April 1975 to April 1976, Office of Naval Research, Virginia: Biomedical and Medical Science Division, May 1976.

19. Schone, H. On the role of gravity in human spatial orientation," Aerospace Medicine, 1964, 35.

20. Stevens, S.S. On the operation known as judgement, American Scientist, 1966, 54, 385.

21. Von Renner, L.C. Extravehicular attitude control by use of head motions. S.M. Thesis, Department of Aeronautics and Astronautics, MIT, 1970.

22. Young, L.R. Role of the vestibular system in posture and movement. V.B. Mountcastle (Ed.) In: Medical Physiology, 13th Edition, Volume I, Chapter 27, St. Louis: C.V. Mosby and Company, 1974.

23. Young, L.R., & Meiry, J.C. A revised dynamic otolith model. Aerospace Medicine, 1968, 39(6),606-608.

24. Young, L.R., & Oman, C.M. Model for vestibular adaptation to horizontal rotation. Aerospace Medicine, 1969, 40,1076-1080.

APPENDIX A: EQUIPMENT CIRCUIT DIAGRAMS

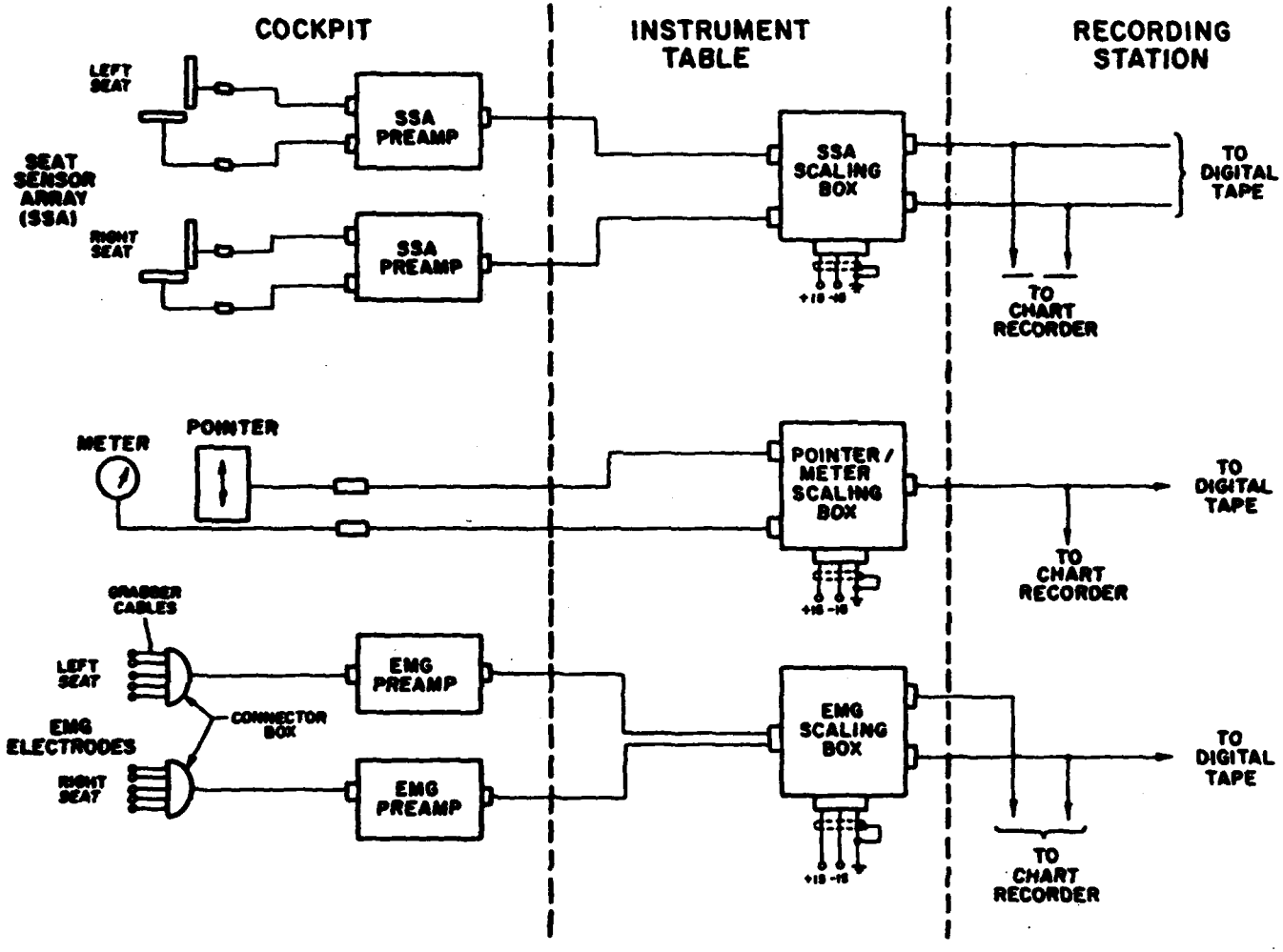

Seat Sensor Array, EMG, and Pointer/Meter Configuration

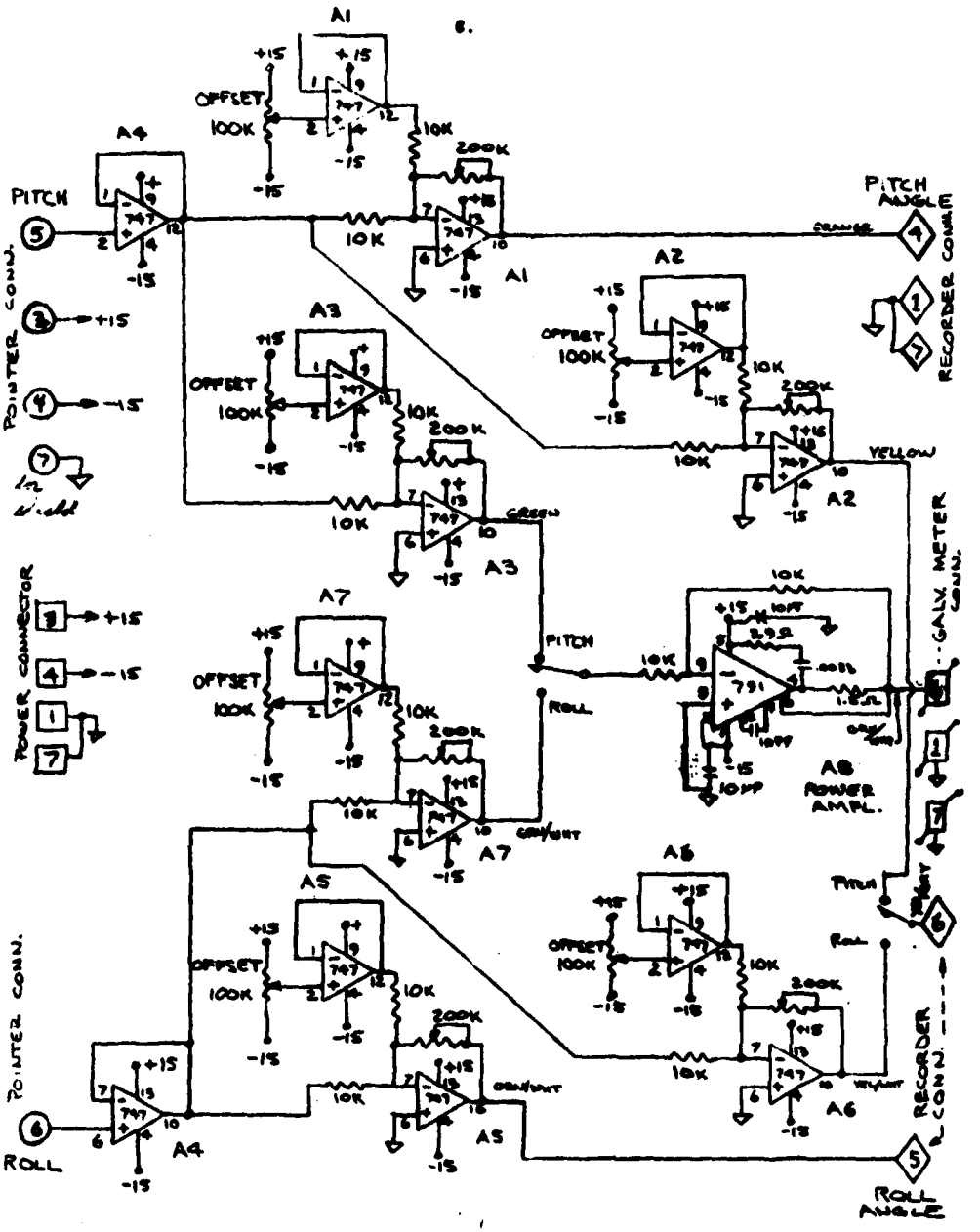

Pointer/Meter Box Wiring Diagram

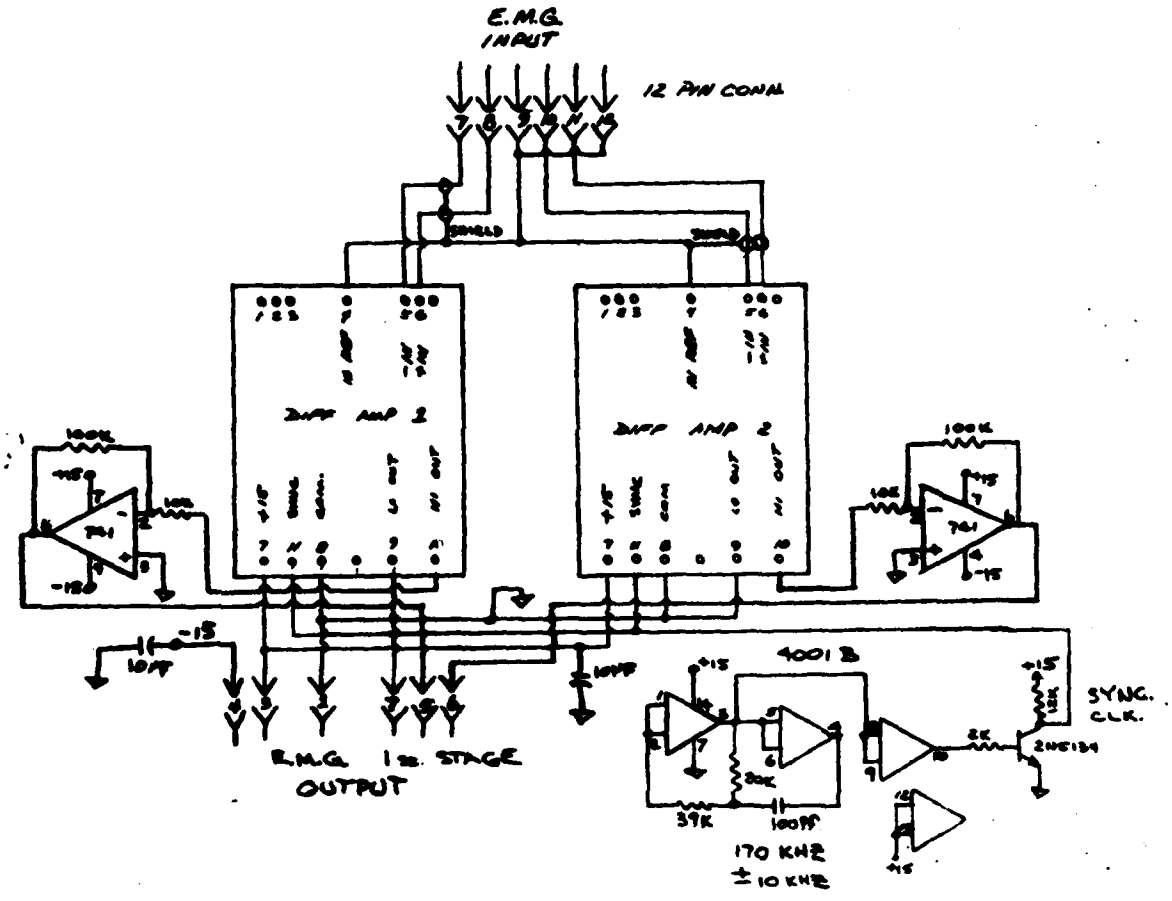

Wiring Diagram EMG Pre-amp Box

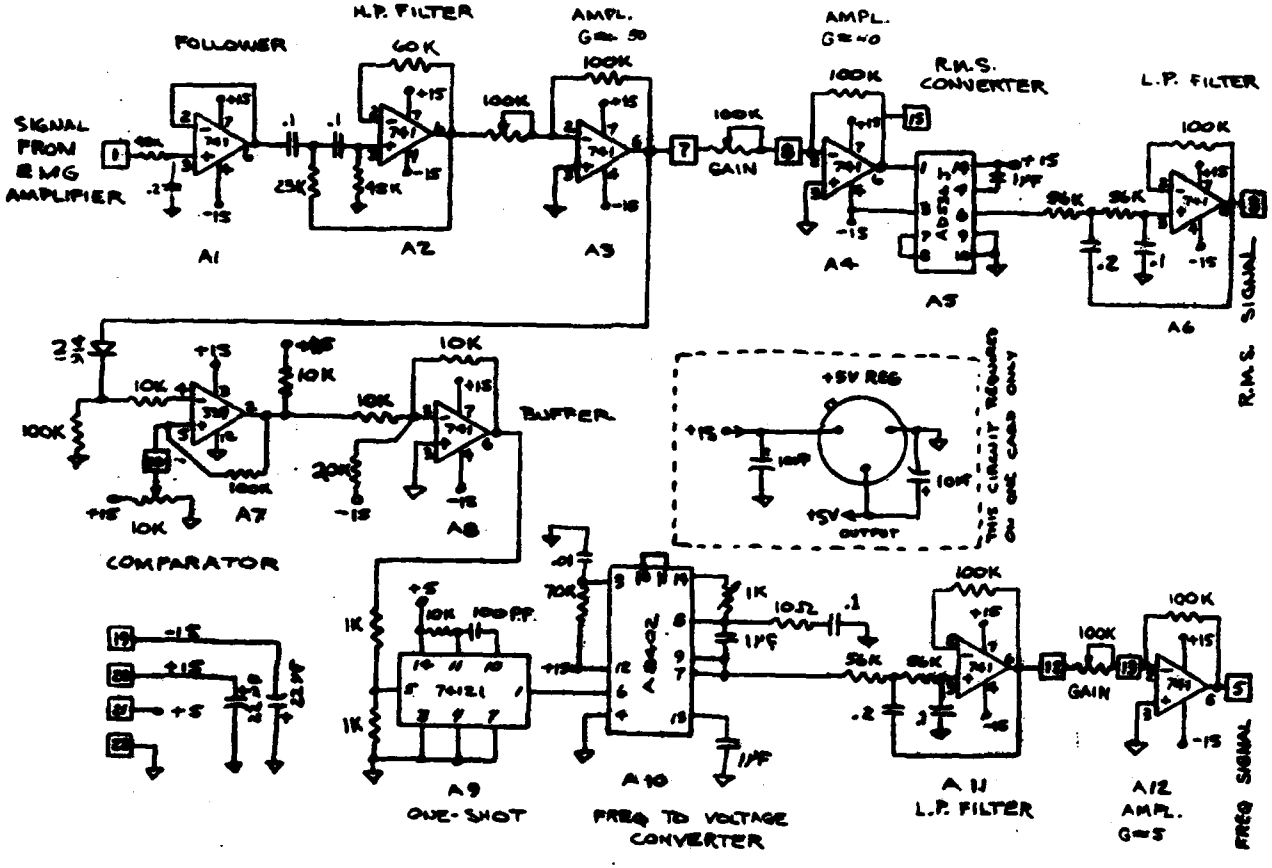

CIRCUIT DIAGRAM FOR EMG PROCESSING BOX LOCATED ON INSTRUMENTATION TABLE

(THE BOX WILL CONTAIN FOUR IDENTICAL CIRCUIT BOARDS - ONE FOR EACH EMG SIGNAL)

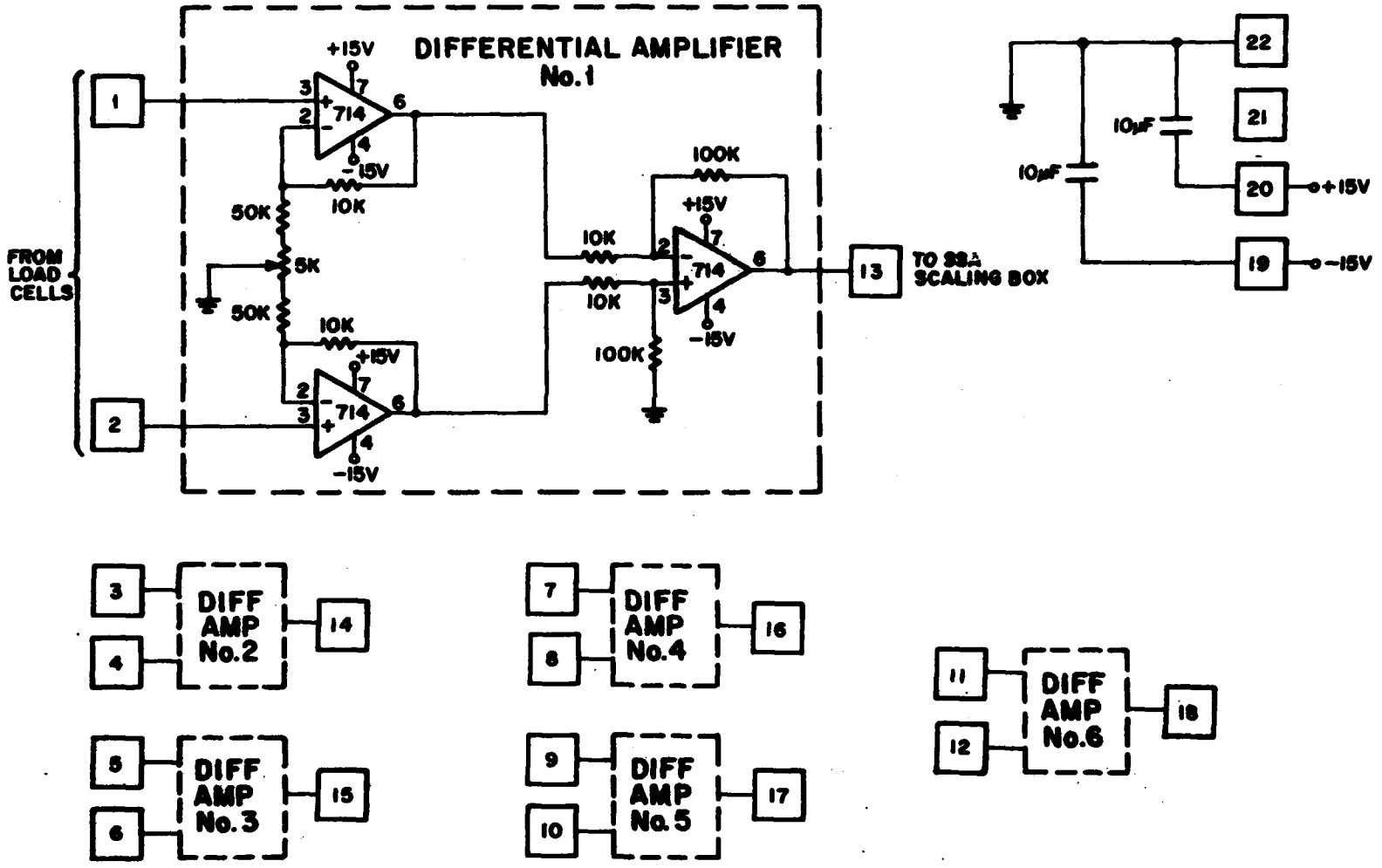

Seat Sensor Array Preamp Card

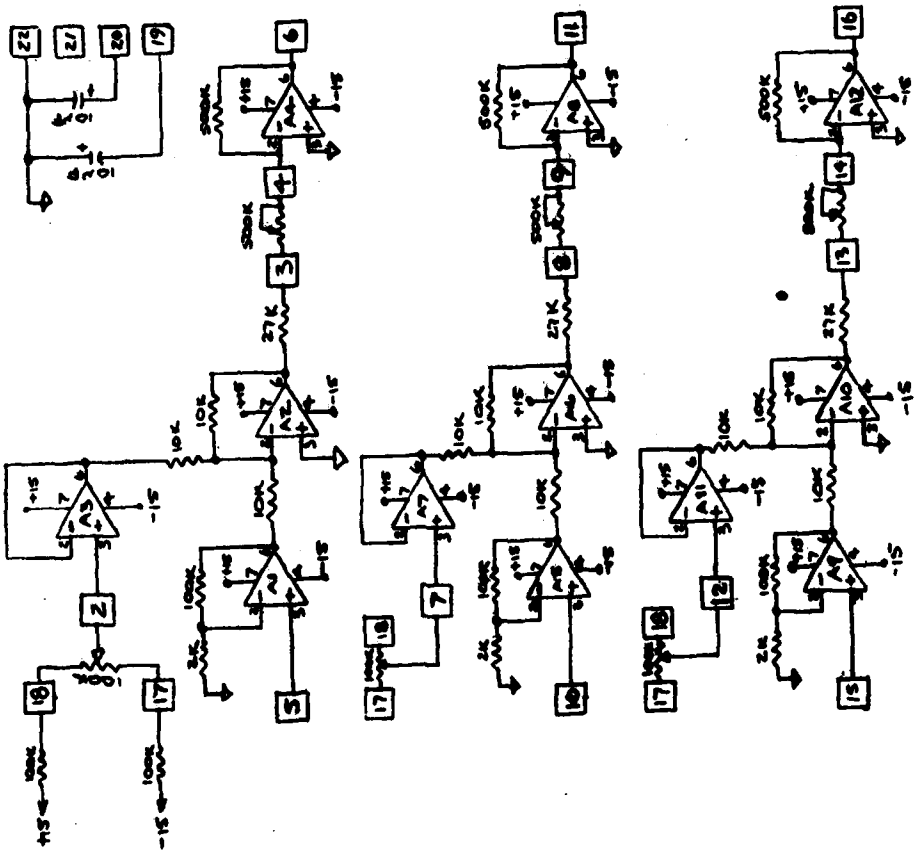

Load Cell Gain and Offset Card - Seat Sensor Array Box

APPENDIX B: DATA TAPE RECORDING LIST

LIST OF SYMBOLS

n_x	Longitudinal acceleration, g units
n_y	Lateral acceleration, g units
Δn_z	Normal acceleration with 1 g removed, g units
p	Roll rate, deg/sec
$\dot{p}$	Roll acceleration, deg/sec^2
q	Pitch rate, deg/sec
$\dot{q}$	Pitch acceleration, deg/sec^2
r	Yaw rate, deg/sec
$\dot{r}$	Yaw acceleration, deg/sec^2
$\Delta\alpha_I$	Change of inertial angle of attack after engage, deg
$\dot{\alpha}_I$	Inertial angle of attack rate, deg/sec
β_I	Inertial angle of sideslip, deg
$\dot{\beta}_I$	Inertial angle of sideslip rate, deg/sec
γ	Flight path angle, deg
δ_a	Total aileron deflection, positive - right trailing edge down, deg
δ_{AS}	Aileron wheel deflection, positive - wheel clockwise, deg
δ_e	Elevator deflection, positive - trailing edge down, deg
δ_{ES}	Elevator wheel deflection, positive - wheel aft, inches
δ_r	Rudder deflection, positive - trailing edge left, deg
δ_{RP}	Rudder pedal deflection, positive - right rudder pedal forward, inches
δ_x	Throttle displacement in cockpit, positive - forward, deg
δ_y	Side force surface deflection, positive - trailing edge left, deg
δ_z	Direct lift flap deflection, positive - trailing edge down, deg
ζ	Servo damping ratio, unitless
$\Delta\theta$	Change of pitch angle after engage, deg
ϕ	Bank angle, deg
ϕ_{a_c}	Coordinated bank angle command
ϕ_{a_u}	Uncoordinated bank angle command
ω_n	Servo natural frequency, Hz

DATA TAPE RECORDING LIST

FOR TIPS FLIGHTS #560-#566

DATA TAPE CHL. NO.	CHANNEL VARIABLE	X	SCALE FACTOR	=	FINAL UNITS
1	P11		0.500		psi
2	P12		1.000		
3	P13		1.000		
4	P14		0.500		
5	P15		0.500		
6	P16		0.500		
7	P17		0.250		
8	P18		0.250		
9	P19		0.250		
10	P110		0.250		
11 (see note (1))	P111		0.250	see note (2)	
12	P21		0.500		
13	P22		1.000		
14	P23		1.000		
15	P24		0.500		
16	P25		0.500		
17	P26		0.500		
18	P27		0.250		
19	P28		0.250		
20	P29		0.250		
21	P210		0.250		
22	P211		0.250		
23 (see note (3))	Meter (θ)		2.000 (20.000)		divisions (deg)
24	n_x		0.050		g
25	n_{y_p}		0.100		g
26	n_{z_p}		0.250		g
27	p		5.000		deg/sec
28	q		2.000		deg/sec
29	r		2.000		deg/sec
30	ϕ		10.000		deg

DATA TAPE RECORDING LIST (CONT'D)

DATA TAPE CHL. NO.	CHANNEL VARIABLE	X	SCALE FACTOR	=	FINAL UNITS	
31	sin θ (θ)		0.050 (3.8648)		--- (deg)	see note (4)
32	sin φ (φ)		0.100 (5.7296)		--- (deg)	
33	V - true		50.000		feet/sec	
34	V_i - IAS		30.000		knots	
35	$\dot{V}_I$ - inertial		2.000		feet/sec/sec	
36	$\hat{\phi}$		4.000		deg	
37	$\hat{\theta}$		4.000		deg	
38	E_{1R}		see note (5)			
39	E_{1F}		↓			
40	E_{2R}					
41	E_{2F}					
42	E_{3R}					
43	E_{3F}					
44	E_{4R}					
45	E_{4F}					
46	α_I		2.000		deg	
47	β_I		2.000		deg	
48	δ_x^R		10.000		deg	
49	δ_y^R		4.000		deg	
50	δ_z^R		4.000		deg	
51	δ_a		4.000		deg	
52	δ_e		2.500		deg	
53	δ_r		2.000		deg	
54	h_p		2500.000		feet	
55	p_c		40.000		deg/sec	
56	ΔV_c		-14.286		feet/sec	
57	q_c		2.000		deg/sec	
58	event marker		1.000		---	
59	time		1.000		sec	
60	identification code		100.000		---	

DATA TAPE RECORDING LIST (CONT'D)

NOTES:

Data recorded on data tape is in integer form as on flight tape. (negative numbers expressed in 2's complement).

Full scale deflection = ± 1023 BITS = ± 10.23 volts.

Use following conversion: (fixed point to floating point).
VARIABLE (final units) = (TAPE VARIABLE/100.0) X SCALE FACTOR

e.g. $p(\text{deg/sec}) = (p_{tape}/100.0) \times 5.00$

(1) Data Tape CHL #11 changed as follows:

Starting at	Chl. Var.	X	Scale Factor	=	Final Units
Flt. #564 rec. #1	ΔP_e		50.000		lbs
Flt. #566 rec. #20	$\dot{\delta}_a^R$		4.000		deg/sec

(2) Nominal scale factors.

(3) Description in ( ) for "PITCH" status.

(4) Description in ( ) for small angle approximation:
i.e., sin $x \approx x$(radians); where $x < 20.$ deg for max. error of 2%.

(5) E_{1F}, E_{2F}, E_{3F}, E_{4F} - scale factor = 54.0 Hertz.
E_{1R}, E_{2R}, E_{3R}, E_{4R} - scale factors vary with individual test subjects.

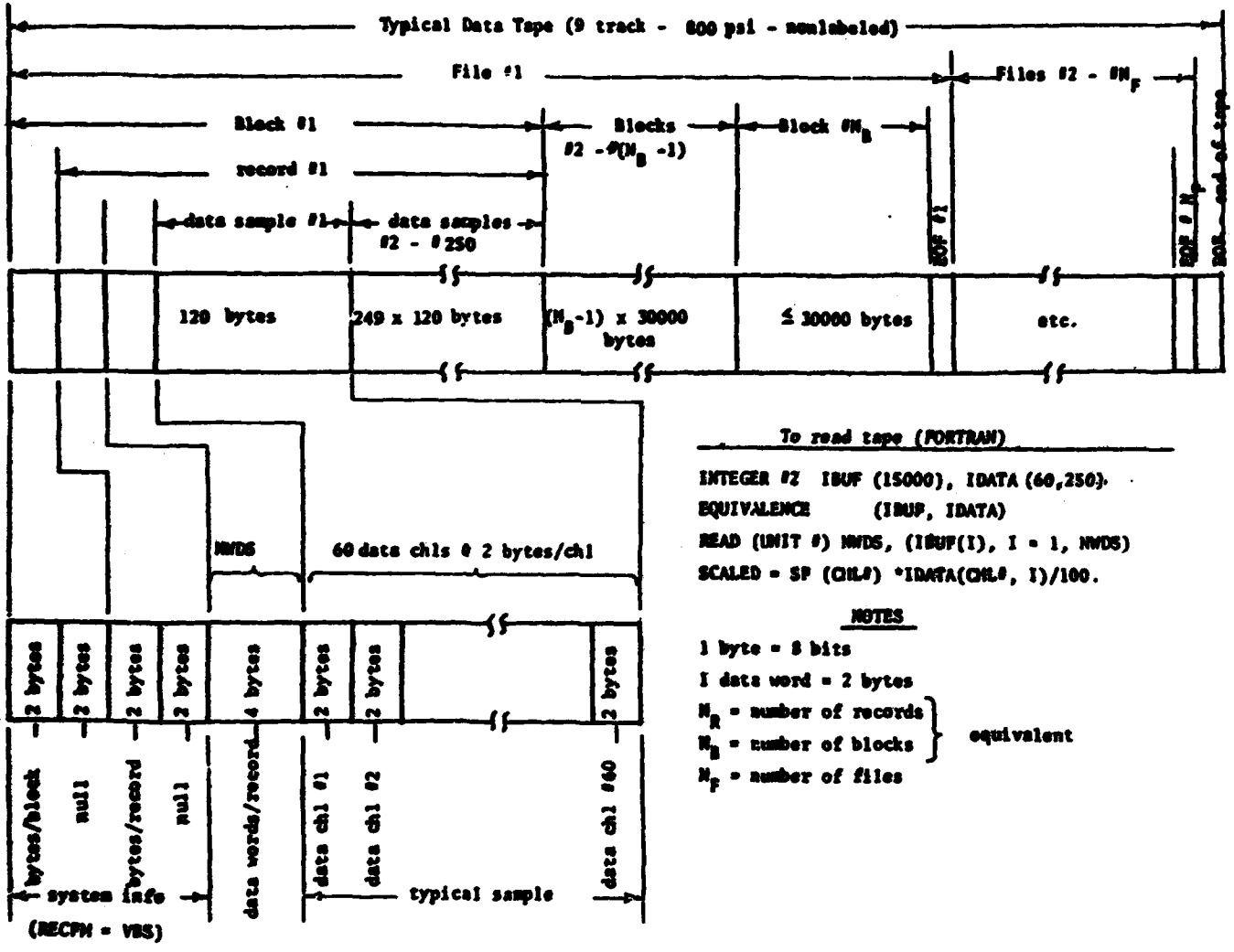

To read tape (FORTRAN)

```
INTEGER *2  IBUF (15000), IDATA (60,250)
EQUIVALENCE       (IBUF, IDATA)
READ (UNIT #) NWDS, (IBUF(I), I = 1, NWDS)
SCALED = SF (CHL#) *IDATA(CHL#, I)/100.
```

NOTES

1 byte = 8 bits

1 data word = 2 bytes

N_R = number of records
N_B = number of blocks
} equivalent

N_F = number of files

APPENDIX C: MOTION SICKNESS QUESTIONNAIRE AND INFORMED CONSENT FORM

MOTION SICKNESS QUESTIONNAIRE

This questionnaire is designed to find out: your familiarity and experience with aircraft flight; medical facts that would be important in interpreting the results of our experiments; and your susceptibility to motion sickness.

Motion sickness susceptibility is revealed by a wide variety of subjective symptoms and objective signs, and may be experienced over a wide range of severity. Common symptoms are stomach discomfort, nausea, vomiting, pallor, sweating. These symptoms are often accompanied by drowsiness, increased salivation, a feeling of warmth (not associated with exercise), and/or headache.

Your replies to all questions will be treated in the strictest confidence.

SUBJECT CODE:_____ DATE:_____ AGE:_____(years)

GENDER:_____ WEIGHT:_____ HEIGHT:_____(inches)

OCCUPATION:_____

SECTION A

1. To your knowledge, do you have any medical condition that affects your sense of balance or spatial orientation?

2. Have you ever experienced repeated episodes of disorientation or vertigo while not in a moving vehicle?

3. Have you ever experienced motion sickness?

4. If you have experienced motion sickness, how long does it usually take you to recover completely when the motion stimulus is removed?

5. When you experience motion sickness, what steps do you usually take to control it (other than getting off the vehicle)?

6. Have you ever piloted an aircraft?

7. Do you hold a pilot's license? (If so, please specify rating)

8. Do you enjoy riding in aircraft?

9. Do you enjoy amusement park rides (roller-coasters, ferris wheels, merry-go-rounds, etc.)?

10. Do you usually use drugs to control motion sickness? If so, which?

11. Do you experience any side effects, such as drowsiness, when you take an anti-motion sickness drug?

12. If you use an anti-motion sickness drug, do you usually take it before motion exposure or when you begin to feel sick?

13. Are you afraid of: heights?_____, darkness?_____.

SECTION B

The following items concern your tendency to develop motion sickness in a variety of situations. Motion sickness refers to a strong and unpleasant stomach awareness or nausea or vomiting. If you have had no experience with a particular motion situation, simply circle 0 under the Number of Experiences column. If you have had experience with a situation, first circle the most appropriate number of experiences, and then circle the letter in the column which describes your general reaction to that situation.

	Number of Experiences				Motion Sickness Occurred				
Motion Situation	0	1-3	4-9	10 or more	Never	Rarely	Sometimes	Often	Almost Always
1. large ships	0	1-3	4-9	10+	a	b	c	d	e
2. small boats	0	1-3	4-9	10+	a	b	c	d	e
3. merry-go-rounds	0	1-3	4-9	10+	a	b	c	d	e
4. roller coasters	0	1-3	4-9	10+	a	b	c	d	e
5. ferris wheels	0	1-3	4-9	10+	a	b	c	d	e
6. other carnival devices	0	1-3	4-9	10+	a	b	c	d	e
7. automobiles (as passenger)	0	1-3	4-9	10+	a	b	c	d	e
8. buses	0	1-3	4-9	10+	a	b	c	d	e
9. trains	0	1-3	4-9	10+	a	b	c	d	e
10. subways	0	1-3	4-9	10+	a	b	c	d	e
11. streetcars	0	1-3	4-9	10+	a	b	c	d	e
12. airplanes (any type)	0	1-3	4-9	10+	a	b	c	d	e
13. elevators	0	1-3	4-9	10+	a	b	c	d	e
14. swings	0	1-3	4-9	10+	a	b	c	d	e
15. hammocks	0	1-3	4-9	10+	a	b	c	d	e
16. ring and bar (gymnastics)	0	1-3	4-9	10+	a	b	c	d	e
17. somersaults	0	1-3	4-9	10+	a	b	c	d	e
18. rollerskating	0	1-3	4-9	10+	a	b	c	d	e
19. ice skating	0	1-3	4-9	10+	a	b	c	d	e
20. dancing	0	1-3	4-9	10+	a	b	c	d	e

TIPS PERCEPTION STUDY

VOLUNTARY INFORMED CONSENT FORM FOR SUBJECT PARTICIPATION

PURPOSE OF TIPS PERCEPTION STUDY

The TIFS Perception Study is being conducted to determine human perception of orientation (feeling of tilt with respect to the horizon), feelings of acceleration, and corresponding motion and force cues during certain aircraft maneuvers. Results from this study will be used to help develop a computer model of the human spatial orientation process, and will also aid in the design and use of ground based aircraft simulation devices.

SUBJECT TASKS

As a subject, you will sit in the right simulation cockpit seat on board the Total In-Flight Simulator during flight. You will be asked to operate a mechanical pointer device to indicate your feeling of orientation, and at other times you will be asked to use a special indicator to estimate your angular velocity and forward acceleration relative to a standard.

INSTRUMENTATION

You will be issued a "flight suit" to wear during the experiment. The seat on which you sit (the right seat of the TIPS simulation cockpit) during the experiment will be equipped with pressure-sensing devices. You will wear head gear containing two small light-emitting diodes and your head motions will be monitored by a TV camera located behind your seat. You will also wear four disposable electrodes on your neck and one disposable reference electrode on your shoulder. The electrodes will be fastened to your skin with a light adhesive, and wires attached to the electrodes will be connected to standard equipment to measure neck electromyographic activity (skin electric potential caused by muscle activity). Skin preparation may include a small surface scratch and the electrodes may cause some slight skin irritation. During most of the flight the windows will be covered and you will not be able to see out.

DURATION

As a subject, you will be asked to participate in one or two flights each lasting from .7 to 1.5 hours.

AIRCRAFT MOTION AND POSSIBLE DISCOMFORT

The aircraft will undergo various tilting, turning, and accelerating motions. For some people, these motions may cause motion sickness discomfort.

WITHDRAWL FROM PARTICIPATION IN THE STUDY

As a subject, you may withdraw from participation in the study at any time, even during the progress of a flight.

SUBJECT COMPENSATION

Calspan employees will receive their regular salary plus flight pay during each flight in which they participate.

PARTICIPANT'S CONSENT

I, , understand that Applied Science Laboratories, a division of Gulf + Western Manufacturing Company, is engaged in research under Contract No. F33615-78-C-0062, with the United States Air Force (Wright-Patterson Air Force Base), and that an experiment, known as TIFS Perception Study, is being undertaken as a part of that research. I am an employee of Calspan Corporation, which operates the Air Force "Total In-Flight Simulator" to be used in the Study, and I have volunteered to participate. I have received a copy of, and have read and understood, the attached description of the TIFS Perception Study and have been afforded the opportunity of asking questions, concerning the Study, of Joshua Borah, an employee of Applied Science Laboratories; or Dr. Phil Reynolds, an employee of Calspan Corporation; or Martin Yohpe, an employee of the United States Air Force. He has explained to me the procedures to be followed and the conditions, sensations and possible discomfort which I may experience. I have also been advised that I am free to withdraw my consent and discontinue participation in the Study at any time.

With the above knowledge and information which has been explained in a manner understandable to me, I voluntarily consent to participate in this research and to act as a subject of the described experiments. I confirm that I am of full age and have the legal capacity to give this consent.

I affirm that I have undergone a physician's examination within the past 2 years, and that, to my knowledge, my state of health is satisfactory.

I also affirm that I have no known history of cardiac arrhythmia or angina.

DATE: _____ _____
(SIGNATURE)

_____
(WITNESS)